UNIVERSITY OF CALIFORNIA SAN DIEGO

Exploring the Metaorganism:

Utilizing the microbiome to improve human health

A dissertation submitted in partial satisfaction of the

requirements for the degree Doctor of Philosophy

in

Biomedical Sciences

by

Joanna Katherine Claire Coker

Committee in charge:

Professor Karsten Zengler, Chair
Professor Victor Nizet, Co-chair
Professor Lars Bode
Professor Hiutung Chu
Professor Philip Gordts

2022

The Dissertation of Joanna Katherine Claire Coker is approved, and it is acceptable in quality and form for publication on microfilm and electronically.

University of California San Diego

2022

DEDICATION

In memory of Louis Coker. I know you’re proud of me. I still wish you could be here.

To my mother Linda Coker, who has always believed I could do anything.

EPIGRAPH

Science may provide the most useful way to organize empirical, reproducible data, but its power to do so is predicated on its inability to grasp the most central aspects of human life: hope, fear, love, hate, beauty, envy, honor, weakness, striving, suffering, virtue.

Paul Kalanithi, *When Breath Becomes Air*

TABLE OF CONTENTS

LIST OF FIGURES

LIST OF TABLES

ACKNOWLEDGEMENTS

I would like to thank all members of the Zengler, Gordts, and Esko labs. You are all amazing people and scientists, and I cannot imagine how I would have finished graduate school without your help and support. Especially Livia, who has been there for my entire grad school journey.

Good mentors are hard to find. But once you find them, you're stuck for life. Thank you to Karsten for always being available when I needed to chat and for trusting me enough to pursue a project in three areas in which I had no expertise before starting in the lab. Thank you to Philip, who gave me as much time and mentorship as any student actually in his lab. Thank you to Joe, Marcy, and Alan, who introduced me to the world of research in such a way that I decided to make it a career. And a heartfelt thanks to my other committee members (Victor Nizet, Hiutung Chu, and Lars Bode), who have taken time out of their busy schedules to make this thesis the best it can possibly be.

I joined a single lab for graduate school, but it came with an entire floor of science family. Special thank you to Livia Zaramela (again), Lisa Marotz, Deepan Thiruppathy, JR Caldera, Daniel Sandoval, and Thomas Mandel Clausen for staying late with me in lab, dragging me out of lab, and making sure I never took my science too seriously. In lab I also had the privilege of working with three incredible undergrads, who have taught me much about science, mentoring, and optimism. Thank you Amber Hauw, Megan Tjuanta, and Nadine Rosete for suffering through my PCR explanations and minutiae enthusiasm.

I would never have made it through this PhD with my sanity intact without my incredible friends. We survived grad school and a pandemic together, and it's still unclear which was more challenging to our mental health. I did more than I ever thought possible

in the great outdoors with my triathlon friends: Rory (“This is the situation”), Ella (no one else I’d rather suffer with on the JMT), Monica (thanks for trusting me for your first backpacking trip), Emily, Paul, Beril, Zack, Michael, Sean, Barry, Amy, and Liana. I lucked out with the best MSTP cohort possible, who accepted my crazy early-to-bed lifestyle and liked me anyway: JakeAlbertEvan (only complained a little about 18 miles in Italy), Andrea, Meghana, Kat, Maribel, Isabel, Juliet, Greg, Ben, Jason, and Lawrence. Bryn and Chris are in a league of their own for feeding me when I wandered into their apartment at random times; I’m still waiting for that spiral staircase.

I would never have made it to the starting line in graduate school without the support of my family. Thank you to my mother Linda, who has always let me be myself and pursue my dreams. She did better than tell me a woman can do anything; she lived it. Thank you to Linda’s partner Stan, who has brought so much laughter into my mother’s life. Thank you to my brothers Carl, who helped me through high school calculus, and Dan, who showed me how to blaze my own path in life.

Chapter 1, in part, has been published in the journal *Gut Microbes*. Coker JK, Moyne O, Rodionov DA, Zengler K. Carbohydrates great and small, from dietary fiber to sialic acids: How glycans influence the gut microbiome and affect human health. Gut Microbes. 2021 Jan-Dec;13(1):1-18. The dissertation author is the primary investigator and author of this material.

Chapter 2, in full, has been submitted as a manuscript for publication in the journal *mSystems*. Coker J, Zhalnina K, Martoz C, Thiruppathy D, Tjuanta M, D’Elia G, Hailu R, Mahosky T, Rowan M, Northen TR, Zengler K. A reproducible and tunable synthetic soil

microbial community provides new insights into microbial ecology. *mSystems. Under revision.* The dissertation author is the primary investigator and author of this material.

Chapter 3, in full, is being prepared as a manuscript for submission for publication of the material. Coker J, Thriuppathy D, Flores-Ramos S, Marotz C, Tjuanta M, Zengler K. A model synthetic skin microbial community allows investigation of cosmetics chemicals and the skin microbiome. *In preparation.* The dissertation author is the primary investigator and author of this material.

Chapter 4, in full, is being prepared as a manuscript for submission for publication of the material. Coker J, Secrest P, Rees S, Quinnell D, Glonek N, Rosete N, Zaramela L, Chang G, Gordts PLSM, Zengler K. Removal of the endothelial non-human sialic acid Neu5Gc reduces atherosclerosis. *In preparation.* The dissertation author is the primary investigator and author of this material.

This research would not have been possible without funding from these sources: National Health Institute of Heart, Lung, and Blood grant number 1F30HL152666 - 01; U.S. Department of Energy, Office of Science, Office of Biological & Environmental Research Awards DE-AC02-05CH11231, DE-SC0021234, and DE-SC0022137.

VITA

2014 Bachelor of Science, Human Biology, University of California San Diego
2022 Doctor of Philosophy, Biomedical Sciences, University of California San Diego

Publications

Coker JK, Moyne O, Rodionov DA, Zengler K. Carbohydrates great and small, from dietary fiber to sialic acids: How glycans influence the gut microbiome and affect human health. Gut Microbes. 2021 Jan-Dec;13(1):1-18.

Bali P*, Coker J*, Lozano-Pope I, Zengler K, Obonyo M. Microbiome signatures in a fast- and slow-progressing gastric cancer murine model and their contribution to gastric carcinogenesis. Microorganisms. 2021 Jan 17;9(1):189.
* These authors contributed equally to the work.

Marotz C, Morton JT, Navarro P, Coker J, Belda-Ferre P, Knight R, Zengler K. Quantifying live microbial load in human saliva samples over time reveals stable composition and dynamic load. mSystems. 2021 Feb 16;6(1):e01182-20.

Sandoval DR, Clausen TM, Nora C, Cribbs AP, Denardo A, Clark AE, Garretson AF, Coker JKC, Narayanan A, Majowicz SA, Philpott M, Johansson C, Dunford JE, Spliid CB, Golden GJ, Payne NC, Tye MA, Nowell CJ, Griffis ER, Piermatteo A, Grunddal KV, Alle T, Magida JA, Hauser BM, Feldman J, Caradonna TM, Pu Y, Yin X, McVicar RN, Kwong EM, Weiss RJ, Downes M, Tsimikas S, Smidt AG, Ballatore C, Zengler K, Evans RM, Chanda SK, Croker BA, Leibel SL, Jose J, Mazitschek R, Oppermann U, Esko JD, Carlin AF, Gordts PLSM. The prolyl-tRNA synthetase inhibitor halofuginone inhibits SARS-CoV-2 infection. bioRxiv. 2021 Mar 26:2021.03.22.436522.

Kawanishi K, Coker JK, Grunddal KV, Dhar C, Hsiao J, Zengler K, Varki N, Varki A, Gordts PLSM. Dietary Neu5Ac intervention protects against atherosclerosis-associated with human-like Neu5Gc loss. ATVB. 2021 Nov;41(11):2370-2739.

Coker J, Zaramela LS, Zengler K. Linking anaerobic gut bacteria and cardiovascular disease. Nat Microbiol. 2022 Jan;7(1):14-15.

Fields of Study

2010 – 2014 Major Field: Microbiology
Professor Joseph Pogliano

2014 – 2015 Major Field: Cancer cell reproduction
Professor Andrea McClatchey

2016 – 2022 Microbiome systems biology and glycobiology
Professor Karsten Zengler

ABSTRACT OF THE DISSERTATION

Exploring the Metaorganism:

Utilizing the microbiome to improve human health

by

Joanna Katherine Claire Coker

Doctor of Philosophy in Biomedical Sciences

University of California San Diego, 2022

Professor Karsten Zengler, Chair

Professor Victor Nizet, Co-chair

The essential role of microbiota in macroscopic organisms has led to a coining of the term “metaorganism”, which encompasses a multicellular host organism and the various microbial communities found within it. Humans depend on the many microbial communities found within and around them to survive. However, reproducible and mechanistic studies of these communities have remained frustratingly elusive in many instances due to the challenges of replicating *in vivo* community behavior in an *in vitro*

laboratory setting. This dissertation seeks to address this problem and demonstrate the benefits for human health that can be obtained through microbiome studies. The first chapters present the development of reproducible synthetic soil and skin microbial communities, to be used for *in vitro* study of community dynamics and targeted interventions on microbiome composition. Studies with these tools show that final community diversity and composition can be modulated by minor adjustments in starting inoculum, with certain organisms driving the final state of the community. This knowledge of community dynamics can be used, for example, to support design of soil microbial communities to increase agricultural plant growth in a sustainable fashion. Additionally, growth of the skin community with cosmetics compounds probes the effect on these compounds on skin microbiota, which has implications for development of skin pathologies. Finally, a later chapter presents the use of a sialidase isolated from the gut microbiome to reduce cardiovascular disease development in a humanized mouse model by removing the sialic acid *N*-glycolylneuraminic acid from the endothelium. This study takes a novel enzyme and applies it in a new way, seeking to use microbiome studies to benefit the host organism on multiple levels. Together this body of work bridges the *in vitro* and *in vivo* aspects of microbiome research to implement novel strategies for partnering with the microbiome to support and advance human health.

Chapter 1: The Microbiome and Human Health

1.1 Introduction

Communities help define function at every level of the tree of life, even—and perhaps especially—the microbial one. The influence of communities stretches beyond the individual levels of life, linking macroscopic host organisms and the individualized communities of microscopic organisms they need to survive. Such interdependence has led to the coining of the term “metaorganism”, to refer to multicellular hosts and the microbial species that live within and around them[1,2]. Humans depend on microbial communities as much as any other species, both within the body and without, which has led to an explosion of research on microbial communities and the microbiome in recent decades. With up to a hundred times more bacterial genes than human genes in the human body, the microbial communities in our body are crucial to human life and play a key role in human development and homeostasis[3]. The following chapter discusses some of the most relevant microbiomes for human health, as well as difficulties in researching and conducting experiments with these communities.

1.2 The human gut microbiome

The human gut microbiome is defined as the sum of genomic DNA of all microbes inhabiting this environment. As in every natural ecosystem, bacteria in the human gut influence the surrounding environment of their host. The human gut microbiota is involved in many essential host functions, such as the processing of nutrients to bioactive molecules like neurotransmitters, vitamins, and fatty acids and protection from pathogens.[4] One of the most well-known examples of this is the breakdown of non-digestible carbohydrates found in plants. As humans do not have the metabolic capability to degrade these complex glycans in the gastrointestinal tract, they reach the colon to be

fermented by gut bacteria and lead to the production of short-chain fatty acids (SCFAs), which participate in the acidification of the digestive tract.[5] Through these and other similar processes, the human gut microbiota has a major impact on the host's physiology in health and disease.

In addition to a greater number of genes and metabolic capabilities than the human genome, the composition of the gut microbiome is also highly malleable.[3] Diet surpasses the role of host genetics in shaping the gut microbiome through modification of the nutritional environment of the bacteria populating the gut.[6–10] Given the influence of the gut microbiome in human health, the ability to alter this microbiome through dietary changes indicates that promoting a healthy microbiome has great potential to improve human well-being and disease prevention and control. Glycans (i.e. carbohydrates) are of major importance in determining the gut microbiome composition.[11] Glycans come in many forms, from long polysaccharide chains that humans are unable to digest (e.g. cellulose, pectins, resistant starch), to oligosaccharide chains attached to proteins and lipids, to individual mono- and disaccharides, such as glucose, lactose, or sialic acids.[11] In this review, we detail how dietary glycans can shape the structure and function of the human gut microbiota and the impact this has on human diseases. We start with an overview of the broad impacts of carbohydrates on gut microbiota composition and metabolic activity. We then focus on the role of sialic acids, a specific monosaccharide class, in shaping the gut microbiome. Sialic acids are a prominent component of the mammalian glycosylation system, and their interactions with the human immune system make their impact on the gut microbiome of particular interest. This review of sialic acids,

the gut microbiome, and impacts on health will summarize recent research and suggest directions for future studies.

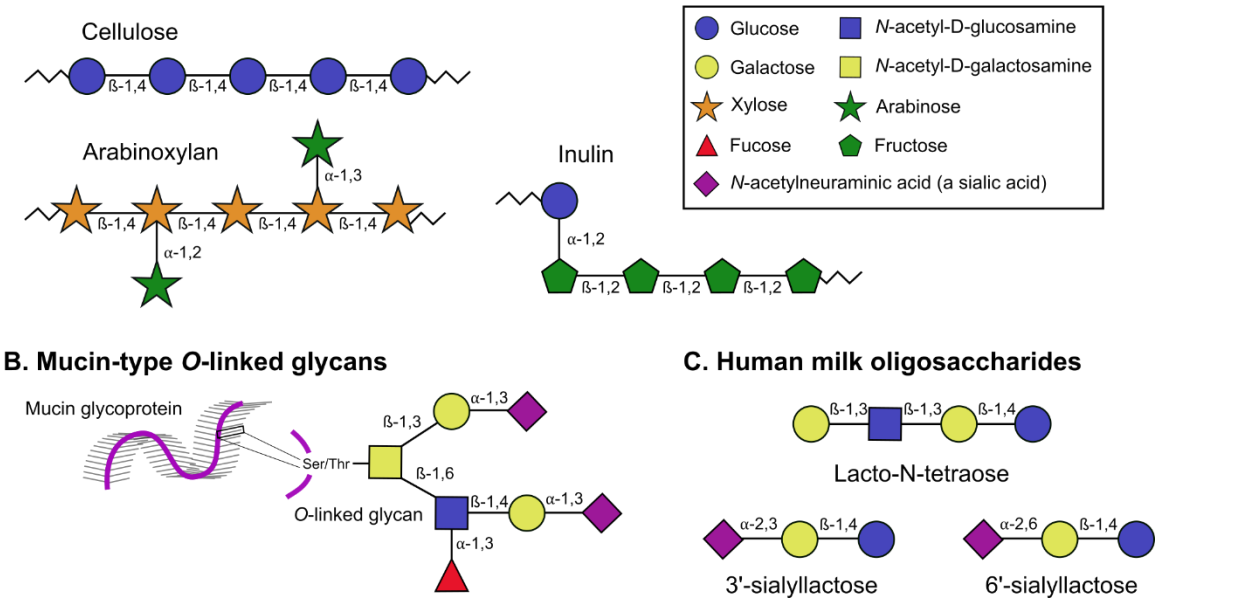

Figure 1.1 Structural composition of common poly- and oligosaccharides. Monosaccharide symbols are represented as in the Symbol Nomenclature for Glycans (assignments for this figure provided in the box).[12,13] The numbers between monosaccharides represent the glycosidic linkage. A) Fiber is a general classification encompassing many types of dietary polysaccharides. Examples of the polysaccharides cellulose, arabinoxylan, and inulin are provided here. B) Mucin-type *O*-linked glycans are host glycans linked to serine or threonine (Ser/Thr) residues on mucin proteins. Like most mammal-derived glycans, they are often tipped with sialic acids such as *N*-acetylneuraminic acid. An example structure is shown; many other monosaccharide and linkage compositions are possible. C) Human milk oligosaccharides (HMOs) are short oligosaccharides found in human breast milk. HMOs are composed of a lactose base (a disaccharide of glucose and galactose) with additional monosaccharides such as *N*-acetyl-D-glucosamine, the sialic acid *N*-acetylneuraminic acid, or fucose attached. Three example structures are shown.

1.2.1 Broad impact of carbohydrates on gut microbiome structure and function

Human studies have repeatedly demonstrated that dietary changes modify the relative abundance of major gut bacterial groups in a rapid and reversible manner.[14,15] For example, low-carbohydrate, weight-loss, and animal-based diets reduce the proportion of the butyrate-producing phyla *Firmicutes* and *Actinobacteria*,[15–17] while high animal product consumption increases the proportion of *Bacteroidetes* and specific *Proteobacteria* like *Bilophila wadsworthia* in the human gut.[15] Lifestyle urbanization and Westernization are key factors influencing dietary behavior, with subsequent impacts on the gut microbiome and potential harmful effects on human health.[18] A rural diet, typically rich in host-indigestible carbohydrates like fiber, is associated with a higher abundance of *Prevotella* and *Xylanibacter spp*., while an urbanized diet, which generally contains more saturated fat and protein from animals, is associated with an increase of *Bacteroides spp*. and a decrease of overall microbiome gene diversity.[19–21] Interestingly, those *Bacteroides*-dominated, less diverse gut communities are associated with a higher incidence of obesity and metabolic syndrome.[22] The loss of diversity and shift from a *Prevotella*- to *Bacteroides*-dominated microbiome has been observed in non-Western immigrants as early as nine months after moving to the USA.[23] These data demonstrate the plasticity of the human gut microbiota in response to dietary carbohydrate changes and the potential impact of these changes on human health.

Many studies examine the impact of plant carbohydrates in particular on the gut microbiome. Diets with high resistant starch intake have been associated with increased relative abundance of *Firmicutes* and particularly *Ruminococcaceae* family members, while resistant potato starch specifically has been associated with increased

Bifidobacterium genera and wheat bran has been associated with increased *Lachnospiraceae* family members.[14,16,24] A recent study also demonstrated rapid modifications of the gut microbiota in mice fed raw versus cooked plant products, due to the improvement of starch digestibility and degradation of plant-derived compounds during the cooking process. Similar observations have been made in the human population, showing that everyday nutritional habits can influence the gut microbiota.[10]

Within plant carbohydrates, dietary fiber is one of the most heavily studied groups. Dietary fiber is generally defined as edible carbohydrate polymers, mostly from plants and edible fungi, that are not digestible by human enzymes.[25] Examples include inulin, dextrin, pectin, cellulose, resistant starch, arabinoxylans, and chitin (Figure 1.1A).[26] Dietary fiber exists in soluble and insoluble forms, although some polymers can be soluble or insoluble depending on conditions like cooking or food processing.[25] Although human metabolism cannot digest fiber, the gut microbiome often contains many enzymes capable of degrading these polymers and utilizing the sugars released for nutrition or other metabolic processes.

Fiber passes mostly undigested through the small intestine and is fermented in the colon by gut bacteria, leading to the production of SCFAs (Figure 1.2).[27] The SCFAs acetate, propionate, and butyrate are the main metabolites produced during microbial fiber fermentation, and they have multiple beneficial effects on the host.[18] Once produced in the colon, SCFAs are rapidly absorbed by host epithelial cells, where the great majority are directly used as an energy source. SCFAs that are not metabolized by the gut epithelium (estimated as <10% of total SCFAs produced)[28,29] are then transported through the portal circulation to the liver, where they can be incorporated by

hepatocytes and used as energy substrates or for the synthesis of glucose, cholesterol, and fatty acids.[30]

A small fraction of the initial SCFAs will reach the main blood circulation and have systemic effects, particularly on the immune system.[30] Notably, SCFAs downregulate the production of pro-inflammatory cytokines by colonic macrophages[31] and promote the differentiation of naive CD4+ T cells into immunosuppressive regulatory T cells (Treg),[32,33] by binding to G-protein coupled receptors[34] or by inhibiting histone deacetylases.[31,35,36] SCFAs derived by the gut microbiota from dietary fiber thus participate in the homeostasis of the immune response, with a demonstrated protective effect against inflammatory diseases, such as multiple sclerosis (MS),[35] inflammatory bowel disease (IBD),[33] and allergic asthma,[37] as well as other pathologies, such as infection[38,39] and carcinogenesis.[20] Colorectal cancer (CRC) is also known to be linked with a gut microbiota dysbiosis characterized by decreased microbial diversity[40] and an under-representation of SCFA-producing bacteria.[41] A high-fiber dietary intake is associated with a lower risk of CRC,[42] while patients with CRC precursor lesions tend to have lower fiber dietary intake than controls.[43]

However, not all studies have shown universal benefits from fiber intake. In a recent study, Singh et al. supplemented the diet of toll-like receptor 5 (TLR5)-deficient mice with fermentable fibers for six months, with the goal of demonstrating the beneficial effect of such a diet on metabolic syndrome. While the authors observed some of the expected effects (reduction of adiposity, amelioration of glycemic control), they also observed that purified fiber supplementation induced icteric hepatocellular carcinoma in 40% of the TLR5-deficient mice.[44] These studies indicate that dietary supplementation

with such purified compounds may have a negative effect on some individuals, and that large-scale enrichment of processed food with purified prebiotic fiber should be taken with great caution.[45] For a more detailed discussion of the gut microbiota and specific health effects of dietary fiber, we refer the reader to ref. 42.[46]

Mono- and disaccharide dietary sugars can affect gut microbiome composition, with potential effects on human health. Fructose and glucose have been demonstrated to specifically inhibit gut colonization by *Bacteroides thetaiotaomicron*, a mammal gut symbiont associated with lean and healthy individuals, by silencing the Roc (regulator of colonization) protein, which promotes competitive colonization in gnotobiotic mice.[47] High fructose intake has also been associated with development of non-alcoholic fatty liver disease (NAFLD) in humans[48] and mouse models.[49,50] The gut microbiome in general plays a causal role in NAFLD development in mouse models,[51] and several studies have established correlations between NAFLD and altered abundance of taxa, such as *Bifidobacterium*,[52] *Lactobacillus*,[52,53] *Bacteroides*, and *Ruminococcus*.[54] Supplementation of *Lactobacillus rhamnosus* in the gut microbiome of mice fed a high-fructose diet to induce NAFLD resulted in decreased liver inflammation and NAFLD disease development.[53] This finding highlights the potential regulatory effects of dietary sugars in the small intestine on gut colonization by beneficial microbes. Later in this review we will discuss in detail recent research on the effects of sialic acids, a biologically important class of monosaccharides, on the gut microbiome and host health.

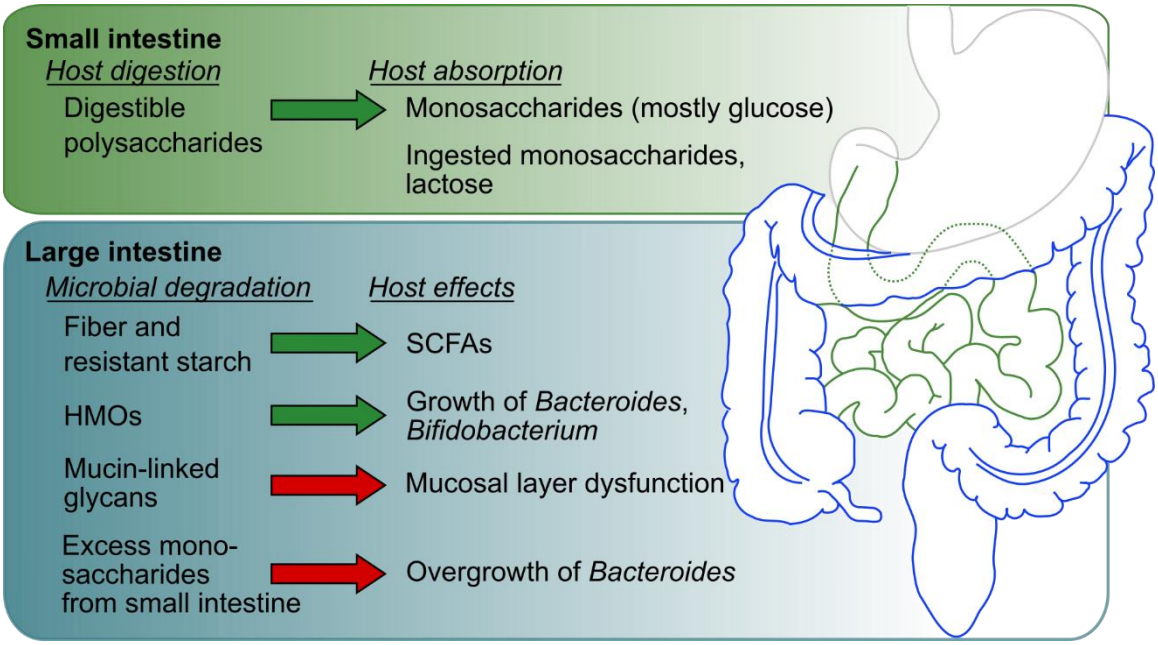

Figure 1.2 Broad overview of carbohydrate digestion and host effects. Other effects are also possible for each glycan. Generally beneficial and detrimental effects are represented by green and red arrows, respectively. Most host digestion and nutrient absorption occurs in the small intestine. Microbes conduct most of the nutrient degradation that occurs in the large intestine, with varying effects on host health and function.

1.2.2 Interplay of dietary fiber and host mucins in the gut microbiome

Although dietary glycans make up the majority of nutrients the gut microbiota consumes, restriction of carbohydrates like fiber from the diet can push microbes to consume glycans produced by the host instead.[55] The colon contains a mucus gel layer composed of two parts: a loose luminal outer layer and a dense mucosal inner layer.[56] The mucosal layer is composed mainly of host mucin proteins with regions of extensive *O*-glycosylation (forming up to 80% of the total mucin mass) (Figure 1.1B).[57] Although microbes do not penetrate the dense inner layer in healthy subjects,[39,58] microbial degradation of the outer layer is thought to be a normal part of mucin turnover and regeneration.[59] For a review of how gut microbiota interact with and degrade the colonic mucosal layer, we direct the reader to ref. 56.[60] Here we focus on how diet can alter the careful balance between gut microbiota and the host mucosal layer.

The section above discussed how the presence of complex polysaccharides, such as fiber, in the diet strongly affects the gut microbiome composition. Many studies have shown that fiber ingestion increases abundance of colonic bacteria capable of fermenting fiber to SCFAs[9,14,17,24], with increased diversity of plant carbohydrates believed to support greater community diversity.[61] Conversely, several studies have shown that a lack of dietary fiber can push bacterial metabolism away from fiber degradation to mucin degradation. Some organisms (e.g. *Bacteroides thetaiotaomicron*) degrade both fiber and mucins and shift their metabolism to mucin degradation when dietary complex polysaccharides are scarce.[55,62] Other organisms (e.g. *Akkermansia muciniphila*) are able to degrade mucins but not fiber and experience expansion of their populations upon complex polysaccharide scarcity.[39,63,64]

Excessive mucin degradation is associated with increased intestinal inflammation[65,66] and increased penetration of bacteria into the dense mucosal mucus layer.[67] In gnotobiotic mice mono-colonized with *B. thetaiotaomicron*, a diet lacking complex polysaccharides (including fiber) resulted in a thinner colonic mucus layer, an increased proximity of colonic microbes to the gut epithelium, and increased expression of the inflammatory marker REG3β.[62] Similarly, it has been shown that dietary fiber deprivation increased the abundance of mucus-degrading bacteria like *A. muciniphila* and *Bacteroides caccae* in mice, subsequently leading to an alteration of the intestinal barrier and higher susceptibility to mucosal pathogens.[39,62] Demonstrating the specific and essential role of the gut microbiome in mucus changes, antibiotic-treated mice fed a low-fiber Western diet but transplanted weekly with gut microbiota from mice fed a high-fiber chow diet had significantly lower mucus penetrability and higher mucus growth than mice transplanted with gut microbiota from Western diet-fed mice.[68] These studies indicate a lack of dietary fiber leads to changes in the gut microbiome that promote dysfunction and increased microbial penetrability of the inner colonic mucus layer.

On the other hand, a recent study suggests potentially beneficial roles of microbial mucus metabolism in ulcerative colitis (UC). Certain organisms are capable of producing the SCFA *n*-butyrate from mucin degradation,[69] and *n*-butyrate as well as mixed SCFAs have been shown to reduce colon inflammation in UC[70,71]. Yamada et al.[69] found decreased mucinase activity and decreased levels of *n*-butyrate in the stool of UC patients, but a significantly higher *O*-glycan-to-mucin protein ratio. Hypothesizing a deficiency in mucin *O*-glycan utilization by gut microbiota, the authors assessed the impact of feeding mice a mucin-enriched diet. After three weeks, they observed an

increased α-diversity; increased relative abundance of *Akkermansia, Allobaculum,* and *Bacteroidales S24-7*; increased cecal SCFAs; and increased colonic Treg and IgA^+ plasma cells.[69] In the setting of UC, mucin degradation may therefore be an important physiologic process to promote.

1.2.3 Impact of the monosaccharide sialic acid on gut microbiome structure and function

Thus far, we have discussed the impact of broad dietary glycan classes on the gut microbiome and host health, including how lack of fiber promotes microbial degradation of host mucus glycans. Next, we focus on the impact of dietary sialic acids, a unique and essential class of monosaccharides, on the gut microbiome and human health. Sialic acids are essential to many physiological processes, play a large role in shaping both the infant and adult microbiome, and allow exploration of how minor chemical modifications in sugar structure can shape the microbiome. Although many authors have reviewed sialic acids in the past, to our knowledge a comprehensive review focusing specifically on dietary sialic acids and the gut microbiome has not been published. In the literature, “sialic acids” is often used to refer to both the group and its most common member, N-acetylneuraminic acid. In this review we will refer to N-acetylneuraminic acid by its abbreviation Neu5Ac and reserve the term sialic acids for the group as a whole.

Sialic acids are acidic 9-carbon monosaccharides, derivatives of neuraminic acid, and ubiquitous in all vertebrate glycosylation systems. Sialic acids often serve as the terminal sugars in *N*-linked and *O*-linked vertebrate glycans that decorate cell-surface proteins and lipids, and as such they are often some of the first monosaccharides encountered in cell-cell interactions.[72,73] They play essential roles in immune system

signaling, cell adhesion, membrane transport, and many other processes.[73–75] The most abundant mammalian sialic acids are Neu5Ac and its close chemical cousin *N*-glycolylneuraminic (Neu5Gc) acid (Figure 1.3A).[73] Humans cannot produce Neu5Gc due to loss of the CMP-*N*-acetylneuraminic acid hydroxylase (CMAH) enzyme,[76–78] and as such Neu5Gc is perceived as a foreign antigenic sugar by the human immune system.[79,80] Sialic acids are present in our diet in *N*- and *O*-linked glycans from animal-derived proteins, and Neu5Gc can be incorporated into human glycoconjugates following ingestion of certain animal-derived foods rich in Neu5Gc, chiefly red meat.[81,82] Neu5Ac and Neu5Gc have drastically different effects on human health, with Neu5Ac a natural and beneficial component of human glycans and Neu5Gc an antigenic and pro-inflammatory component.[83–87]

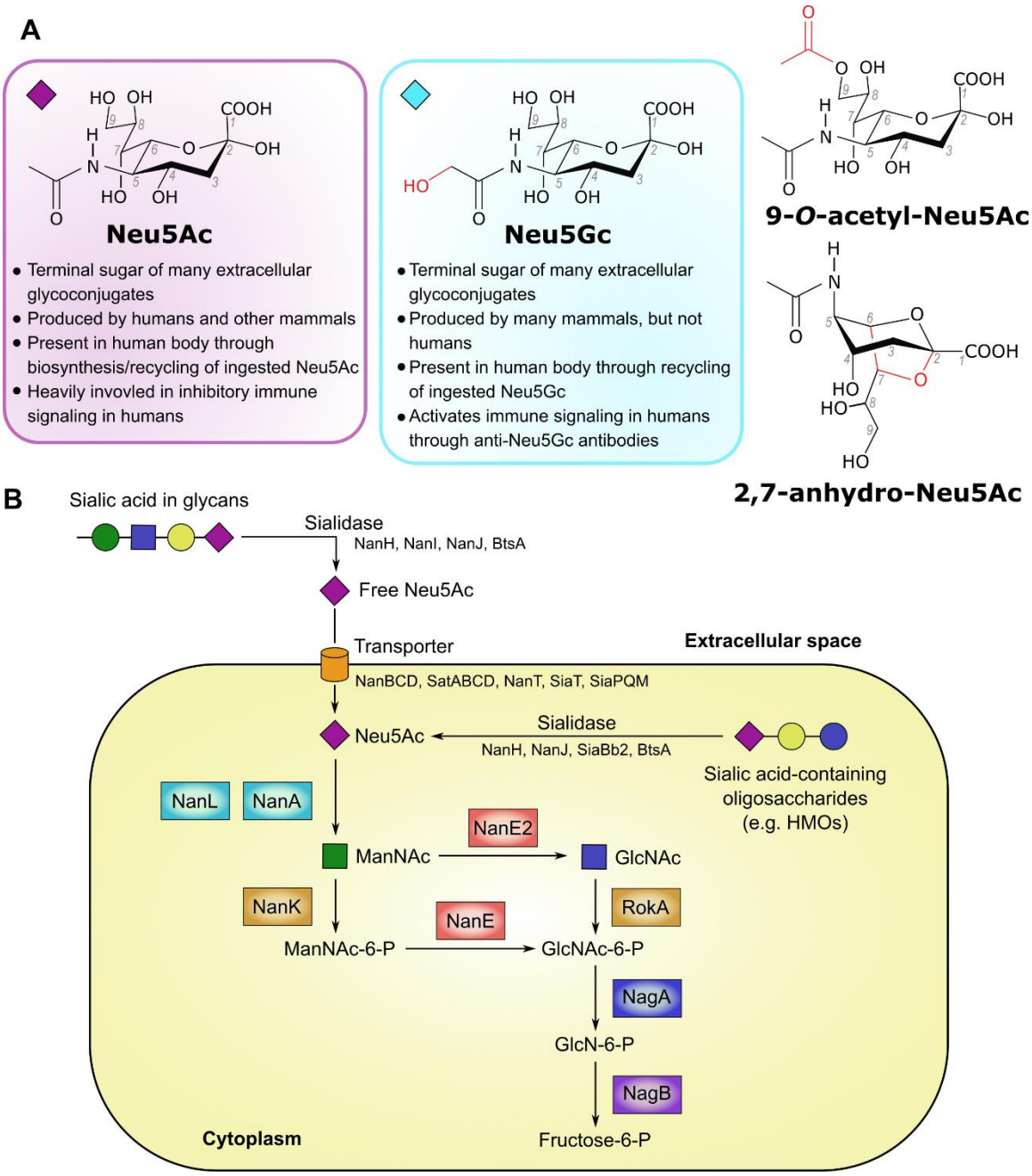

Figure 1.3 Sialic acids overview and metabolism. A) Structures of the sialic acids discussed in this review. Changes from the Neu5Ac structure are shown in red. Differences between Neu5Ac and Neu5Gc with regards to human physiology are listed below those structures. Diamonds by Neu5Ac and Neu5Gc structures depict the Symbol Nomenclature for Glycans symbol for each. B) Schematic of general Neu5Ac metabolism in bacterial cells. Steps with multiple characterized enzymes (sialidase and transporter) have protein names listed below the general enzyme name. Steps with one well-characterized enzyme have the enzyme name next to the arrow. The exception is the conversion of Neu5Ac to ManNAc, which has 2 well-characterized enzymes. Enzymes are color-coded based on function. References for enzyme functions: NanAEE2KL, RokA, NagAB;[88] NanHIJ;[89] NanBCD;[90] NanT;[91] SiaBb2;[92] BtsA;[93] SatABCD;[94] SiaT;[95] SiaPQM.[96]

1.2.4 Sialic acid metabolism by gut bacteria

Human-associated bacteria, including gut microbiota, use sialic acids primarily as either a nutrient source or as a signaling molecule to interact with their host.[97] For example, given the role of Neu5Ac on host cells in inhibiting autoimmune signaling through Siglec proteins,[98] some pathogens evade the immune system by prominently displaying Neu5Ac on their cell surfaces.[99,100] For an extensive review of sialic acids catabolism by human pathogens all over the body, we refer to ref. 87.[100] Bacteria can synthesize sialic acids *de novo* or scavenge from the surrounding environment.[74,97] Complete metabolism of sialic acids requires a sialidase to release the monosaccharide from the glycan, a transporter protein to transport the monosaccharide inside the cell, and a suite of intracellular enzymes to convert sialic acids into a sugar fed into different metabolic pathways (Figure 1.3B).[74] Many common gut microbes contain genes for part of or for this entire pathway, affecting their role in the gut microbial community, and through that the community's potential effects on human health.

The first full Neu5Ac metabolism pathway was described in *Escherichia coli* in 1999[101] and the ability of *E. coli* to metabolize Neu5Ac has since been shown to be important for gut colonization in mice.[102] The *Nan* gene cluster in *E. coli* encodes the sialic acids uptake transporter NanT and three catabolic enzymes (NanA lyase, NanK kinase, and NanE epimerase) that catalyze the conversion of Neu5Ac to pyruvate and *N*-acetylglucosamine-6-phosphate. This is further metabolized through the *N*-acetylglucosamine (GlcNAc) catabolic pathway (Figure 1.3B). Neu5Gc is transported and catabolized by *E. coli* using the same NanT transporter and NanA lyase but producing glycolate instead of pyruvate.[103] Similar Neu5Ac catabolic gene clusters with variations

in the identity of sialic acid transporter were identified in 46 out of 1,902 bacterial genomes examined in a 2009 study.[104] However, 91% of these 46 organisms were able to colonize humans, indicating the ability to metabolize sialic acids is particularly valuable for bacteria in human-associated niches. Nine of these organisms were gut commensals (*Anaerotruncus colihominis, Dorea formicigenerans, D. longicatena, Faecalibacterium prausnitzii, Fusobacterium nucleatum, Ruminococcus gnavus, Lactobacillus sakei, L. plantarum,* and *L. salivarius*), while several others were known gut pathogens (*E. coli, Shigella* (species unspecified)*, Salmonella enterica, Yersinia enterocolitica, Vibrio vulnificus,* and *V. cholerae*).[104] A similar analysis in 2015, of 4,497 genomes in NCBI at the time, found that 5.9% of species contained genes for the full pathway of Neu5Ac metabolism; again, these organisms primarily colonize humans or animals.[100] An alternative Neu5Ac utilization pathway was identified in the gut commensal *Bacteroides fragilis* (Figure 1.3B) and involves a putative sialic acid transporter from the MFS superfamily (NanT), a non-orthologous Neu5Ac lyase (NanL), and two novel catabolic enzymes, epimerase NanE3 and kinase RokA.[88] The *nanLE2T* gene cluster from *B. fragilis* was further identified in many colonic bacteria from the *Bacteroidetes* phylum, including *B. vulgatus* and *Parabacteroides distasonis*, but not in *B. thetaiotaomicron,* which encodes a sialidase but lacks the *nanLE2T* genes to fully metabolize sialic acids.[105] Other microbes like *Clostridioides difficile* or *E. coli* lack a sialidase but encode a complete pathway to metabolize sialic acids.[106]

We analyzed the distribution of sialic acids utilization pathway and sialidase genes across a reference set of 2,662 genomes representing ~700 species and ~200 genera of bacteria from the human gut.[107] For genomic identification of genes encoding

sialidases, Neu5Ac transporters, and catabolic enzymes (Figure 1.3B), we used a subsystems-based approach implemented in the SEED platform.[108] Each reference genome was assigned binary phenotypes reflecting the presence/absence of: (i) a complete Neu5Ac utilization pathway; and (ii) sialidase enzyme(s) (Figure 1.4). Approximately 1,040 strains were predicted as Neu5Ac-utilizing strains, representing ~80 bacterial genera. Among these, a sialidase was identified in 40% of the strains, including prominent colonic bacteria from the *Akkermansia*, *Bacteroides*, *Bifidobacterium*, *Clostridium*, *Flavonifractor*, *Parabacteroides*, and *Prevotella* genera. Another subgroup of strains that lack a sialidase but are capable of sialic acid utilization includes both human gut symbionts such as *Anaerococcus*, *Blautia*, *Escherichia*, *Eubacterium*, *Faecalibacterium*, *Fusobacterium*, and also a number opportunistic pathogens including *Clostridioides*, *Staphylococcus*, and *Streptococcus spp*. Finally, ~100 strains from 27 microbial genera possess a sialidase but apparently lack the sialic acid utilization capability. These include 18 *Bacteroides* strains (e.g. *B. faecis, B. intestinalis, B. thetaiotaomicron*), 6 *Porphyromonas* strains, and 6 *Coprobacillus* strains. The high prevalence of many of these strains in the gut microbiome suggests even strains that solely release Neu5Ac from underlying glycans contribute to the overall sialic acid degradation capability of gut communities.

These mixed catabolic capabilities fit with studies showing ingested complex polysaccharides can be digested and metabolized by different gut organisms, in a syntrophic or synergistic interaction network.[109] In support of this, recent studies of *Salmonella enterica* and *C. difficile* showed that these organisms expand following antibiotic treatment through scavenging of sialic acids liberated from ingested food by

other gut microbes such as *B. thetaiotaomicron*.[110] Colonization with *B. thetaiotaomicron* lacking a sialidase inhibited *C. difficile* expansion in the mouse gut, while feeding with exogenous Neu5Ac reversed these effects.[110] Similarly, Huang et al.[111] showed that increased sialidase activity from *B. vulgatus* drives *E. coli* expansion in a mouse model of colitis. Hence sialic acids released in the gut by one organism can be scavenged and metabolized by other organisms lacking a sialidase, causing effects that ripple through the metabolic network.

Although most research has been done on Neu5Ac, microbes can also act on modifications of Neu5Ac or on other sialic acids (Figure 1.3A). Neu5Ac modified with an *O*-acetyl group is generally resistant to release by sialidases. However, recent studies of *B. fragilis* show the *O*-acetylesterase EstA removes 9-*O*-acetyl esterifications, allowing sialidases to release these modified Neu5Ac molecules and promote *in vitro* growth of *E. coli*.[112] Although not confirmed *in vivo* yet, this could provide another example of bacterial interactions to share metabolic capabilities. Previous studies of the commensal anaerobe *Ruminococcus gnavus* showed it cannot grow on unmodified Neu5Ac alone and instead uses an intramolecular *trans*-sialidase to release 2,7-anhydro-Neu5Ac from α2-3-linked sialic acids.[113] 2,7-anhydro-Neu5Ac is then selectively transported across the *Ruminococcus* cell membrane and converted back to Neu5Ac for further metabolism.[114] This strategy, which prevents other organisms from utilizing the uncommon 2,7-anhydro-Neu5Ac, seems designed to conserve resources for *R. gnavus* as opposed to the cross-talk seen in other sialic acid processing pathways. While the major part of sialidase research focuses on Neu5Ac, some recent studies have examined the activity of gut microbe sialidases on Neu5Gc. Zaramela et al.[115] reported the

discovery of Neu5Gc-preferential sialidases from the gut microbiome of the Hadza hunter-gatherer group,[6] with four out of the five selected *Bacteroides* sialidases displaying preferential release of Neu5Gc over Neu5Ac in at least one of the tested conditions. Further exploration of metabolism of these and other sialic acid modifications will undoubtedly reveal more novel microbial strategies to harvest sialic acids.

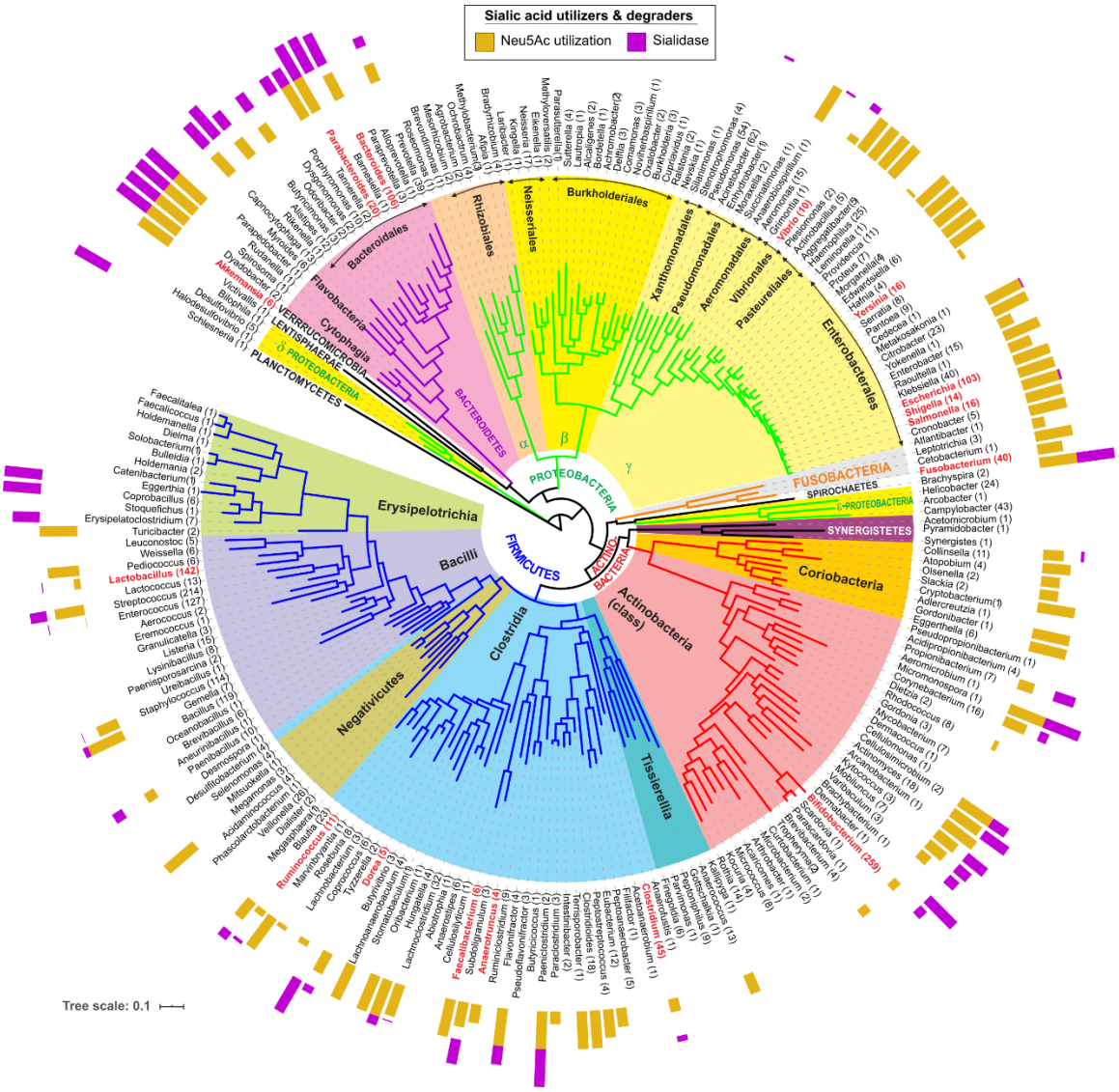

Figure 1.4 Genomic distribution of Neu5Ac utilizers and degraders in human gut microbiome strains. The phylogenetic tree was constructed using concatenated sequences of universal ribosomal proteins from approximately 2,600 human gut microbial genomes from the PATRIC genomic database[116] by RAxML version 8,[117] then shrunk to genus representatives and visualized via iTOL.[118] Numbers next to genera in the outermost level of the tree indicate the number of analyzed genomes per genus. Bars adjacent to each genus indicate the proportion of genomes that contain genes for: a Neu5Ac transporter and full Neu5Ac catabolism pathway (gold bars); and one or more Neu5Ac sialidase genes (purple bars). Genera mentioned in this review are shown in red text.

1.2.5. Sialylated HMOs and the infant gut microbiome

The infant gut microbiome is thought to start developing in utero through fetal ingestion of amniotic fluid.[119] Peri- and post-natally, the microbiota composition is heavily influenced by mode of fetal delivery (vaginal versus Cesarean section) and infant food source (breast milk versus formula).[119,120] Human milk oligosaccharides (HMOs) represent a potent source of sialic acids (and other monosaccharides) that is unique to the infant diet (Figure 1.1C). HMOs are a group of over 200 oligosaccharide structures present in human breast milk, making up the third most abundant component of milk at 5-15 g/L (following lactose at 70 g/L and lipids at 40 g/L).[121] The composition and overall amount of HMOs in breast milk varies by woman and by time since delivery.[122] The majority of HMOs are not absorbed by the infant in the small intestine for nutrition, but instead persist into the colon where they have a significant impact on infant health (Figure 1.2).[123] For example, HMOs have been shown to directly inhibit infant gut colonization by pathogens like enterotoxic *E. coli*, *V. cholerae* toxin, *Campylobacter jejuni*, rotaviruses, and noroviruses.[124–126]

HMOs in general, and sialylated HMOs (HMOs containing sialic acid) in particular, also promote growth of particular beneficial microorganisms in the infant gut. Of the taxa studied from the infant gut microbiome, only the *Bifidobacterium* and *Bacteroides* genera have been shown to metabolize a broad range of HMOs.[127,128] The gut microbiome of breast-fed infants is typically dominated by *Bifidobacterium*, representing up to 70% of gut microbiota in breast-fed infants compared to 31% in formula-fed infants.[129] A study of individual gut microbes in isolation showed that the sialylated HMOs 3’-sialyllactose (3’SL) and 6’-sialyllactose (6’SL) specifically promoted growth of seven *Bifidobacterium*

longum strains, as well as *B. vulgatus* and *B. thetaiotaomicron*.[128] 6'SL but not 3'SL promoted growth of *Lactobacillus delbrueckii*, although *L. rhamnosus* did not show appreciable growth on HMOs.[128] In particular, *B. longum* subsp. *infantis* is capable of fully metabolizing all HMOs studied to date and of growing on Neu5Ac alone in vitro.[130] The *B. longum* subsp. *infantis* genome contains a 43-kb gene cluster (HMO1) with 16 glycoside hydrolases and many oligosaccharide transport proteins, as well as two sialidases, *nanH1* in the HMO1 gene cluster and *nanH2*.[120,130,131] Intriguingly, *B. longum* subsp. *infantis* appears to transfer oligosaccharides into its cytoplasm and digests HMOs to monosaccharides within the cell;[120,132,133] by contrast other microorganisms (e.g. *Bacteroides* and *Bifidobacterium bifidum*) are thought to break down HMOs to di-/monosaccharides extracellularly and transport these components into the cytoplasm.[120,134]

Other *B. longum* strains contain genes for specific portions of the sialic acids catabolism pathway (Table 1.1). *B. longum* subsp. *bifido* can release monosaccharides, including Neu5Ac, from HMOs but is unable to catabolize Neu5Ac, fucose, or N-acetylglucosamine.[131] In contrast, *B. longum* subsp. *breve* can ferment these monosaccharides but may or may not be able to release them from HMOs, in a strain-dependent manner.[135,136] *Bacteroides* species also have variable sialic acids metabolic capabilities (Table 1.1). Similar to *Bifidobacterium*, *B. fragilis* can cleave and fully metabolize Neu5Ac from HMOs, while *B. thetaiotaomicron* can cleave but not metabolize Neu5Ac.[105] *Bacteroides* and most *Bifidobacterium* species metabolize HMOs through the same enzymatic pathways as host mucin glycan degradation.[105] However, despite its facility at HMO digestion, *B. longum* subsp. *infantis* does not appear

to digest host mucins.[133] These results indicate dietary Neu5Ac in HMOs is heavily involved in shaping the infant gut microbiome by promoting colonization of *Bifidobacterium* and *Bacteroides* species, potentially laying the foundation of a life-long synergy between host and gut microbes.

Table 1.1 Summary of the ability of bacteria in the infant gut microbiome to release and metabolize the sialic acid Neu5Ac from HMOs.

Genus	Species	Neu5Ac release	Neu5Ac metabolism
Bifidobacterium	*Longum* subsp. *infantis*	**+**	**+**
	longum subsp. *bifido*	**+**	**-**
	longum subsp. *breve*	**-/+**	**+**
Bacteroides	*fragilis*	**+**	**+**
	thetaiotaomicron	**+**	**-**

As in sialic acids metabolism, studies of sialic acids and the infant microbiome focus primarily on Neu5Ac. Research on the effect of Neu5Gc on the infant microbiome is virtually nonexistent. Studies in the past have not identified Neu5Gc in human breast milk, although it is readily present in bovine milk.[129,137,138] However, a recent study of human milk composition discovered that breast milk from all 16 mothers tested (split between women who consumed cow's milk and dairy-free almond beverages) contained HMOs with Neu5Gc, indicating that diet-derived monosaccharides can be incorporated into breast milk HMOs.[139] The presence of Neu5Gc in breast milk further adds another possible mechanism for the development of anti-Neu5Gc antibodies, which appears in infants within the first six months of life.[140] Anti-Neu5Gc antibodies drive a process of chronic low-level inflammation called xenosialitis, which has been shown in animal models to contribute to inflammatory pathologies, such as liver cancer,[86] atherosclerosis,[87] and other autoimmune diseases.[98] Other possible mechanisms for anti-Neu5Gc antibody development include the presence of Neu5Gc in commercial baby foods and exposure to Neu5Gc on the surface of bacteria like non-typeable *Haemophilus influenzae*.[83,140]

Isolating the impact of ingested HMOs containing Neu5Ac on the infant gut microbiome is relatively simple, arguably simpler than in adults given the stereotyped diets of infants. However, tying these changes to infant health outcomes is much more difficult. A study in 2016 provides one of the most comprehensive experimental investigations of this question. Researchers inoculated germ-free mice with a defined microbial community of 25 strains isolated from the gut microbiota of a growth-stunted Malawian infant.[141] Mice were then fed a typical Malawian diet with or without purified

sialylated bovine milk oligosaccharides. Mice receiving the oligosaccharides treatment showed significantly increased weight gain, lean mass, and long bone growth, compared to the control group (caloric intake was equivalent between the groups). These effects were not seen in germ-free mice treated with oligosaccharides, indicating the microbiome plays a critical role in the health benefits observed. Similar results were seen in gnotobiotic piglets.[141] Intriguingly, despite the gut microbiome-dependent nature of the effects, the composition of the gut community was not significantly different between oligosaccharides and control groups after treatment. However, significant transcriptional changes were observed in *B. fragilis* and *E. coli*, including upregulation of genes in the polysaccharide utilization locus of *B. fragilis*. The researchers also noted that the two *B. longum* subsp. *infantis* strains included in the community failed to colonize in the gut community in both the treatment and control groups, although strains of *B. longum* subsp. *breve, B. bifido,* and *B. catenulatum* did colonize.[141] This is surprising given the ubiquity of *B. longum* subsp. *infantis* in the gut microbiota of human infants and its superior abilities to digest and metabolize HMOs. However, recent research indicates the ability of bacterial strains to successfully colonize the infant gut is affected by many different factors.[142] Follow-up studies on the mechanism of increased long bone growth with sialylated oligosaccharide treatment indicated the effect came from decreased osteoclast generation and activity, in a microbiota-dependent manner.[143] Much work remains to be done to investigate the connections between the gut microbiome and infant health.

1.2.6. Sialic acids and the adult gut microbiome

In contrast to studies of infants and dietary sialic acids, where studies focus on microbiome composition but often do not address direct health impacts, studies of adults

and dietary sialic acids focus mainly on health impacts and rarely assess microbiome composition. The ubiquity of sialic acids in mammalian glycoconjugates gives them a role in many physiological and pathological processes, from brain development to immune regulation, infections, heart disease, and diabetes.[73] Many of these pathological processes have been associated with hypo-sialylation, or low Neu5Ac levels, of relevant molecules. Several studies have therefore looked at the effect of exogenous Neu5Ac-feeding on disease development and progression. Neu5Ac-feeding in *apoE*$^{-/-}$ mice (a model of atherosclerosis through knockout of ApoE, a protein heavily involved in lipid circulation and metabolism)[144] reduced atherosclerosis plaque area, as well as lipid liver deposition, triglyceride and cholesterol levels, and expression of inflammatory cytokines and intracellular adhesion factors in aorta endothelial cells and liver cells.[85] In a different study, oral supplementation of the Neu5Ac precursor N-acetyl-D-mannosamine in mice on a high-fat diet (to study type II diabetes) resulted in a restoration of IgG sialylation and preserved insulin sensitivity.[145] The mechanism of action in these studies is unknown and changes in the microbiome were not investigated in either case. However, given the established connections between the gut microbiome and atherosclerosis and diabetes[146–148] and the impact sialic acids can have on the microbiome, an investigation of gut microbiome composition in response to Neu5Ac in these disease models would be intriguing.

The impact of dietary sialic acids on the adult gut microbiome is often difficult to tease apart, given the varied diets of adults. In 2017, researchers analyzed the gut microbiota of the Hadza people, a community living an ancestral hunter-gatherer lifestyle in Tanzania, where diet composition is determined by seasonal food availability.[6] A

longitudinal analysis revealed important modifications of the microbiome over the course of a year, following shifts between dry and wet seasons that corresponded to periods of meat- and plant-based diets, respectively. Metagenomic sequencing revealed both an increased diversity and increased number (as reads per million) of carbohydrate-active enzymes (including sialidases) in dry season samples, when the Hadza diet is dominated by meat, a food rich in sialic acids.[6] A different study, focusing specifically on sialidases, re-analyzed the Hadza data and found specific enrichment of an organism encoding a sialidase to release Neu5Gc from glycans in the dry season samples.[115] Since Neu5Gc is not made by humans, but is specifically enriched in red meat, this finding indicates that a Neu5Gc-metabolizing microbe becomes more abundant in the Hadza gut microbiota when levels of Neu5Gc increase in the diet.

The ability of non-human mammals to produce Neu5Gc, through the functional CMAH enzyme that humans lack, has led to a great difficulty in studying the effects of anti-Neu5Gc inflammation in animal models. However, researchers have been able to work around this through the generation of *Cmah*$^{-/-}$ animals that, like humans, produce only Neu5Ac.[149,150] The presence of Neu5Gc in human glycoconjugates has been implicated in numerous disease processes, such as liver cancer and atherosclerosis.[86,87] Neu5Gc-feeding in mouse models deficient in Neu5Gc exacerbates these diseases. Of particular interest, *Cmah*$^{-/-}$ knockout in a background knockout of the low-density lipoprotein receptor (*Ldlr*$^{-/-}$) reproduces the human-specific Neu5Gc deficiency in a classic atherosclerosis model.[87] Neu5Gc-feeding in this *Cmah*$^{-/-}$ *Ldlr*$^{-/-}$ mouse model demonstrated significantly more atherosclerosis plaque size and necrotic core volume, compared to control groups.[87] Feeding of Neu5Gc in a *Cmah*$^{-/-}$

mouse model (without the *Ldlr*$^{-/-}$ deletion) showed distinct changes in the gut microbiome, with *Bacteroides*, *Barnesiella*, *Clostridium*, *Parabacteroides*, *Roseburia*, and *Turicibacter* significantly enriched compared to feeding with Neu5Ac.[115] Examining the effects of Neu5Gc-feeding on the microbiome of the *Cmah*$^{-/-}$ *Ldlr*$^{-/-}$ model and potential relationships between these changes and atherosclerosis could further our current understanding of the role the gut microbiome plays in cardiovascular disease.

1.3. The soil microbiome

Plant-microbiome interactions have been the focus of an increasing number of studies in recent years, especially with the potential to optimize agricultural production through the promotion of plant growth and soil health[151–153]. These studies clearly show that plant microbiome communities are heavily influenced by the location of microbial colonization on the plant[154–156] and the host plant genotype[157,158]. Each of these studies, some explicitly and some implicitly, are searching for what has been termed the “minimal microbial community”, the minimal set of organisms required to accurately reproduce natural community functions[159]. The number of community microbes in studies ranged from under 10[156,157] to between 20 and 40[155,158,160,161], although some studies starting with a high number of microbes reported that only a small number of organisms consistently colonized plant sites[156,160]. In addition to loss of starting organisms, *in vitro* microbial communities commonly lose α-diversity over time, compared to the starting community[162–164]. The vast majority of synthetic microbial communities are constructed with equal amounts of each organism, although Bai et al.[155] compared an equal (1:1:1:1) ratio of four represented phyla to an unequal ratio (1:1:1:0.25) but found the final community

compositions were similar. However, it has recently been shown that starting ratios, even in a simple co-culture, can have a significant effect on community growth and composition[165,166]. To what extent equal ratios in the starting inoculum produce the most reproducible and diverse synthetic community is still an open question[166]. When generating soil communities, we hypothesized that synthetic community α-diversity could be increased by adjustment of starting organism ratios, with higher levels of organisms that decrease in abundance during growth of an equally-mixed community.

The scientific community has developed robust model systems for research in animals, plants, and individual microbes[167,168]. These systems allow experiments to be repeated and validated across research groups, leading to a body of research that grows on the work of others. However, microbiome research currently lacks widely-accepted reproducible model systems, despite the recognition that microbial communities play a fundamental role in biological systems[151,169,170]. Indeed, host organisms and their microbiota are often referred to as one meta-organism, requiring both parts of the system to thrive[2,153,171]. Several groups have worked to develop reproducible microbial systems, such as a microbial chemostat[172]; the Lubbock chronic-wound biofilm model[173]; or *in vitro* gut systems incorporating microbes[174–176], most notably the Altered Schaedler Flora community[177,178]. These systems address important research questions about the interactions between microbes and their host environment. However, they normally do not probe the mechanisms of host-community interactions, particularly in plant-microbe communities under environmental perturbations.

To address specific questions pertaining to the inner workings of microbial communities, researchers must be able to alter the presence and abundance of specific

organisms, introduce genetic alterations as necessary, and maintain strict control of growth conditions like temperature, humidity, acidity, and light[153,159,179,180]. At present, experiments with synthetic microbial communities are the only viable method to design research studies within these constraints[153,156,181,182]. Although the use of bioengineering tools to introduce specific changes in natural microbial communities shows promise in this area[183–185], these systems still lack an ability to predict the effect of engineering outcomes on the community as a whole[185]. The field of microbiome research, and soil microbiome research in particular, would benefit from development of a standardized synthetic community system to test hypotheses and compare results.

1.4. The human skin microbiome

Human skin, the largest and most exposed organ in the body, harbors a diverse microbiota that aids in defense against microbial pathogens and other skin pathologies[186–188]. Disruptions to the skin microbiome have been associated with multiple skin diseases, such as acne, atopic dermatitis, and seborrheic dermatitis[186,189,190]. Furthermore, the use of topical products such as make-up[191], deodorant[192], and skin care products have been shown to alter microbiome composition and diversity for weeks after the time of application[193]. Understanding how skin care products affect the skin microbiome, and through that their effect on skin health, would support the development of personalized skin treatment regimens for microbiome dysbiosis issues[186].

The composition of this microbial community is modulated by physical factors of the skin microenvironment, such as pH, temperature, moisture, oxygen availability, and

topography[188,194,195]. The community is further influenced by microbial interactions and intercellular metabolite exchanges, which help determine community structure and function[186,188,195,196]. This suggests that establishing a synthetic representation of this fixed skin microbiome could permit studies of the complex microbe-microbe, microbe-metabolite and microbe-host interactions that govern skin and host health. A major barrier to standardized studies of the skin microbiome is the lack of a reproducible *in vitro* system. Despite being dynamically modified by multiple external and internal factors, studies documenting skin microbiome composition across multiple body sites and time points indicate that composition is largely represented by a select few "fixed" organisms[194,197]. The recent advent of many reconstructed human epidermis models (RHEs) that accurately represent the physiological complexities of skin, such as Epiderm, Labskin, or NativeSkin, has allowed studies of the microenvironmental factors that regulate skin microbial community structure[198,199]. However, as with the soil microbiome, we still lack a robust, standardized microbial community that can be used to probe the community dynamics of the skin microbiome[199].

1.5. Summary

Microbial communities impact human health in a wide variety of settings, from the soil in which we grow our food to the digestion of that same food within our bodies. However, studying these communities in controlled and reproducible settings is exceedingly difficult given the countless factors that shape *in vivo* community development. Developing standardized and reproducible tools to study these communities is therefore essential to advance the current body of knowledge about the

microbiome, just as standardized models have been irreplaceable for the study of individual bacterial and mammalian organisms.

The following chapters in this thesis explore how such tools can be developed and implemented to gain new knowledge of microbial communities, and furthermore to apply knowledge gained from these communities to ameliorate human disease. Chapter 2 focuses on developing a standardized synthetic soil community that can be grown with agricultural plants and uses this community system to probe the effect of starting inoculum ratios on final community dynamics. Chapter 3 moves to developing a standardized skin community to investigate skin microbial community dynamics, with an emphasis on investigating the effect of chemicals found in cosmetics products on the skin microbiota. Chapter 4 moves beyond *in vitro* community systems to apply an enzyme isolated from the mouse gut microbiome to the treatment of cardiovascular disease. Together these studies explore multiple levels of the human metaorganism and cover a broad range of microbiome applications, from *in vitro* investigatory and screening tools to *in vivo* medical treatment strategies.

1.6. Acknowledgements

Chapter 1, in part, has been published in the journal *Gut Microbes*. Coker JK, Moyne O, Rodionov DA, Zengler K. Carbohydrates great and small, from dietary fiber to sialic acids: How glycans influence the gut microbiome and affect human health. Gut Microbes. 2021 Jan-Dec;13(1):1-18. The dissertation author is the primary investigator and author of this material.

Chapter 1, in part, has been submitted as a manuscript for publication in the journal *mSystems*. Coker J, Zhalnina K, Martoz C, Thiruppathy D, Tjuanta M, D'Elia G, Hailu R,

Mahosky T, Rowan M, Northen TR, Zengler K. A reproducible and tunable synthetic soil microbial community provides new insights into microbial ecology. *mSystems. Under revision.* The dissertation author is the primary investigator and author of this material.

Chapter 1, in part, is being prepared as a manuscript for submission for publication of the material. Coker J, Thriuppathy D, Flores-Ramos S, Marotz C, Tjuanta M, Zengler K. A model synthetic skin microbial community allows investigation of cosmetics chemicals and the skin microbiome. *In preparation.* The dissertation author is the primary investigator and author of this material.

Chapter 2: A reproducible and tunable synthetic soil microbial community provides new insights into microbial ecology

2.1 Abstract

Microbial soil communities form commensal relationships with plants to promote the growth of both parties. Optimization of plant-microbe interactions to advance sustainable agriculture is an important field in agricultural research. However, investigation in this field is hindered by a lack of model microbial community systems and efficient approaches for building these communities. Two key challenges in developing standardized model communities are maintaining community diversity over time and storing/resuscitating these communities after cryopreservation, especially considering the different growth rates of organisms. Here, a model community of 17 soil microorganisms commonly found in the rhizosphere of diverse plant species, isolated from soil surrounding a single switchgrass plant, has been developed and optimized for use with fabricated ecosystem devices (EcoFABs). EcoFABs allow reproducible research in model plant systems, with precise control of environmental conditions and easy measurement of plant-microbe metrics. The model soil community grows reproducibly *in vitro* between replicates and experiments, with high community α-diversity achieved through growth in low-nutrient media and adjustment of starting composition ratios for the growth of individual organisms. The community additionally grows in EcoFAB devices and regrows with a similar composition to unfrozen communities following cryopreservation with glycerol, allowing for dissemination of the model community. Our results demonstrate the generation of a stable microbial community that can be used with EcoFAB devices and shared between research groups for maximum reproducibility.

2.2 Introduction

Here, we present the generation of a diverse, reproducible, and tunable synthetic microbial community, composed of soil bacteria isolates obtained from switchgrass agricultural fields. Using a picoliter liquid printer to allow precise control of the initial bacterial inoculum, we tested over 20 community starting composition ratios to generate a synthetic community with maximum robustness and α-diversity. We then used this community to probe the effect of DNA from dead cells on sequencing composition results. To further support the reproducibility of this model community, we additionally determined a method for the cryopreservation of the community enabling it to be shared with other research groups. The 17-member community can readily be applied to EcoFAB devices, which allow reproducible research in model plant systems with precise control of environmental conditions and easy measurement of plant-microbe metrics[180,200].

2.3 Results

2.3.1 Strain Selection

Our overall goal was to generate a stable, reproducible microbial community for use with EcoFAB devices to study plant-microbe interactions in the rhizosphere. To this end, we selected 18 microbial strains isolated from the rhizosphere and bulk soil surrounding a single switchgrass plant that span the typical diversity found in the rhizosphere of grasses or food crops (Table 2.1). One strain was later eliminated to result in a final 17-member community, described below. These strains were all from different genera, to facilitate community diversity and ease of strain identification through 16S rRNA gene sequencing in the final community. All strains can be grown axenically *in vitro*

under aerobic conditions without shaking in liquid Reasoner's 2A (R2A) media at 30 °C (see Materials and Methods).

Table 2.1 Strain isolates used in this study and examples of plants associated with them in previous publications.

Genus	Strain	Associated plants[a]
Lysobacter	OAE881	Nicotiana tabacum L, tomato, pepper[201–203]
Burkholderia	OAS925	Zea mays L, Betula, Equisetum, Quercus, Senecio vulgaris, Triticum aestivum, Zantedeschia, Coffea, Saccharum officinarum, Zea mays L, Zea mays L, Lolium multiflorum, citrus, wheat[204–209]
Variovorax	OAS795	Citrus, maize, tomato, wheat[208,210,211]
Chitinophaga	OAE865	Tomato, Oryza sativa L, Cymbidium goeringii, ginseng[212–215]
Niastella	OAS944	Hibiscus syriacus L, persimmon tree, Populus euphratica, Korean ginseng[216–219]
Mucilaginibacter	OAE612	Gossypium hirsutum L, Angelica sinensis, ginseng, Dokdo Island (S Korea)[220–223]
Sphingomonas	OAE905	Citrus, wheat, Oryza sativa L[208–210,224,225]
Rhizobium	OAE497	Citrus, Oryza sativa, Dioscorea alata, Dioscorea esculenta[210,226,227]
Bradyrhizobium	OAE829	Citrus, Vaccinium angustifolium, wheat, Brazilian sugarcane[208,210,228,229]
Bosea	OAE506	Zea mays L, Cyperus rotundus L[230,231]
Methylobacterium	OAE516	Eucalyptus spp., Oryza sativa cv. Dongjin and Lycopersicon esculentum L. cv. Mairoku, maize[232–234]
Arthrobacter	OAP107	Ginkgo biloba L, Quercus ilex, Triticum aestivum L (wheat)[235–237]

Table 2.1 Strain isolates used in this study and examples of plants associated with them in previous publications, continued.

Genus	Strain	Associated plants[a]
Mycobacterium	OAE908	Soil from Haikou (China), tomato, Oryza sativa L. cv. Wusimi[238–240]
Rhodococcus	OAS809	Zea mays L, Oryza sativa L.[230,241]
Brevibacillus	OAP136	Zea mays L, Lolium perenne, Pinellia ternata, Nicotiana tabacum L, Gossypium hirsutum[230,242–245]
Paenibacillus	OAE614	Solanum lycopersicum, Oryza sativa L, wheat[246–248]
Bacillus	OAE603	Zea mays L, Triticum aestivum L (wheat), Lolium perenne, Nicotiana tabacum L[230,237,242,244]
Pseudomonas simiae	WCS417	Wheat, citrus, Zea mays L, Nicotiana tabacum L[209,210,230,244]

[a]References were found through PubMed searches (conducted on 8/17/2021) of “<genus> rhizosphere”, “<genus> soil isolation”, and/or “<genus> plant isolation”. Plant scientific names are listed when included in the references; otherwise plant common names are used.

We assembled these strains into synthetic communities using a SCIENION CellenONE liquid-handling robot printer (SCIENION US Inc., Phoenix, AZ) (Figure 2.1). The CellenONE machine is capable of dispensing droplets from 300-450 picoliters. Liquid samples can be taken up into the piezo dispense capillary (PDC), then dispensed in individual drops of precise volume through a piezoelectric pulse. The machine can be programmed to dispense drops from the PDC in specific locations or patterns on a target of the operator's choosing. For the soil communities, individual strains in diluted liquid culture were taken up from wells of a 96- or 384-well plate and dispensed to a target 96-well plate with fresh liquid growth media. However, samples can also be dispensed to targets such as 384-well plates, microscope slides, or agar plates. Use of this system allowed the 18 strains to be combined in varying starting ratios by programming a different number of starting drops per strain for each community. Individual strains were diluted to an optical density at 600nm (OD_{600}) of 0.025 for each experiment.

Following community assembly, communities were allowed to grow for up to 11 days. Growth was monitored through OD_{600}. Community growth was halted at the desired time point by freezing the communities at -20 °C. DNA was extracted from communities by heating samples to 95 °C in a PCR machine for 10 minutes. 5µl of undiluted supernatant from heated community samples was used to generate 16S rRNA gene sequencing libraries. This method was confirmed to produce the same 16S sequencing results as DNA extraction with a commercial DNA extraction kit (Qiagen PowerSoil Pro) (Figure 2.2A-B).

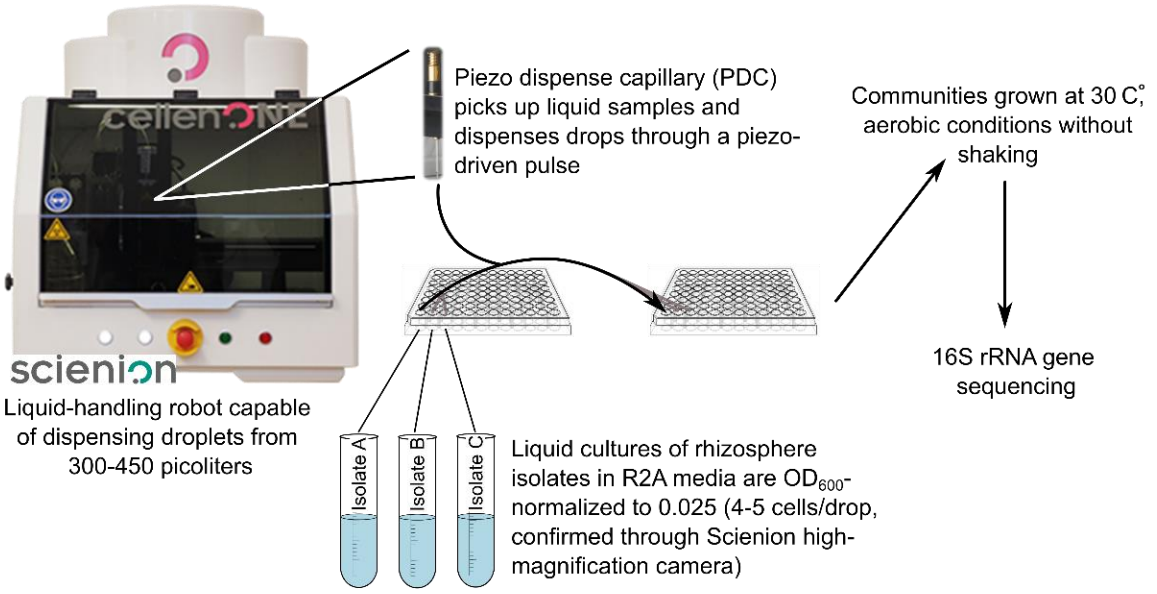

Figure 2.1 Schematic of synthetic rhizosphere community generation using a piezo dispense capillary (PDC) device. Isolates were grown for 3-4 days in liquid R2A media, then OD_{600}-normalized to 0.025 and loaded into individual wells in the probe plate. The PDC drew liquid up from one well of the probe plate and dispensed a programmed number of drops in desired wells of the target plate. This process was repeated for each isolate to result in a final mixed community. Communities were grown aerobically for the desired amount of time, then analyzed for composition and diversity with 16S rRNA sequencing.

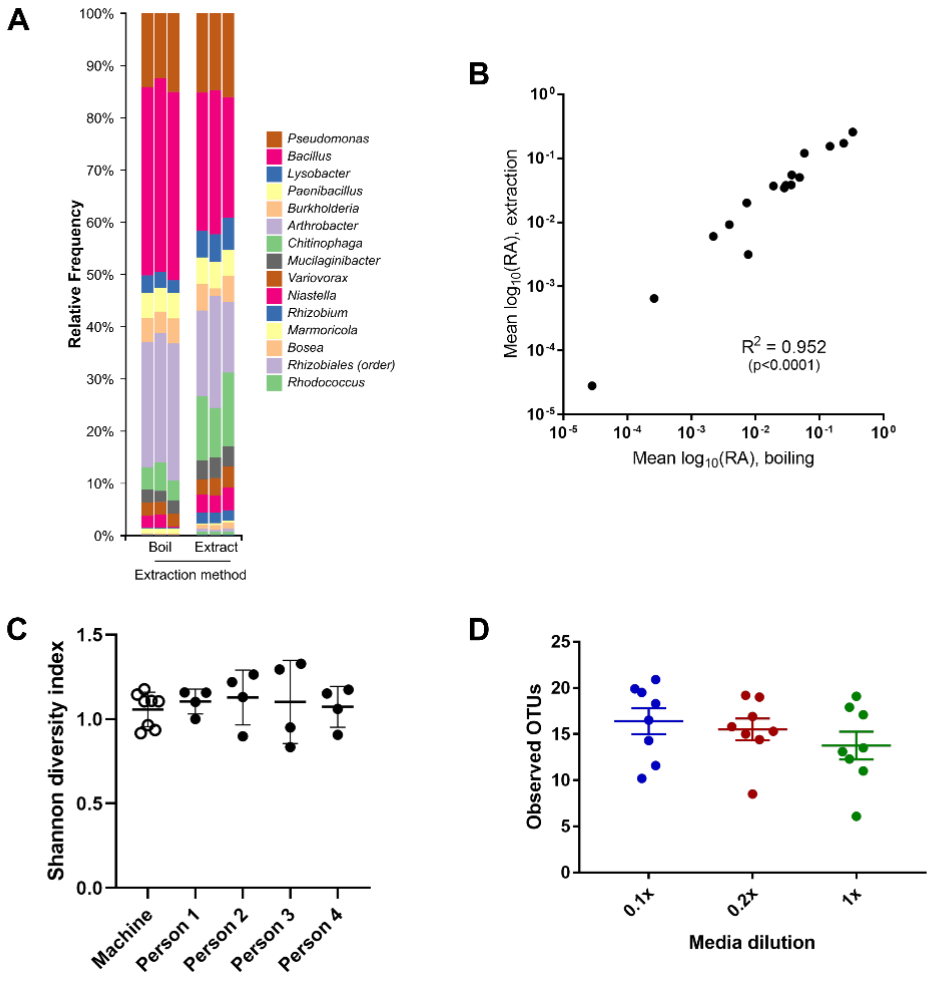

Figure 2.2 Supplement to Figure 2.1 *Comparison of boiling and conventional kit DNA extraction for rhizosphere isolates (A-B).* Isolates were mixed in equal amounts, as determined by OD normalization. DNA was extracted either by heating to 95°C for 10 minutes in a PCR machine (boiling) or using a conventional extraction kit (Qiagen PowerSoil Pro) (extraction). (n=3 per condition) A) Taxonomy of samples through 16S sequencing. B) Comparison of a logarithmic transformation of mean relative abundance values in boiling and extraction samples. Pearson's correlation coefficient is shown on the plot. *Community diversity between assembly methods and media dilutions (C-D).* C) Shannon diversity index of machine-assembled and human-assembled communities from 4 different people (n=4-8 each). D) Observed operational taxonomic units (OTUs) for equally-mixed community grown in 1X, 0.2X, and 0.1X R2A media for 3 days (n=8 each).

2.3.2 Automated assembly of synthetic communities produces similar results to hand assembly

The use of the picoliter printer to assemble synthetic communities was chosen to increase throughput and to potentially reduce variability from human and calibration error during pipetting. We therefore compared the diversity and composition of eight replicates of an automated-assembly community (machine) to sixteen replicates of a hand-assembly community (human) after 3 days of growth in 0.1X R2A media. The hand-assembled communities were composed of 4-6 replicates each from 4 different lab members. The growth rate and final OD_{600} value was the same between machine- and hand-assembled communities (Figure 2.3A). The β-diversity metric of Bray-Curtis distance showed a significantly larger dissimilarity between communities assembled by hand compared to machine for two of the four people (one-way ANOVA with Benjamini-Hochberg FDR, * $p<0.05$ *** $p<0.001$) (Figure 2.3B). Similarly, α-diversity showed a greater spread in hand-assembled than machine-assembled communities for two of the four people (Figure 2.2C). These results indicate that community assembly with the automated printer will, on average, result in less variability than community assembly by different people.

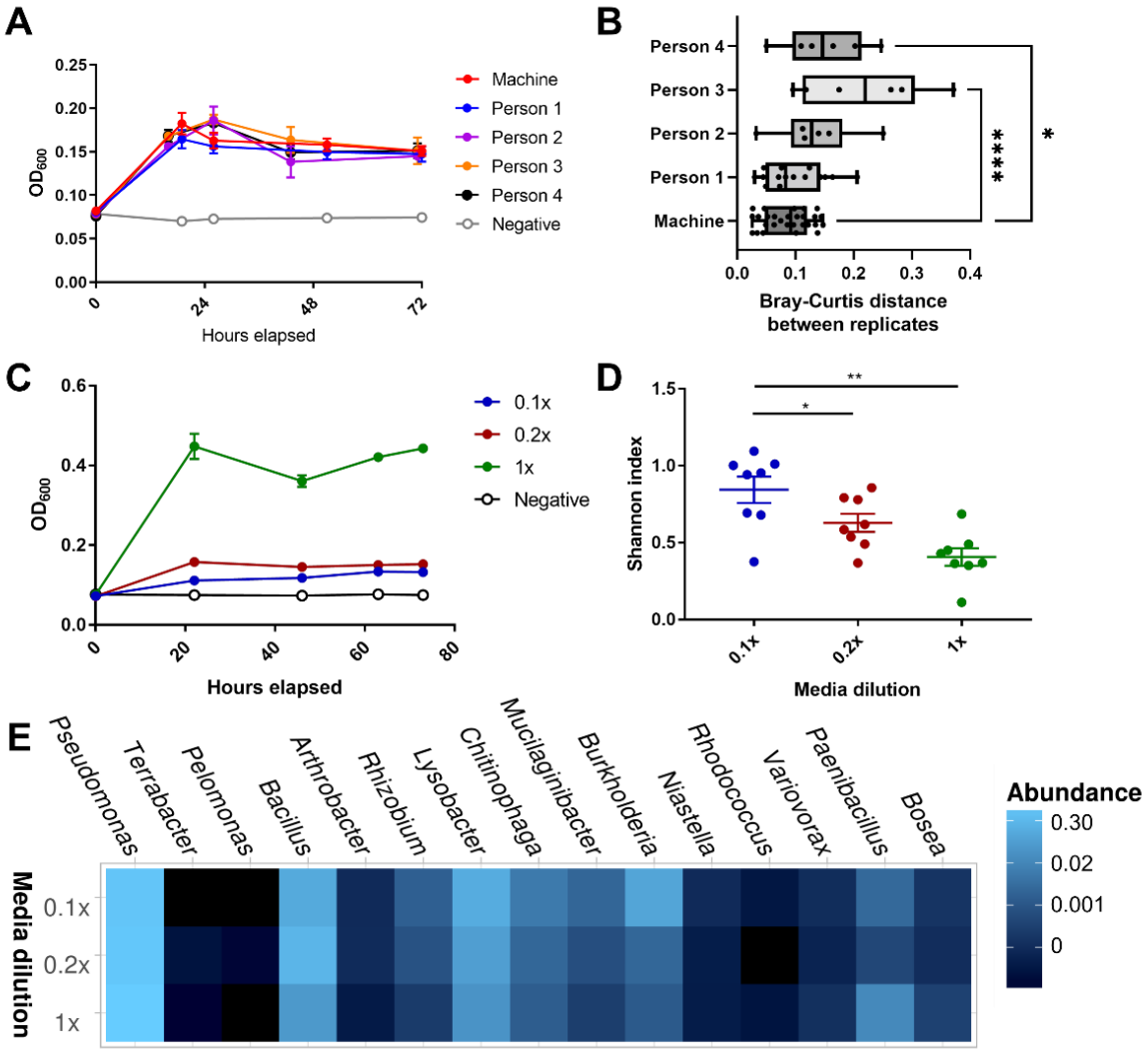

Figure 2.3 Community diversity with hand-assembly and media dilutions. A) OD_{600} values of human-assembled (human) and machine-assembled communities (machine) over 3 days (72 hours) of growth (n=6-8 each). B) Bray-Curtis distance on 16S rRNA gene amplicon sequencing between replicates of the human- and machine-assembled communities. C) OD_{600} values of machine-assembled equally-mixed communities in 1X, 0.2X, and 0.1X R2A media over 3 days (n=8 each). D) Observed OTUs (left) and Shannon diversity index (right) of media dilution communities (Student's t-test, * = $p<0.05$, **** = $p<0.001$). E) Heatmap of taxonomy relative abundance of media dilution communities from 16S sequencing. Taxonomic order was determined by PCoA clustering of the Bray-Curtis distance. Replicates for each condition were merged with the Phyloseq command merge_samples(group = "Media_dilution").

2.3.3 Alpha-diversity of the synthetic soil community is enhanced through low-nutrient conditions

We next sought to test if nutrient availability affected the growth of individual strains within the community. We compared the growth and diversity of an equally-mixed community of all 18 strains between 1X, 0.2X, and 0.1X R2A media (n=8 for each condition) after 3 days of growth. As expected, total community growth was highest in 1X media, followed by 0.2X and 0.1X media (Figure 2.3C). However, the α-diversity metrics of observed OTUs and Shannon diversity index were lowest in 1X media and increased as media dilution increased (Figure 2.3D, Figure 2.2D). Taxonomy analysis of 16S sequencing data revealed that the *Pseudomonas* strain commonly grew to a high final proportion of the final community, regardless of media dilution (Figure 2.3E). However, the 0.1X communities displayed higher relative abundances of other, less-dominant strains, such as *Chitinophaga, Burkholderia,* and *Mucilaginibacter*. Individual growth curves of all organisms can be found in Figure 2.4.

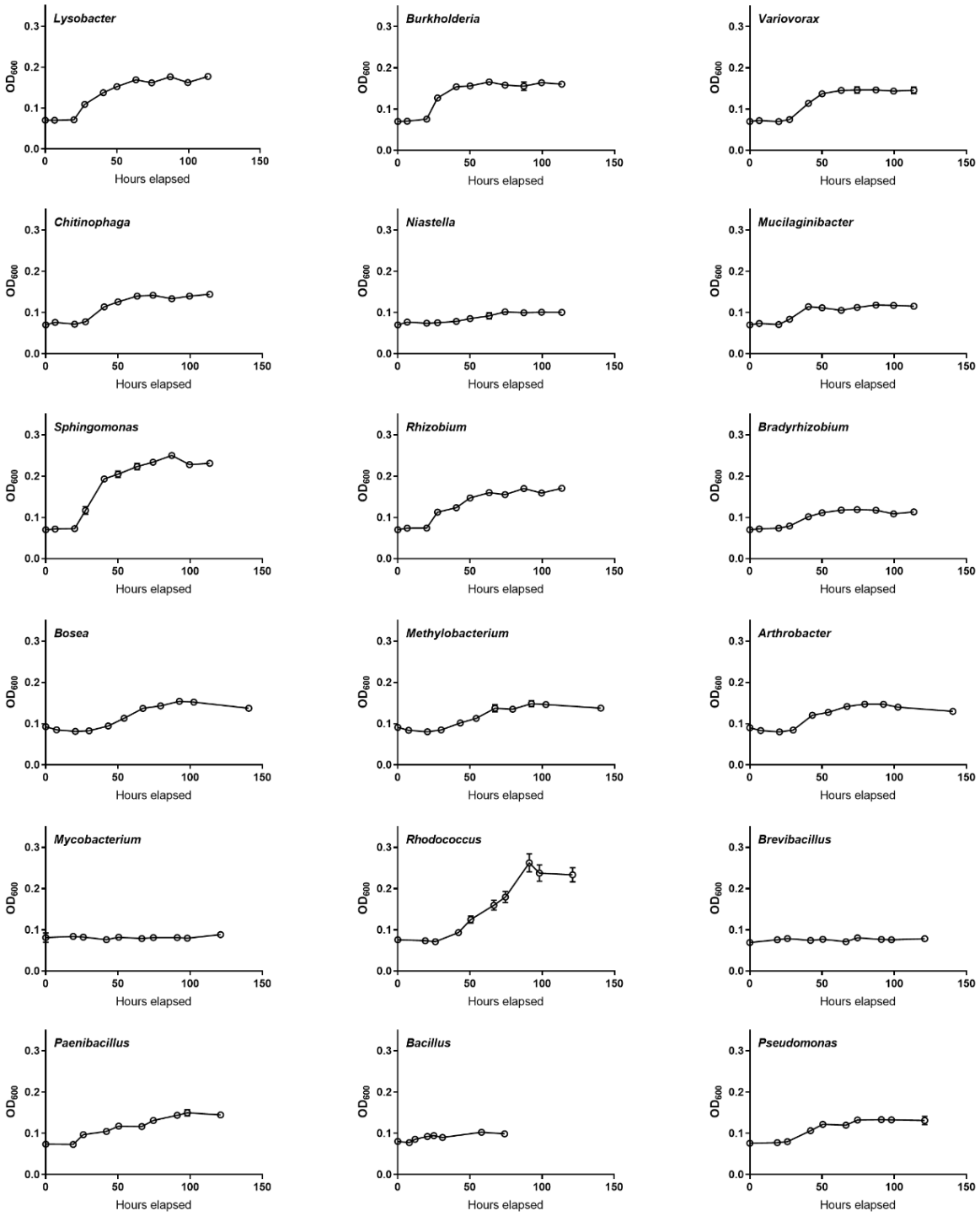

Figure 2.4 Supplement to Figure 2.3. Growth curves of individual rhizosphere isolates in 0.1X R2A media.

2.3.4 Alpha-diversity of the synthetic soil community is maximized through adjustment of starting community ratios

We next sought to maximize community diversity through adjustment of community starting ratios, meaning organisms were mixed in the starting community in ratios other than 1:1. We tested 11 different starting ratios with and without *Pseudomonas* (22 ratios total; Figure 2.5A). The exact calculations and ratios are provided in Tables 2.2-2.3. Briefly, the ratios were calculated based on the change in relative abundance after 3 days of growth from an equally-mixed inoculum. The starting relative abundance (SRA; relative abundance in the inoculum), final relative abundance (FRA; relative abundance after 3 days of growth), and FRA/SRA ratio (FSR) values were applied with various equations to try to design communities with high α-diversity. When designing the community compositions, we hypothesized that starting with lower amounts of organisms with a high SRA or FSR and higher amounts of organisms with a low SRA or FSR would increase α-diversity (Figure 2.5A, “FSR-based” and “SRA-based” compositions). We also included 4 compositions with different starting amounts of an equally-mixed community (Figure 2.5A, “Equal” compositions). For this study, two identical 96-well plates were assembled at the same time with the picoliter printer and allowed to grow for 2 and 6 days, respectively.

Table 2.2 Relative abundance values of organisms from an equally-mixed community.

	SRA[a]	FRA[b]	F/S ratio (FRA/SRA)[c]
Lysobacter OAE881	0.029507	0.160573	5.44179057
Pseudomonas simiae WCS417	0.139359	0.570065	4.09063447
Sphingomonas OAE905	0.000018	0.000053	2.8754562
Burkholderia OAS925	0.044979	0.117325	2.60846168
Rhizobium OAE497	0.001012	0.001477	1.45909576
Bacillus OAE603	0.363800	0.137535	0.37805086
Chitinophaga OAE865	0.044788	0.007738	0.17275925
Mucilaginibacter OAE612	0.023927	0.002400	0.10030911
Bosea OAE506	0.001536	0.000085	0.0554598
Rhodococcus OAS809	0.000219	0.000012	0.05523912
Paenibacillus OAE614	0.047480	0.002502	0.05269173
Niastella OAS944	0.016974	0.000045	0.0026626
Variovorax OAS795	0.024828	0.000059	0.00237307
Arthrobacter OAP107	0.250202	0.000049	0.0001968
Bradyrhizobium OAE829	0.001405	0.000000	0
Methylobacterium OAE516	0.001405	0.000000	0
Mycobacterium OAE908	0.000120	0.000000	0
Brevibacillus OAP136	0.000000	0.000019	0

[a]SRA = starting relative abundance; RA reported by 16S sequencing at time 0 of an equally-mixed community.

[b]FRA = final relative abundance; RA reported by 16S sequencing after 3 days growth of an equally-mixed community.

[c]F/S ratio = fold-change in relative abundance between time 0 and 3 days, calculated as FRA / SRA

Table 2.3 Equations for starting community ratios and number of CellenONE printer drops per organism.

	2 everyone	20 everyone	200 everyone	2000 everyone	2x cutoff	3x cutoff	Linear correction	Log correction	RA (exp)	RA (linear)	Weighted abundance
Equation[a]	2 drops	20 drops	200 drops	2000 drops	2 or 2000 drops	2, 200, or 2000 drops	Drops = (10-FSR)*10	Drops = (10-FSR)^{10}/2e6	Drops = 100/SRA^2	Drops = 1/SRA*10	Drops = 100*2^((1-SRA)*(1-FSR))
Lysobacter	2	20	200	2000	2	2	46	2	2	3	200
Pseudomonas	2	20	200	2000	2	2	59	26	2	2	16
Sphingomonas	2	20	200	2000	2	2	71	168	2986	5464	27
Burkholderia	2	20	200	2000	2	2	74	243	2	2	34
Rhizobium	2	20	200	2000	2	2	85	1033	2	99	73
Bacillus	2	20	200	2000	2	200	96	3401	2	2	132
Chitinophaga	2	20	200	2000	2	200	98	4200	2	2	173
Mucilaginibacter	2	20	200	2000	2	200	99	4520	2	4	184

Table 2.3 Equations for starting community ratios and number of CellenONE printer drops per organism, continued.

	2 everyone	20 everyone	200 everyone	2000 everyone	2x cutoff	3x cutoff	Linear correction	Log correction	RA (exp)	RA (linear)	Weighted abundance
Bosea	2	20	200	2000	2	200	99	4730	2	65	192
Rhodococcus	2	20	200	2000	2	200	99	4731	21	457	192
Paenibacillus	2	20	200	2000	2	200	99	4743	2	2	187
Niastella	2	20	200	2000	2000	2000	100	4987	2	6	197
Variovorax	2	20	200	2000	2000	2000	100	4988	2	4	196
Arthrobacter	2	20	200	2000	2000	2000	100	4999	2	2	168
Bradyrhizobium	2	20	200	2000	2000	2000	100	5000	2	71	200
Methylo-bacterium	2	20	200	2000	2000	2000	100	5000	2	71	200
Mycobacterium	2	20	200	2000	2000	2000	100	5000	70	837	200

Table 2.3 Equations for starting community ratios and number of CellenONE printer drops per organism, continued.

	2 everyone	20 everyone	200 everyone	2000 everyone	2x cutoff	3x cutoff	Linear correction	Log correction	RA (exp)	RA (linear)	Weighted abundance
Brevibacillus	2	20	200	2000	2000	2000	100	5000	5739	7575	200

[a]FSR = F/S ratio, as defined in Table 2.2. The minimum number of drops per organism was set at 2.

Figure 2.5 Community diversity with starting ratio adjustments and removal of relic DNA. A) Representation of the 11 community starting ratios used in this study, as both relative (top) and absolute (bottom) abundances. Descriptive names of the ratios are on the x-axis. For equal communities, all organisms were added in equal but increasing amounts; the number refers to the number of drops released by the printer for each organism. For FRA-based and SRA-based adjusted communities, the number of drops for each organism was calculated as shown in Tables 2.2-2.-3. For communities without *Pseudomonas*, *Pseudomonas* was not added. B) Shannon diversity index of each community ratio, 2 and 6 days combined. Communities without *Pseudomonas* are on top, communities with *Pseudomonas* on bottom. Communities are shown in order of decreasing average Shannon index for communities without *Pseudomonas*. (n = 4 each) C) PCA of robust Aitchison distance between communities with different starting ratios. Symbols of communities with *Pseudomonas* have reduced opacity. GR = growth rate; RA = relative abundance. D) Number of sequencing reads passing quality filtering per sample for PMA- and mock-treatment conditions. E) PCA of Aitchison distance between PMA- and mock-treatment communities. F) Heatmap of taxonomic composition of the 5 community ratios after 16 hours of growth. Sample order on the x-axis was determined by hierarchical clustering of Bray-Curtis distance in the Phyloseq package. PMA-treated (yellow) and mock-treated (red) communities are marked in the rug plot at the bottom of each heatmap.

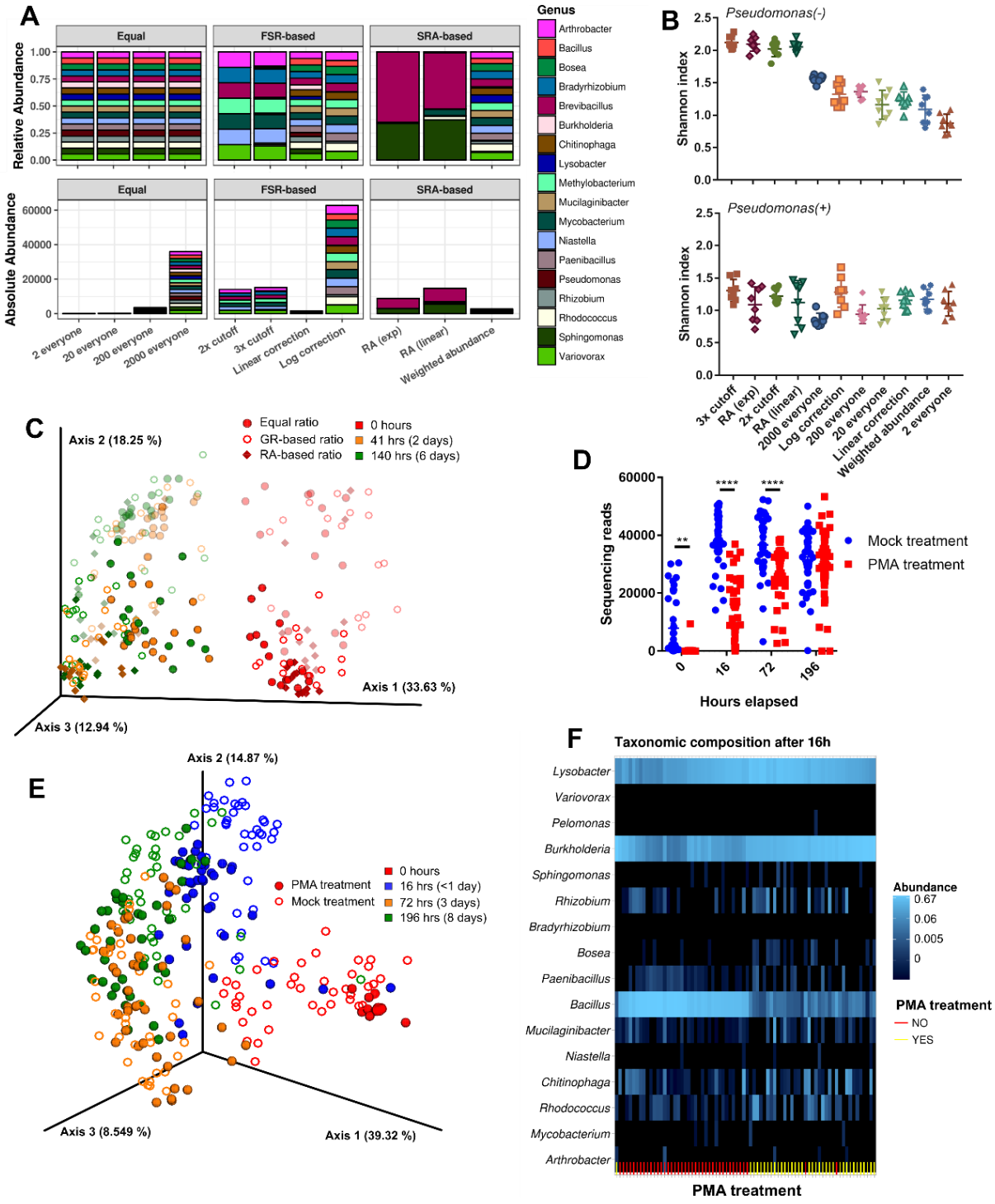
A
Equal
FSR-based
SRA-based
Relative Abundance
Absolute Abundance
2 everyone
20 everyone
200 everyone
2000 everyone
2x cutoff
3x cutoff
Linear correction
Log correction
RA (exp)
RA (linear)
Weighted abundance
Genus
Arthrobacter
Bacillus
Bosea
Bradyrhizobium
Brevibacillus
Burkholderia
Chitinophaga
Lysobacter
Methylobacterium
Mucilaginibacter
Mycobacterium
Niastella
Paenibacillus
Pseudomonas
Rhizobium
Rhodococcus
Sphingomonas
Variovorax
B
Pseudomonas(-)
Pseudomonas(+)
Shannon index
3x cutoff
RA (exp)
2x cutoff
RA (linear)
2000 everyone
Log correction
200 everyone
20 everyone
Linear correction
Weighted abundance
2 everyone
C
Axis 2 (18.25 %)
Axis 1 (33.63 %)
Axis 3 (12.94 %)
Equal ratio
GR-based ratio
RA-based ratio
0 hours
41 hrs (2 days)
140 hrs (6 days)
D
Sequencing reads
Hours elapsed
Mock treatment
PMA treatment
E
Axis 2 (14.87 %)
Axis 1 (39.32 %)
Axis 3 (8.549 %)
PMA treatment
Mock treatment
0 hours
16 hrs (<1 day)
72 hrs (3 days)
196 hrs (8 days)
F
Taxonomic composition after 16h
Lysobacter
Variovorax
Pelomonas
Burkholderia
Sphingomonas
Rhizobium
Bradyrhizobium
Bosea
Paenibacillus
Bacillus
Mucilaginibacter
Niastella
Chitinophaga
Rhodococcus
Mycobacterium
Arthrobacter
Abundance
PMA treatment
NO
YES

In general, communities containing *Pseudomonas* grew to slightly higher OD_{600} values than communities without *Pseudomonas* (Figure 2.6). α-diversity, as measured by Shannon index, was highest in the following communities without *Pseudomonas*: 2x cutoff, in which organisms with FSR<0.05 received 2000 drops from the starting isolate culture while organisms with FSR>0.5 received 2 drops; 3x cutoff, in which organisms with FSR>1, FSR 0.05-1, and FSR<0.05 received 2000, 200, and 2 drops respectively; RA (exp), in which the number of drops decreases exponentially with FRA; and RA (linear), in which the number of drops decreases linearly with FRA (Figure 2.5B). Analysis of robust Aitchison distance, as a metric of β-diversity, showed that 2- and 6-day communities were significantly different from starting communities (Figure 2.5C; pairwise PERMANOVA with Benjamini-Hochberg FDR correction, $p = 0.0015$). Communities also separated between those with and without *Pseudomonas* (pairwise PERMANOVA with Benjamini-Hochberg FDR correction, $p = 0.001$)

A well-known issue with genomics analysis is the inability to distinguish DNA from dead cells or other extracellular sources (“relic DNA”) from live cell DNA after sequencing[249–251]. To determine the effect of relic DNA on our synthetic community samples, we compared untreated communities to communities treated with propidium monoazide (PMA) to remove extracellular DNA prior to sequencing[251]. The communities with the five highest α-diversity values from Figure 2.5B were chosen to examine the effect of relic DNA. Four identical plates were prepared with the picoliter printer, with plates collected as time points at 0, 16, 72, and 196 hours. Overall community growth was not significantly different between communities (Figure 2.7A-B).

16S rRNA gene sequencing of PMA-treated communities showed significantly fewer reads passing quality filtration at the 0-, 16-, and 72-hour timepoints compared to mock-treatment communities, although the gap decreased as time increased (Figure 2.5D). No difference was seen in the number of reads between mock- and PMA-treated communities at 196 hours. PCA of Aitchison distance between the communities showed a separation between the 0-hour and other timepoints (Figure 2.5E). PMA-treated samples were significantly different from the mock-treated samples at 0, 16, and 196 hours, but not at the 72-hour time point (pairwise PERMANOVA with Benjamini-Hochberg FDR correction, $p = 0.001$-0.005). Hierarchical clustering by Bray-Curtis distance near-perfectly separated communities between PMA-treated and mock-treated samples, regardless of starting community ratios (Figure 2.5F, rug plot). Taxonomy analysis shows all mock-treatment communities had high relative abundance of *Bacillus* at 16 hours, an organism with a low relative abundance in the 16-hour PMA-treated samples (Figure 2.5F). This was not observed at the 72- and 196-hour time points (Figure 2.7C-D). This suggests that many of the *Bacillus* reads detected in the mock-treatment samples before 24 hours could come from nonviable cells (presumably either spores or dead cells), while after 24 hours this is no longer the case.

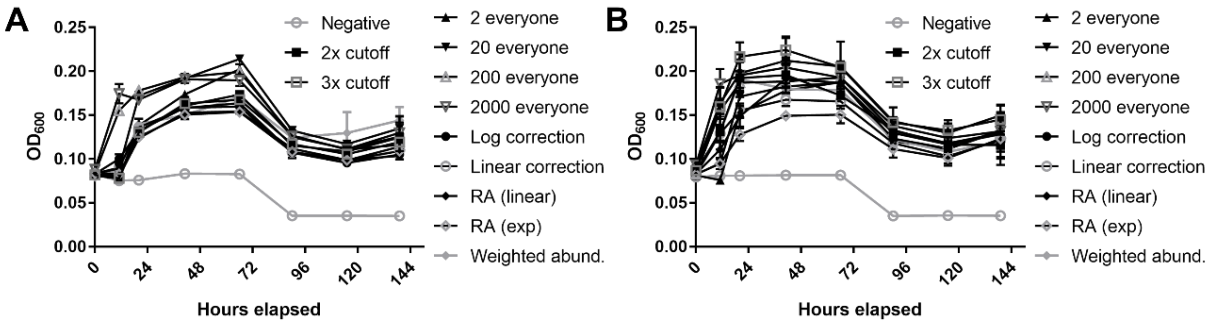

Figure 2.6 Supplement to Figure 2.5. Growth curves of communities with adjusted starting ratios. Community growth was monitored through OD_{600} for 6 days. A) Growth of communities without *Pseudomonas simiae*. B) Growth of communities with *Pseudomonas simiae*.

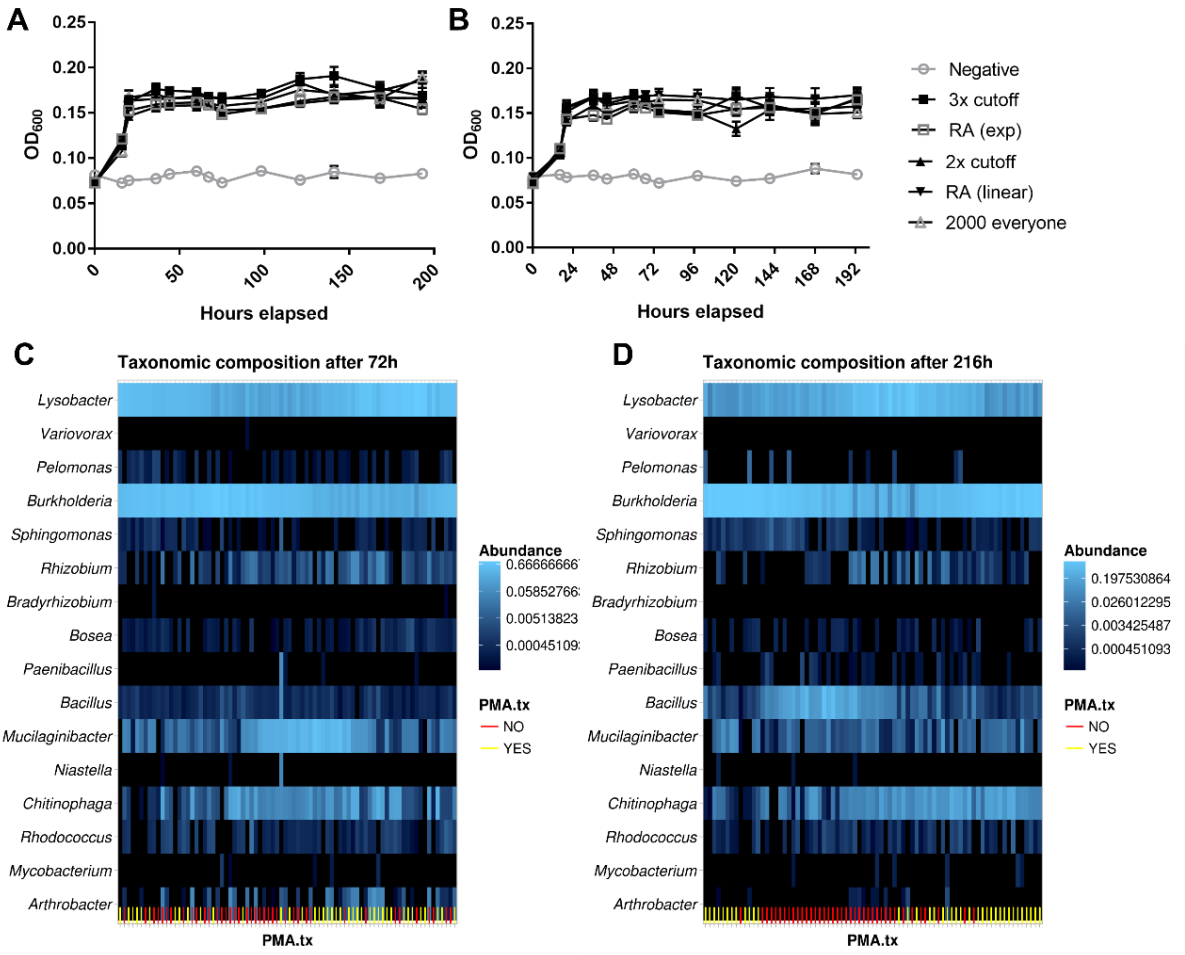

Figure 2.7 Supplement to Figure 2.5. Growth curves and taxonomic composition of PMA-treated and mock-treated communities. Community growth was monitored through OD_{600} for 8 days (n=4 for each condition). A) Growth of communities that were not treated with PMA before sample collection B) Growth of communities treated with PMA before sample collection. C) Heatmap of taxonomic composition after 72 hours of growth, all community ratios combined. D) Heatmap of taxonomic composition after 196 hours (8 days) of growth, all community ratios combined. PMA-treated (yellow) and mock-treated (red) communities are marked in the rug plot at the bottom of each heatmap.

2.3.5 Community diversity dynamics are driven by presence of a few taxa

After determining that the highest α-diversity was observed in the 3x cutoff community composition, we sought to determine if the presence of specific taxa was required to generate this high-diversity community. For example, would there be a taxon or group of taxa whose removal caused community diversity to decrease sharply? To address this question, we started with the 3x cutoff composition and removed combinations of one or more organisms from the starting community. The absolute number of drops for the remaining organisms was left the same as before. We tested a total of 18 combinations within the 3x cutoff community (Figure 2.8A). We compared composition of the community with all 17 strains to the community with only “fast-growing” strains (strains that received 2 drops during community assembly), only “slow-growing” strains (received 2000 drops), and combinations that removed 1, 2, or 3 strains at a time, or removed the fast-growing strains one-by-one without replacement.

We first examined the effect of the total number of strains on community α-diversity, measured by Shannon diversity index (Figure 2.8B). There was a significant but very weak positive correlation between the number of strains in the starting community and final α-diversity (Spearman’s correlation coefficient R^2=0.157, p=0.002). However, we were most interested in community combinations that deviated from the linear regression trendline shown in Figure 2.8B. We therefore analyzed the composition of the communities with 13 and more organisms for patterns that could explain large differences in α-diversity between communities. Each of these communities contained a “base community” of 14 organisms, with additional combinations of the fast-growing *Lysobacter*, *Burkholderia*, and *Chitinophaga* strains (Figure 2.8C, x-axis).

α-diversity varied significantly depending on the combination of 4 organisms present in the community. The addition of *Lysobacter* or *Chitinophaga* to the base community increased α-diversity, but the addition of *Burkholderia* did not. However, adding both *Lysobacter* and *Chitinophaga* did not significantly increase diversity over adding one of those organisms. Additionally, adding *Burkholderia* with *Lysobacter* or *Chitinophaga* did not reduce diversity. These results indicate that community α-diversity is not a simple additive effect of the individual organisms.

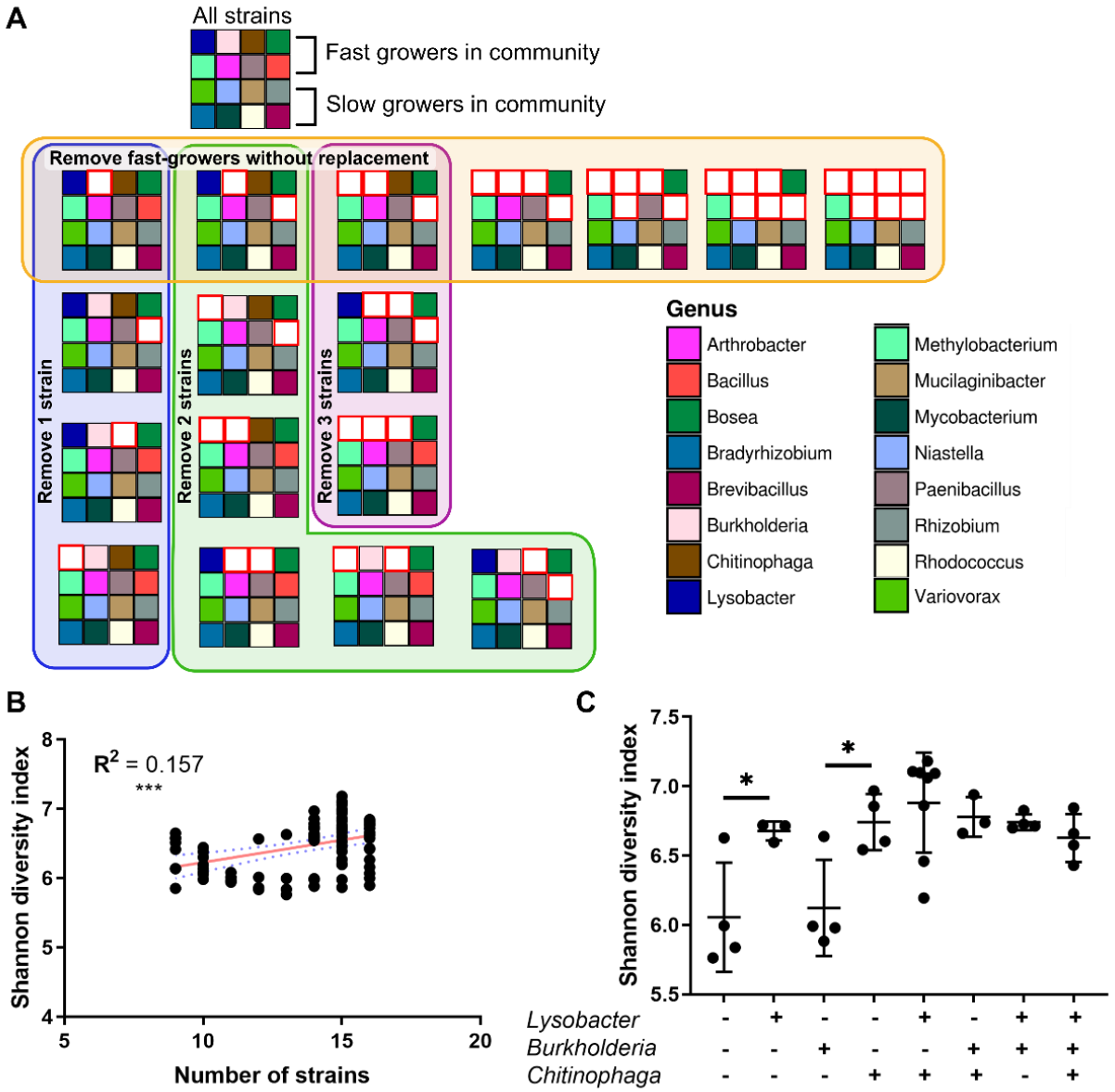

Figure 2.8 Investigation of individual strains in community dynamics. A) Schematic of 18 tested combinations of the 3x cutoff community, with each large square representing a different combination. Each small colored square represents an individual strain (see bottom right legend). White squares with a red border indicate the organism in that position was not included in that combination. For this experiment, strains were divided into fast-growing and slow-growing strains as indicated. *Sphingomonas* was not included in this experiment due to suspected contamination. B) The number of strains in each community combination plotted against the Shannon diversity index (n = 3-8 per combination). A linear regression trendline with 95% confidence interval is shown on the plot in red and blue, respectively. Spearman's correlation coefficient is reported on the plot (*** p<0.001). C) Shannon diversity index for combinations with 13 or more strains. Communities are divided into groups based on the presence/absence of *Lysobacter, Burkholderia,* and *Chitinophaga* (* p<0.05).

2.3.6 Synthetic community is able to colonize the rhizosphere in EcoFAB system

To further our goal of developing a template for a model rhizosphere microbial community, we integrated our community with the EcoFAB device (https://eco-fab.org/), an existing system developed for reproducible studies with plants[159,180,200]. Colonization of plants in EcoFAB devices by the rhizosphere isolates would show these communities can be easily transferred to a current plant-microbiome system. To investigate this, sterile *Brachypodium distachyon* Bd21-3 seedlings were transferred into the EcoFAB device at 3 days after germination. 12-day-old plants were then inoculated with an equally-mixed community, either with or without *Pseudomonas*, and allowed to grow for 7 days (n=4-5). Rhizosphere community composition was then assessed with 16S sequencing and compared to the original inoculant.

Synthetic communities grown on plants were significantly different from the original inoculant, as determined by Bray-Curtis distance (Figure 2.9A; pairwise PERMANOVA with Benjamini-Hochberg FDR correction, $p = 0.036$). Communities with *Pseudomonas* were not significantly different from communities without *Pseudomonas*. However, a heatmap of relative abundance shows obvious changes in community composition between the inoculant and rhizosphere communities collected after 7 days on the plant (Figure 2.9B). *Burkholderia, Rhizobium*, and *Mucilaginibacter* increased in relative abundance, while several other organisms decreased in relative abundance. The increase in *Burkholderia* mirrors the presence of *Burkholderia* in the *in vitro* synthetic communities.

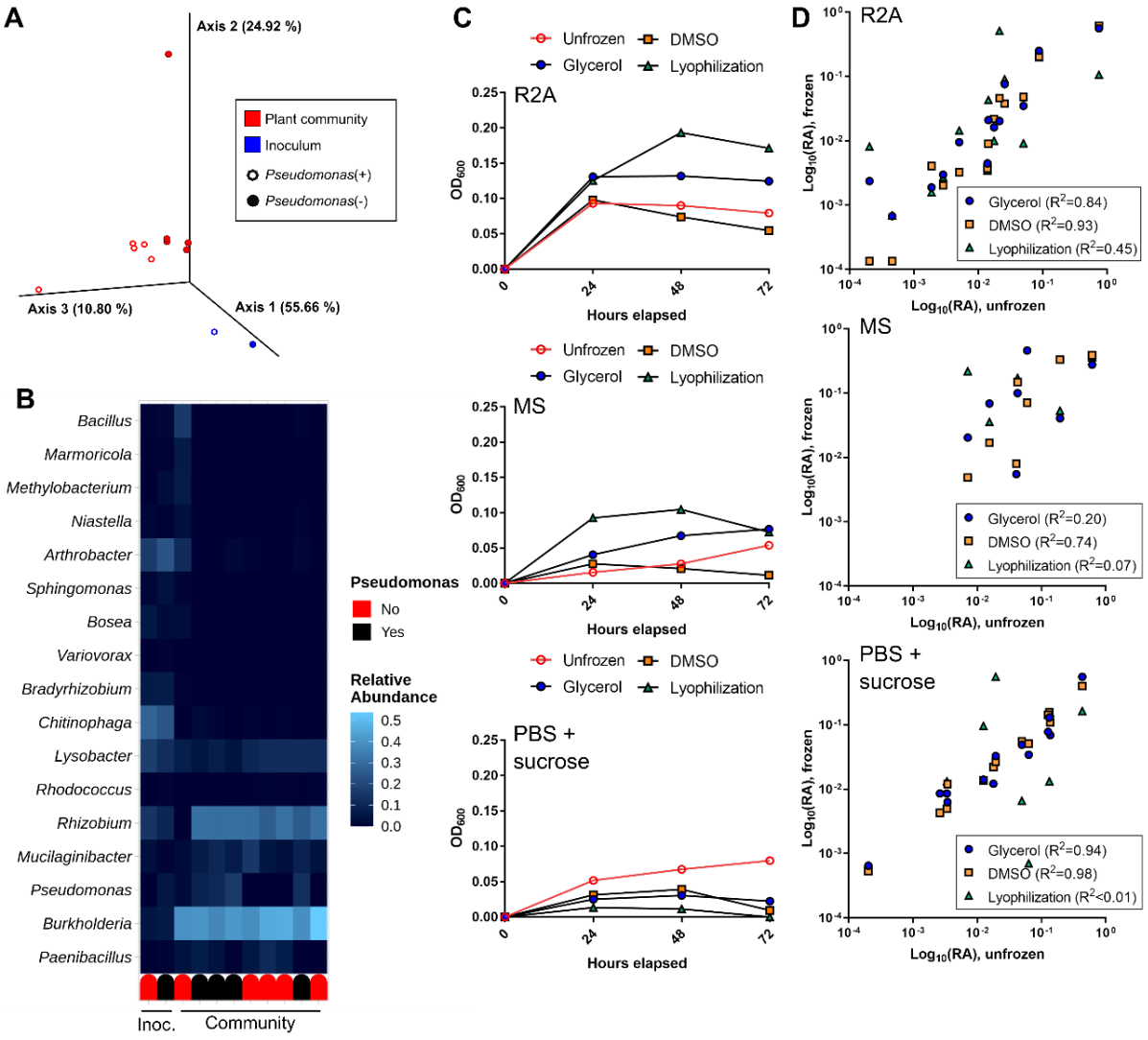

Figure 2.9 Community growth and composition with plant colonization and following cryopreservation. A-B) An equally-mixed community was inoculated to 12-day old *Brachypodium* plants, with or without *Pseudomonas*, and allowed to grow for 7 days. A) PCoA of Bray-Curtis distance between rhizosphere communities grown on plants for 7 days (n=5 each) and original inoculant (n=1). B) Heatmap of relative abundance of starting inoculum (Inoc.) and rhizosphere communities grown on plants for 7 days. Rug plot indicates presence (black) or absence (red) of *Pseudomonas* in inoculant. C-D) An equally-mixed community was preserved with 20% glycerol, 20% DMSO, or lyophilization and re-grown in R2A media (left panel), MS media (middle panel), or PBS with 10% sucrose (right panel). Growth and composition was compared to a community that was not frozen. C) Community growth measured through OD_{600}. The unfrozen control community is shown in red. (n = 1) D) Comparison of $\log_{10}$(relative abundance) from 16S sequencing between frozen and unfrozen communities for each cryopreservation method. Each point represents the $\log_{10}$(relative abundance) of an individual genus in the frozen vs unfrozen community. Pearson's correlation coefficient is reported for each comparison.

2.3.7 Cryopreservation allows for community re-growth that recapitulates original community composition

To enable collaborative and comparable microbiome research, any synthetic community must grow and act reproducibly between different researchers and research institutions. We sought to determine which method of cryopreservation would best preserve community fidelity to an unfrozen community, to facilitate distribution of the synthetic rhizosphere community presented here to other research groups. We tested the growth and composition of an equally-mixed community following three methods of cryopreservation, compared to an unfrozen control community. The unfrozen community was allowed to grow for 72 hours in three types of media (R2A media, MS media, or PBS with 10% sucrose [the lyophilization medium]). Our cryopreserved communities were frozen at -80 °C for 3 days after lyophilization, or with either 20% glycerol or 20% DMSO as a cryopreservant. After freezing, the communities were subsequently grown for 3 days in the same media as the unfrozen community.

Community growth was highest in R2A media and lowest in PBS with 10% sucrose (Figure 2.9C). Comparison on log-transformed relative abundance values from 16S sequencing shows large differences in community composition between cryopreservation methods (Figure 2.9D). Lyophilization consistently produced the lowest Pearson's coefficient of determination (R^2 value) between frozen and unfrozen communities in all media. Glycerol and DMSO showed similar high coefficients in R2A and PBS with 10% sucrose media, although the DMSO coefficient was much higher than glycerol in MS media (R^2=0.74, compared to R^2=0.20).

2.4 Discussion

In this study, we sought to develop a method to assemble and manipulate a synthetic soil community, while maintaining high levels of community α-diversity. Our results demonstrate the advantages of using a liquid-handling robot system to prepare synthetic communities. Direct comparison of hand-assembled and robot-assembled communities showed that machine-assembled communities have a generally lower level of dissimilarity than communities assembled by hand (Figure 2.3B). Examining community α-diversity (Figure 2.3C), two of the four hand-assembly subjects produced communities with a similar standard deviation to the machine-assembled communities. However, the other two subjects produced communities with a larger standard deviation, indicating the differences inherent between hand-assembly subjects. Machine-assembly eliminates this source of variability in community production.

Other studies starting with a large number of community members[156,160] reported a loss of detection of many organisms after the community was applied to plants. Of our 17 starting organisms (excluding *Pseudomonas*), 11 were found consistently throughout all experiments and timepoints. *Pseudomonas simiae* was excluded from our later community experiments due to its tendency to proliferate rapidly in the community and decrease overall α-diversity. Additionally, community α-diversity was substantially increased by adjustment of starting organism ratios based on the growth rates of community members. Starting ratios containing orders of magnitude more of slower-growing organisms (2x cutoff and 3x cutoff) resulted in higher Shannon diversity index values than the 4 equally-mixed conditions (Figure 2.5B). The increases in α-diversity were seen even after 6 days of community growth. This indicates that synthetic

community diversity can be increased over the diversity seen in typical 1:1 ratio communities by determining the growth rate of individual members and adjusting the starting ratios accordingly. As presented in this study, these ratios can also be determined through calculation of relative abundance changes during growth of an equally-mixed community.

In our 3x cutoff community without *Pseudomonas*, which displayed the highest α-diversity of the tested starting compositions, we further investigated the specific combination of organisms driving community diversity. We did not see a strong relationship between α-diversity and the total number of organisms in the starting community (Figure 2.8B). However, in communities with 14 or more organisms we noticed a range of α-diversity. We therefore analyzed the changes in α-diversity with the presence or absence of 3 specific fast-growing organisms in the community (*Bukholderia, Lysobacter,* and *Chitinophaga*). Our results indicate that different combinations of these organisms within the 3x cutoff community produce surprising non-linear diversity results. The addition of *Lysobacter* or *Chitinophaga* to the 13-member base community resulted in significant increases in α-diversity (Figure 2.8C), while the addition of *Burkholderia* did not change the α-diversity. Adding both *Lysobacter* and *Chitinophaga* to the base community resulted in a slight increase in diversity in most replicates, although this did not reach significance. However, adding *Lysobacter, Chitinophaga,* and *Burkholderia* together reduced diversity to levels similar to *Lysobacter* or *Chitinophaga* alone. These results show that community α-diversity is not driven solely by additive effects of individual community members. Interactions between organisms can alter the effect of individual

microbes on diversity. How these interactions move beyond diversity to affect individual organism metabolism is still an open question.

To address the potential influence of relic DNA on our sequencing results, we tested the effect of PMA treatment on the community ratios with highest α-diversity. Our results indicate that relic DNA can have a significant effect on sequencing results from <24 hours of community growth. Significantly fewer quality sequencing reads were detected in PMA-treated communities after 0, 16, and 72 hours of growth. However, the taxonomy relative abundance values were similar from 72 hours out to 196 hours (8 days). This indicates that while relic DNA can significantly alter sequencing results in our system in short-term growth studies, this effect diminishes at later time points (between 24 and 72 hours).

After investigating and optimizing α-diversity for our synthetic rhizosphere community, we next sought to display the utility of this community in a controlled model microbiome system. We tested community colonization of the EcoFAB device, a system designed for reproducible plant-microbiome system studies. The synthetic community was able to colonize the rhizosphere of *Brachypodium distachyon* plants grown in the EcoFAB device and was significantly different from the original inoculant after 7 days growth on the plant (Figure 2.9A-B). The presence of *Pseudomonas* did not significantly change the community in the EcoFAB system, unlike what was seen in our *in vitro* synthetic community system. The high relative abundance of *Burkholderia* in the rhizosphere communities was similar to levels of *Burkholderia* seen in the *in vitro* community, while other organisms had different relative abundance levels. These differences were expected given the addition of the *Brachypodium* plant, which produces

factors that affect soil microbe growth and metabolism. Indeed, aspects of plant-associated microbiomes have been shown to change rapidly in the natural environment based on climatic factors[252]. Future studies will focus on improving the accuracy of the *in vitro* by adding plant factors to the growth media.

We additionally determined the optimal method for community cryopreservation and re-growth. Although sequencing results indicated a high correlation between the glycerol and DMSO frozen communities and unfrozen community in PBS with 10% sucrose, the low OD_{600} values in this medium indicates this fidelity is likely due to a lack of growth following thawing. Preservation of 20% glycerol and re-growth in MS media led to similar growth by OD_{600} as the unfrozen community, but sequencing results revealed a poor correlation. However, glycerol preservation and re-growth in 0.1X R2A media resulted in community re-growth that closely re-capitulated the unfrozen community in both OD_{600} and sequencing results.

Community reproducibility, diversity, and preservation are essential questions to be addressed in the development of reproducible microbiome model communities. Developing a defined and reproducible synthetic microbial community, accounting for various starting organism ratios, and the ability to preserve communities for dissemination are key elements to aid reproducible microbiome sciences. Additionally, we have shown that our synthetic community can be used in EcoFAB devices to reproducibly study plant-microbe interactions in the rhizosphere. The methods and workflows developed here can be readily adapted for the design and study of other model communities and to standardize microbiome research.

2.5 Materials and Methods

2.5.1 Isolate selection

Isolates were selected from a collection obtained from the rhizosphere and soil surrounding a single switchgrass plant grown in marginal soils described elsewhere[253,254]. Isolates are available from the Leibniz Institute German Collection of Microorganisms and Cell Cultures GmbH (DSMZ) under accession numbers DSM 113524, DSM 113525, DSM 113526, and DSM 113527.

2.5.2 Soil isolate growth conditions

Individual isolates were grown in 3-5mL liquid cultures of 1X R2A media (Teknova, cat # R0005) in 14-mL culture tubes in aerobic conditions, 30 °C, without shaking. Isolates were allowed to grow for 5-7 days before diluting for community generation. 0.2X and 0.1X media was made by diluting 1X media with water purified by a Milli-Q water purification system and vacuum-filtering through a 0.22μM filter. Growth curves for individual isolates were conducted in 96-well plates. Isolates cultured in 1X R2A media were diluted to a starting OD_{600} of 0.05 in 200 uL of 0.1x R2A. Sterile R2A media served as the negative control.

2.5.3 Synthetic community growth conditions

Communities were grown in 200μL of liquid R2A media in 96-well plates in aerobic conditions, 30 °C, without shaking. To prevent condensation, each plate lid was coated with 3mL of an aqueous solution with 20% ethanol and 0.01% Triton X-100 (Sigma, cat # X100-100ML). Excess liquid was removed after 30 seconds and the lid was allowed to air-dry for 30min under a UV light for sterilization. To further prevent condensation, plates were set on 4 100mm-diameter Petri dishes (2 stacks of 2 dishes) filled with ~20mL water

each to generate a humid environment around the plates. Optical density readings at 600nm, to normalize isolates and monitor community growth, were taken with a Molecular Devices SpectraMax M3 Multi-Mode Microplate Reader (VWR, cat # 89429-536).

2.5.4 Synthetic community assembly using the CellenONE printer

Communities were assembled using a SCIENION CellenONE machine (https://www.scienion.com/). Individual isolate cultures were OD_{600}-normalized to 0.025 (after subtracting media blank), then transferred from a 384- or 96-well probe plate to a 96-well target plate using a CellenONE piezo dispense capillary (PDC) (size medium; Scienion, cat # P-20-CM) with droplet size set to 390-420 picoliters. The number of drops per isolate for each community was programmed by hand using the provided Scienion software (v1.92). The number of drops per organism for each ratio can be found in Table 2.3. Droplet integrity was confirmed before and after each isolate spotting run using the droplet camera and automated droplet detection. The PDC was cleaned between isolates by flushing the PDC interior with 0.5mL water. 200 drops of R2A were added to negative control wells as the last step in each experimental setup, to ensure no contamination occurred due to incomplete flushing of the PDC between isolates. For the community dynamics experiment, organisms receiving 2000 drops were added to communities with a multichannel pipettor.

2.5.5 Treatment with PMA to remove relic DNA

PMA (Biotium, cat # 40013) was added to communities to a final concentration of 10μM directly prior to sample collection (PMA-treatment); 5μL water (mock-treatment) was added to control communities. Communities were then incubated in the dark for 5 minutes at room temperature, then placed <15cm from a direct fluorescent light source

and incubated on ice for 30min. Communities were then frozen at -20 °C until processing for sequencing.

2.5.6 Plant colonization experiment

Brachypodium distachyon Bd21-3 seeds were dehusked, sterilized, and germinated on 0.1X Murashige and Skoog (MS) basal salt mixture M524 plates, pH 5.7 (Phyto Technology Laboratories) in a 250 µmol/m^2 s−1 16-hr light/8-hr dark regime at 24 °C for three days. EcoFABs were sterilized as previously described[180], and seedlings transferred to EcoFAB chambers filled with 0.1X MS at 3 days after germination. Twelve-day old plants were inoculated with an equally-mixed community of 17 or 18 bacterial isolates, as described above. To mix the community, the OD_{600} of each isolate was measured, with the assumption that OD_{600} of 1 is equal to ~10^9 CFU (colony-forming units)/mL[161]. Isolates were combined at 10^5 CFU/mL per isolate in the final EcoFAB volume. Plants were harvested seven days after inoculation. Microbial communities were detached from the plant root by vortexing the root in 0.1 phosphate-buffered saline (PBS) for 10 minutes at maximum speed, followed by centrifugation at 10000g, at 6 °C. DNA was extracted by using the Qiagen DNeasy PowerSoil Pro kit according to manufacturer's instructions (cat # 47014).

2.5.7 Community cryopreservation and re-growth

All community members were OD_{600}-normalized to 0.1 after 3 days of growth in 1X R2A and mixed equally to a final estimated total CFU count of 7.2*10^8 CFU. The community was then centrifuged (5000g, 5min) and resuspended in 4mL of 0.1X R2A media. 250µL of the community was inoculated into 4mL of 0.1X R2A, MS media (RPI, cat # M10200), or PBS + 10% sucrose (w/v) as the "unfrozen" control community. 500µL

of the community was mixed with 500µL of either 40% glycerol, 40% DMSO, or PBS with 20% sucrose (w/v). The glycerol and DMSO stocks were frozen immediately at -80 °C. The PBS with 10% sucrose stock was lyophilized on a Labconco FreeZone Plus Freeze Dry System (cat # 7386030) and then stored at -80 °C. Stocks were thawed after 3 days and 250µL of stock was inoculated into the same 3 types of media as the unfrozen community. Samples from all communities were frozen at -20 °C after 3 days of growth for 16S sequencing analysis.

2.5.8 DNA extraction and sequencing

DNA extracted with a kit was processed with the Qiagen DNeasy PowerSoil Pro kit according to manufacturer's instructions (cat # 47014). DNA extracted by boiling was processed by thawing community samples, transferring 100µL to a PCR plate, and heating the plate in a PCR machine at 100 °C for 10 minutes. 5µL of undiluted sample was used as DNA input for the 16S rRNA gene amplicon library protocol. 16S libraries for the cryopreservation, adjusted community ratios, PMA, and boil-extraction comparison experiments were prepared using 515F-806R primers according to the Earth Microbiome Project protocol[255] and sequenced on an Illumina MiSeq platform with a paired-end 150 V2 kit as previously described[256,257]. 16S libraries for the community dynamics experiment were prepared using 341F-805R primers (F 5'-CCTACGGGNGGCWGCAG-3' R 5'-GACTACHVGGGTATCTAATCC-3') and sequenced on an Illumina MiSeq platform with a paired-end 150 V2 kit. 16S libraries for the plant experiments were prepared using 515F-806R primers and sequenced on an Illumina NovaSeq platform with a paired-end 250 V2 kit. Shotgun metagenomics libraries for the human-/machine-assembled experiment were prepared using 1ng DNA input and Nextera XT indexes and

sequenced on an Illumina MiSeq platform with a paired-end 150 V2 kit. DNA sequences generated through this study are available on the NCBI Sequence Read Archive (BioProject ID PRJNA807292).

2.5.9 16S rRNA sequencing analysis and statistical analyses

All 16S sequences were analyzed using QIIME2[258] (v2020-11). Paired-end reads were joined using the “qiime vsearch join-pairs” command and quality-filtered and denoised (using default parameters) with Deblur[259]. Reads were trimmed as appropriate for quality for each experiment (150bp for human-/machine-assembled, cryopreservation, adjusted community ratios, and PMA experiments; 200bp for plant experiment). α- and β-diversity was calculated using the “qiime diversity” set of commands, with alpha rarefaction used to determine an appropriate sampling depth. Robust Aitchison distance was calculated using the DEICODE plugin[260]. Microbial taxonomy was assigned to the filtered sequences with the “qiime feature-classifier classify-sklearn” command, using a scikit-learn classifier created from a custom database of the 16S rRNA gene sequences for the isolates used in the study. Heatmaps and relative abundance plots were generated using R[261] (v3.3.2) with the packages dplyr[262], phyloseq[263], ggplot2[264], and scales[265]. β-diversity plots were generated using QIIME2. All other plots were generated using GraphPad Prism 7 software. All code used to process and analyze sequencing results can be accessed through Github at https://github.com/jkccoker/Soil_synthetic_community.

2.5.10 Shotgun metagenomics sequencing analysis

Shotgun sequencing data were quality-filtered during adapter trimming with Trimmomatic[266] (v0.36) using the settings “ILLUMINACLIP:NexteraPE-PE.fa:2:30:10

LEADING:10 TRAILING:10 SLIDINGWINDOW:4:15 MINLEN:36". Trimmed reads were aligned to a custom database of community strain genomes using bowtie2[267] (v2.2.3) using default settings. α- and β-diversity was calculated in phyloseq. β-diversity plots were generated using phyloseq. All other plots were generated using GraphPad Prism 7 software.

2.6 Acknowledgements

Chapter 2, in full, has been submitted as a manuscript for publication in the journal *mSystems*. Coker J, Zhalnina K, Martoz C, Thiruppathy D, Tjuanta M, D'Elia G, Hailu R, Mahosky T, Rowan M, Northen TR, Zengler K. A reproducible and tunable synthetic soil microbial community provides new insights into microbial ecology. *mSystems. Under review.* The dissertation author is the primary investigator and author of this material.

The development of the technologies and research described in this chapter were funded through Trial Ecosystem Advancement for Microbiome Science Program and the Microbial Community Analysis and Functional Evaluation in Soils (m-CAFEs) Science Focus Area Program at Lawrence Berkeley National Laboratory funded by the U.S. Department of Energy, Office of Science, Office of Biological & Environmental Research Awards DE-AC02-05CH11231. This material is also based upon work supported by the U.S. Department of Energy, Office of Science, Office of Biological & Environmental Research under Awards DE-SC0021234 and DE-SC0022137.

Chapter 3: A model synthetic skin microbial community allows investigation of cosmetics chemicals and the skin microbiome

3.1 Abstract

Human skin harbors diverse communities of microbes, the genomes of which makes up the skin microbiome. These microbial communities work with host processes to make up a first line of defense against pathogens and other skin disorders. Changes in the skin microbiome have been associated with multiple skin pathologies, such as acne, atopic dermatitis, or seborrheic dermatitis. Use of cosmetics, including make-up, deodorant, and skin care products, has also been associated with changes in skin microbiota. However, research into the impacts of these changes has been hampered by a lack of reproducible *in vitro* model communities. Here we present a reproducible synthetic skin community that can be assembled and grown in an efficient and high-throughput manner. We show the final diversity and composition of this community can be determined by minor adjustments in the starting inoculum. This system also allows the growth of *Cutibacterium acnes* in an oxic community setting, although in monoculture *C. acnes* is only able to grow in anoxic conditions. Finally, we use this community to assess the effect of four compounds commonly found in skin cosmetics on community growth and function. The detergents SLS, SLES, and rhamnolipid all decreased community growth and caused similar changes in community composition. The amino acid derivative creatine did not substantially alter community growth but did increase the relative abundance of *C. acnes* in certain conditions. In summary, this synthetic community can serve as a platform for reproducible *in vitro* skin microbiome investigations and as a first-pass system to screen the effect of topical compounds on the skin microbiome.

3.2 Introduction

In this study, we have used a picoliter liquid printer to create a 9-member bacterial community designed to represent the average human skin microbiome. We constructed these communities using a Scienion CellenONE-X1 pico-liter printing microfluidic device that uses piezo-electric technology to dispense pico-liter droplets at nanometer accuracy. This method ensures that the communities generated are defined, down to the number of cells added at the time of community construction, and highly reproducible. This method also supports high-throughput community production, allowing the study of many replicates relatively quickly and cheaply. We assemble communities from five different starting inoculum proportions and use shotgun metagenomic sequencing to assess the model community's alpha-diversity and taxonomic composition in an investigation of community dynamics. We then take one of these communities forward to test the effect of four chemicals commonly found in skin cosmetics on microbial growth and composition. This study both establishes a model skin microbial community that can be used for *in vitro* investigations and demonstrates its utility in assessing the effect of cosmetics chemicals on skin microbes.

3.3 Results

3.3.1 Selection and characterization of individual isolates

Although the composition of a healthy skin microbial community varies between body sites and individuals[194,195], the community is typically dominated by a few broad categories of microbes[194,197]. We therefore decided to construct a broadly representative synthetic skin microbial community using 9 highly bacterial strains found most frequently across most body sites[188,268]: *Cutibacterium acnes* (ATCC

KPA17202), *Staphylococcus epidermidis (*ATCC 12228)*, Staphylococcus aureus* (ATCC SA113)*, Staphylococcus hominis* (ATCC 27844, strain DM 122), *Staphylococcus capitis* (ATCC 27840, strain LK 499), *Staphylococcus warneri* (ATCC 27836, strain AW 25), *Streptococcus mitis* (ATCC 49456, strain NCTC 12261), *Corynebacterium afermentans* (ATCC 51403, strain CIP 103499 [LCDC 88199]), and *Micrococcus luteus* (ATCC 4698). We selected these strains as an initial starting point to construct the average skin microbiome, with the potential to further modify it as needed to represent specific body-site microbiomes.

We used OD600 based spectrometric measurements to characterize growth rates of the strains in isolation in complex media (Brain Heart Infusion, BHI) (Figure 3.1). Although the surface of the skin is exposed to oxygen, oxygen gradients in the skin allow the growth of anaerobic bacteria such as [187,188,269]. We therefore tested growth in both aerobic and anaerobic conditions for each strain. Aerobic growth was monitored for 72 hours, while anaerobic growth was monitored for 180 hours. All strains were able to grow aerobically and anaerobically except *C. acnes*, which grew only anaerobically. *S. warneri* grew to the highest maximum OD600 in both conditions, while *S. mitis* and *M. luteus* grew to the lowest maximum OD600 aerobically and anaerobically, respectively.

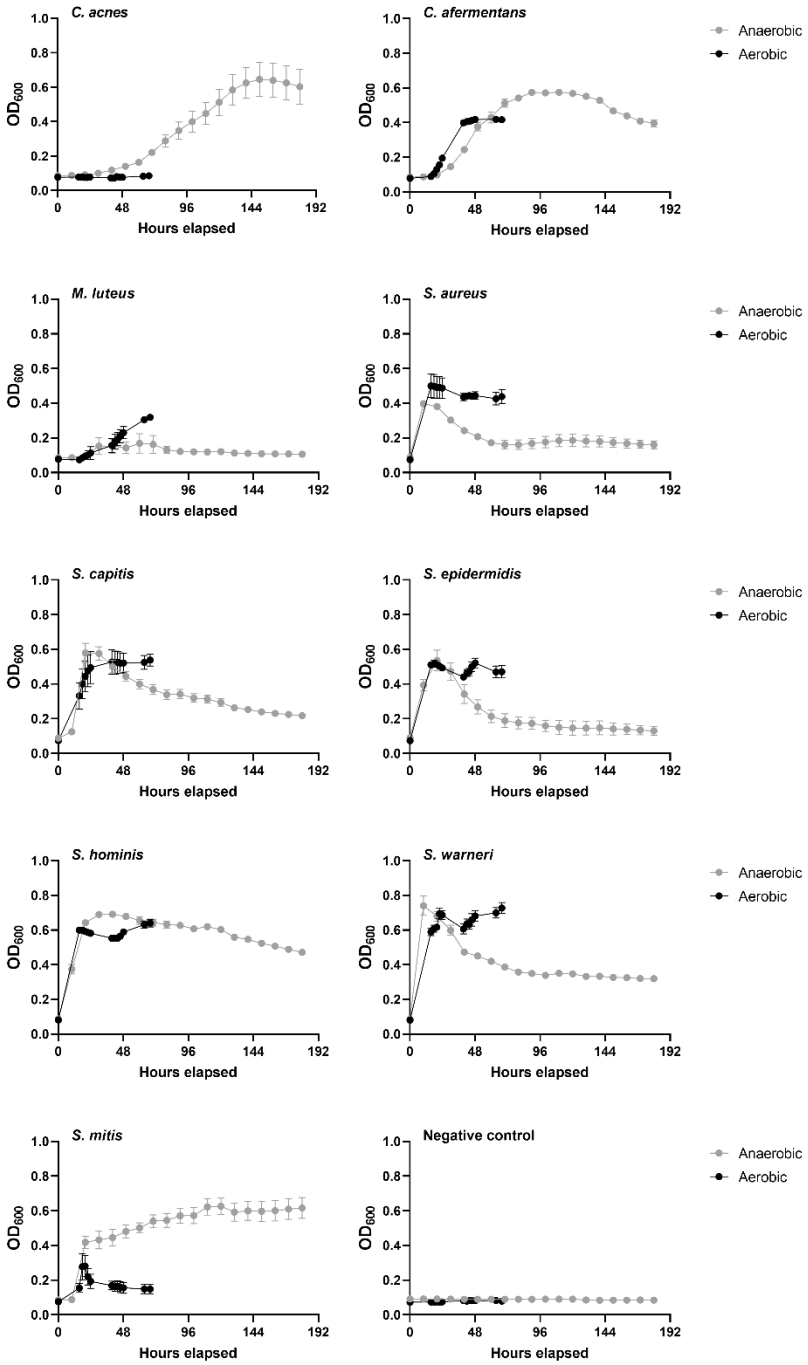

Figure 3.1 Growth curves of individual strains. Growth of individual strains in aerobic and anaerobic conditions, measured by OD600. Strains were grown in 200 uL of 1X BHI medium. Aerobic and anaerobic growth was monitored for 72 and 180 hr, respectively.

3.3.2 Combination of strains into a community

After characterizing the individual strains, we next sought to combine the strains into a community that would reach a stable OD600 and maintain a reasonable level of community diversity to model a diverse skin microbiome. We used BHI as the growth medium because all strains were able to grow in that medium. The isolates were combined into a community in a 1:1 ratio using a Scienion CellenONE liquid printing machine in an aerobic setting. This machine allows printing of liquid droplets in the picoliter size range with high precision and accuracy. Individual isolates were grown for 3 days in a liquid BHI culture, then diluted to OD = 0.065 after subtracting the value of blank media. 80 nanoliters of each diluted isolate (200 drops of 400 picoliters each) was then added to 200 uL of 1X or 0.1X BHI in a 96-well plate (n = 8 each). 80 nL of sterile BHI was added to negative control wells (n = 8). The plate was then grown in an anaerobic chamber maintained at 37 °C for 5 days, with OD600 readings taken approximately every hour for the first 48 hr and a final reading at 118 hr.

The OD600 readings showed very similar growth profiles within biological replicates, but different profiles between 1X and 0.1X BHI conditions (Figure 3.2A). The 1X BHI condition OD600 rose sharply within the first 10 hr before decreasing and maintaining a steady OD between 48-118 hr. The 0.1X BHI condition rose to a lower maximum OD than the 1X communities and maintained a steady OD between 24-48hr, but declined at some point between 48-118 hr.

We next conducted shotgun metagenomic sequencing of the 118-hr samples (n = 4 per condition) to assess community diversity and composition after 5 days of growth. The Shannon diversity index, a metric of alpha-diversity, showed that communities grown

in 0.1X BHI had significantly lower diversity than those grown in 1X BHI (Figure 3.2B). This is in contrast to results seen in our previous research with soil microbes (Coker et al 2022, in revisions), showing that diluted media can increase diversity in some communities. Analysis of the Bray-Curtis distance between samples showed a significant difference between 0.1X and 1X BHI communities (Figure 3.2C). We therefore looked at the taxonomic composition of the samples (Figure 3.2D). All communities in both conditions contained reads from all isolates except *C. afermentans*, indicating that 8 of the 9 starting isolates were able to survive and grow in the community. The 0.1X BHI communities had higher relative abundance of C. acnes, while 1X communities had higher *S. aureus, S. epidermidis*, and *S. mitis*.

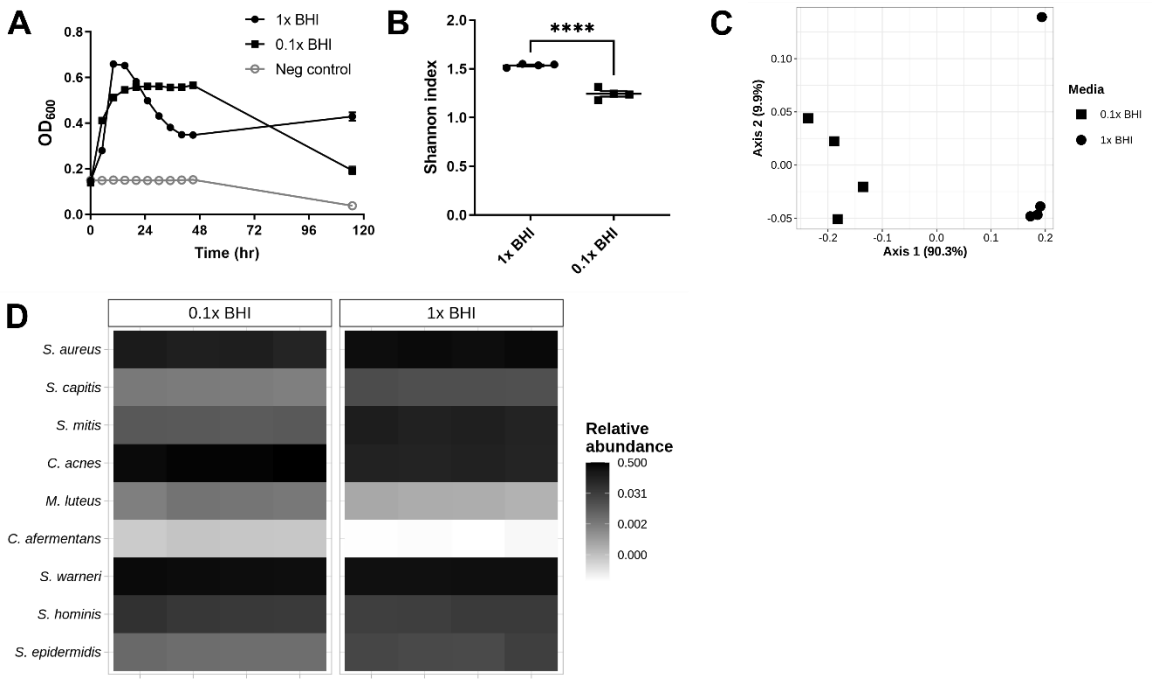

Figure 3.2 Combining isolates into a community in a 1:1 ratio. A) OD600 readings of communities grown in 0.1X or 1X BHI in anaerobic conditions (n = 8 per condition). Readings were taken every hour, but only every 5 hours are shown for clarity. B) Shannon diversity index of 1X and 0.1X BHI communities (n = 4 each). (Student's t-test, $p < 0.0001$). C) PCA of Bray-Curtis distance of 1X and 0.1X BHI communities (n = 4 each). (PERMANOVA, $p = 0.032$). D) Relative abundance of 1X and 0.1X BHI communities (n = 4 each).

3.3.3 Optimizing community diversity through strain starting ratios

Previous work in our group showed that alpha-diversity can be increased in a synthetic soil community by modifying the starting ratio of organisms from the traditional 1:1 combination (Coker et al 2022, in revision). We therefore generated community inoculums with 4 different starting ratios and compared the results to the equally-mixed (EM) community. The starting ratios were designed to have a lower amount of faster-growing organisms and a higher amount of slower-growing organisms, based on data from the isolate growth curves (Figure 3.1). The 2x and 3x cutoff starting proportions were determined by growth rate; the GC slope adjusted (GCS) starting proportions were determined by the slope of the isolate growth curve; and the GC time adjusted (GCT) starting proportions were determined by the time to halfway through the growth curve (Figure 3.3A). The absolute and relative proportions of the inocula are represented in Figure 3.3A, and the exact starting amounts can be found in Table 3.1.

Figure 3.3 Growth, diversity, and composition of skin community with varied starting ratios. A) Relative and absolute abundances of starting inoculum for each starting ratio. Absolute abundance is shown as the number of drops dispensed by the CellenONE printer. B) Growth profile of communities from different starting ratios (n = 8 per condition), in 1X and 0.1X BHI. Communities were grown anaerobically in 200 uL of liquid medium. C) Shannon diversity index of communities grown in 1X and 0.1X BHI (n = 4 per condition; Student's t-test, *** $p < 0.001$, **** $p < 0.0001$). D) PCA of Bray-Curtis distances between communities in 1X and 0.1X BHI. (PERMANOVA, $p < 0.001$) E) Heatmap of relative abundance of RPKM of communities grown in 1X and 0.1X BHI. Community starting ratio is indicated in the rug plot below the heatmap.

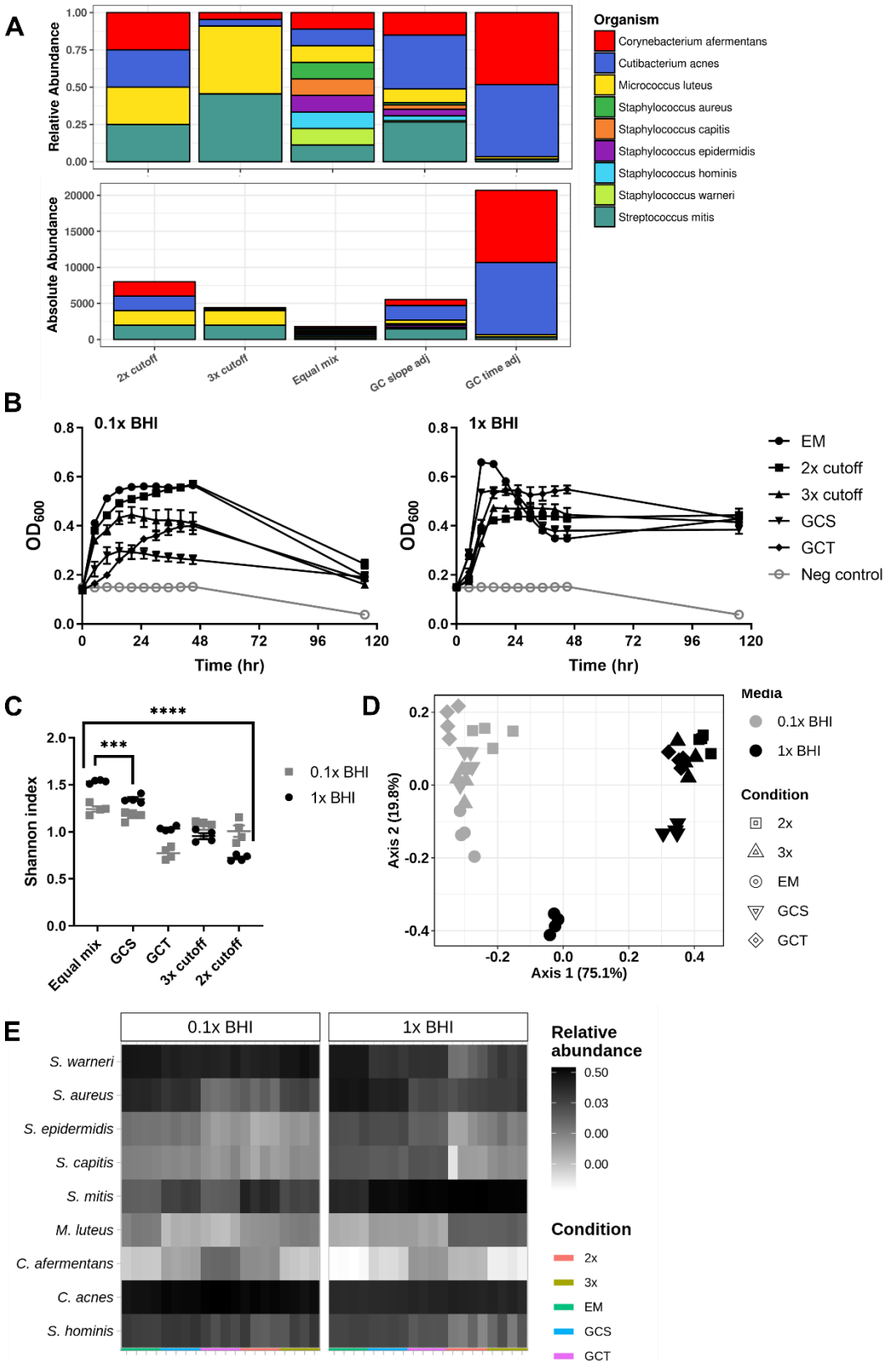
A
Relative Abundance
1.00
0.75
0.50
0.25
0.00
Absolute Abundance
20000
15000
10000
5000
0
2x cutoff
3x cutoff
Equal mix
GC slope adj
GC time adj
Organism
Corynebacterium afermentans
Cutibacterium acnes
Micrococcus luteus
Staphylococcus aureus
Staphylococcus capitis
Staphylococcus epidermidis
Staphylococcus hominis
Staphylococcus warneri
Streptococcus mitis
B
0.1x BHI
1x BHI
OD600
Time (hr)
EM
2x cutoff
3x cutoff
GCS
GCT
Neg control
C
Shannon index
****
***
Equal mix
GCS
GCT
3x cutoff
2x cutoff
0.1x BHI
1x BHI
D
Axis 2 (19.8%)
Axis 1 (75.1%)
Media
0.1x BHI
1x BHI
Condition
2x
3x
EM
GCS
GCT
E
0.1x BHI
1x BHI
S. warneri
S. aureus
S. epidermidis
S. capitis
S. mitis
M. luteus
C. afermentans
C. acnes
S. hominis
Relative abundance
0.50
0.03
0.00
0.00
Condition
2x
3x
EM
GCS
GCT

Table 3.1 Starting drops of skin strains in five different community inoculum ratios.

Organism	Equal mix	2x cutoff	3x cutoff	GC[a] slope adjusted	GC[a] time adjusted
C. afermentans	200	2000	200	835	10000
C. acnes	200	2000	200	2000	10000
M. luteus	200	2000	2000	510	304
S. aureus	200	2	2	83	3
S. capitis	200	2	2	161	27
S. epidermidis	200	2	2	242	7
S. hominis	200	2	2	178	9
S. warneri	200	2	2	54	6
S. mitis	200	2000	200	1472	319

[a] GC = growth curve

Communities were constructed in the same manner and grown in the same conditions as described for the EM community. The EM community grew to the highest maximum OD600 in both 1X and 0.1X BHI, but all communities displayed a similar final OD600 (Figure 3.3B). The GCS community had the lowest maximum OD600 in 0.1X BHI but the second-highest in 1X BHI. On the other hand, the 2x cutoff community had the lowest OD600 in 1X BHI but the second-highest in 0.1X BHI. Alpha-diversity was significantly different between the different starting ratios, with the highest diversity in the EM communities and the lowest in the 2x cutoff communities (Figure 3.3C). Communities were significantly different by Bray-Curtis distance between 0.1X and 1X BHI (Figure 3.3D).

When choosing a community for future studies, we evaluated factors of both alpha-diversity and taxonomic composition. The EM community in 1X BHI had the highest alpha-diversity, but it also contained the highest abundance of *S. aureus* of all communities (Figure 3.3E). *S. aureus* is a common source of skin infection and has been correlated with skin diseases such as atopic dermatitis (Khadka 2021, Domenico 2019, Byrd). Furthermore, the EM community grew quickly to a high maximum OD600 in 1X BHI but then dropped rapidly, suggesting the community undergoes rapid growth and death in contrast to the steady state of the skin microbiome. We therefore decided to pursue further experiments with the GCS community in 1X BHI. The GCS community has a similar alpha-diversity to the EM community, but a lower abundance of *S. aureus* and a more stable OD600 growth profile.

3.3.4 Effect of cosmetics chemicals on community growth and diversity

Following optimization of the skin community diversity and composition with the GCS community, we next sought to use this community to evaluate the effect of chemicals commonly found in cosmetics on skin microbes. As investigation of the skin microbiome has highlighted its role in skin health and dermatological conditions, the effect of skin cosmetics on the microbiome has been increasingly studied[193,270,271]. However, there is no unified system for testing the effect of compounds in skin products on the microbiome. Synthetic communities offer a quick and cost-effective way to predict how these compounds will affect skin microbes.

We therefore grew the GCS community in the presence of 4 compounds commonly found in skin and personal hygiene products: sodium laurel sulfate (SLS, also known as sodium dodecyl sulfate), sodium laureth sulfate (SLES), rhamnolipid (RL), and creatine (Crt) (Figure 3.4A). SLS is an anionic detergent that produces the cleansing effect of many soaps and shampoos and is commonly used as an inducing agent in models of irritant contact dermatitis[272]. SLES is also an anionic detergent, thought to be less harsh on skin than SLS, although it can still cause irritation[273]. Rhamnolipids are a group of surfactants produced in various forms by several types of bacteria, most notably *Pseudomonas aeruginosa*. Rhamnolipids are generally regarded as less toxic, more biodegradable, and more environmentally-friendly than detergents like SLS and SLES[274]. Creatine is a compound made naturally by the human body and involved in energy homeostasis in cells[275]. Topical application of creatine is thought to improve skin cellular health and decrease wrinkles[275–277]. To study the effect of these compounds on the skin microbiome, each compound was added to the community in 2-

3 concentrations (*w/v*) either at the point of inoculation (0 hr of growth) or after 24 hr of community growth, to simulate applying the compound to an established skin microbiome (Figure 3.4A). The communities were then incubated aerobically for 72 hr before processing for sequencing. Aerobic incubation was used because the area of the skin to which products are normally applied is an oxic environment.

Figure 3.4 Effect of skin product compounds on synthetic community growth and composition. A) Schematic of skin compound experiment. Compounds were added at either time of inoculation (0 hr) or 24 hr post-inoculation; the time compounds were added is marked with a red arrow. Compounds were added in 2-3 concentrations (w/v) (n = 4 per condition). Compound structures are shown on the right. B) Community growth in the presence of the compounds, as measured by OD600. A black arrow marks the time of compound addition for each plot. The growth profile of the community without any compounds (Community alone; blue line) is provided on each plot for reference. C) Changes in community taxonomic composition in the presence of rhamnolipid and creatine, as determined by shotgun metagenomic sequencing. RPKM of the indicated compound and concentration (Creatine 0.1%, Rhamnolipid 0.5%), added at 0h or 24h, is plotted against RPKM of the community alone. The gray dotted line represents no change between communities (x = y). The blue line represents a linear regression of the community comparison, with a 95% confidence interval indicated by the shaded gray area. RPKM is averaged between the 4 replicates for each condition, with error bars representing the standard error of the mean. D) Growth of C. acnes alone in the same conditions as the community was grown in, measured by OD600 (n = 4). E) Volcano plot of RPKM fold-change between creatine or rhamnolipid (all concentrations combined) and control community. Dotted gray line indicates fold-change of 0. Vertical red line indicates fold-change of 2. Horizontal red linen indicates p-value = 0.05. Samples with significance below $p < 0.05$ are labeled.

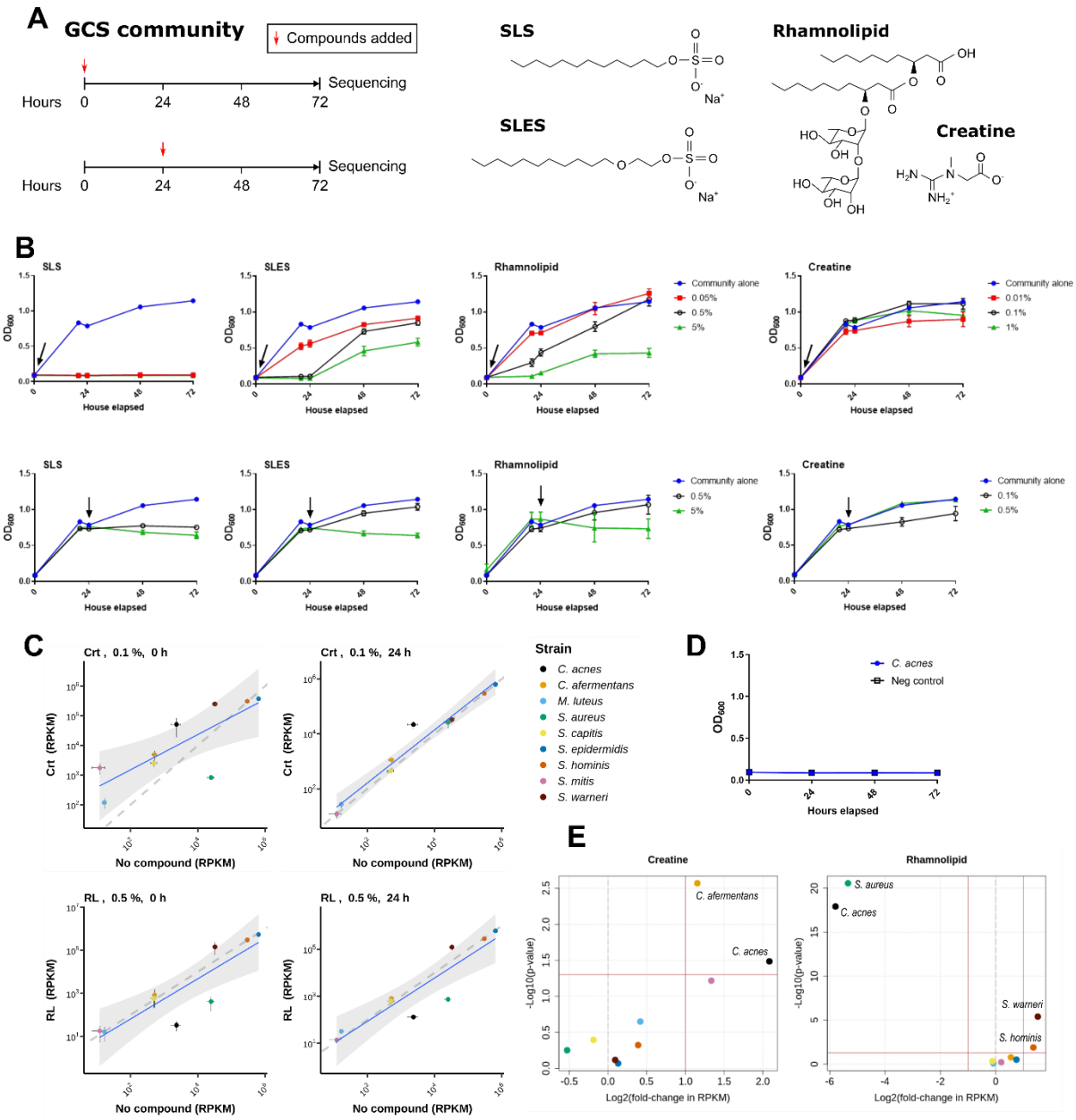
A
GCS community
Compounds added
Hours 0 24 48 72
Sequencing
SLS
SLES
Rhamnolipid
Creatine
B
SLS
SLES
Rhamnolipid
Creatine
OD600
House elapsed
Community alone
0.05%
0.5%
5%
0.01%
0.1%
1%
C
Crt , 0.1 %, 0 h
Crt , 0.1 %, 24 h
RL , 0.5 %, 0 h
RL , 0.5 %, 24 h
Crt (RPKM)
RL (RPKM)
No compound (RPKM)
Strain
C. acnes
C. afermentans
M. luteus
S. aureus
S. capitis
S. epidermidis
S. hominis
S. mitis
S. warneri
D
C. acnes
Neg control
OD600
Hours elapsed
E
Creatine
Rhamnolipid
-Log10(p-value)
Log2(fold-change in RPKM)
C. afermentans
C. acnes
S. aureus
S. warneri
S. hominis

SLS prevented all microbial growth when added at time of inoculation or at 24 hr post-inoculation, even at the lowest concentration of 0.05% (Figure 3.4B). SLES and RL inhibited microbial growth in a dose-dependent manner when added at time of inoculation, with SLES having a more severe effect than RL. SLES and RL prevented further microbial growth upon 5% treatment at 24 hr, although 0.5% treatment did not have a strong effect on growth. Creatine treatment did not cause strong and consistent changes in the growth profile of the community. Microbial growth was lower in 0.01% at inoculation and 0.1% at 24 hr conditions, but these changes were not significant.

We next investigated the effect of these compounds on skin community composition. We focused our investigation on the RL and Crt conditions, as these compounds allowed substantial community growth in almost all treatment conditions. By comparing the reads per kilobase million (RPKM) for communities treated with a compound to the RPKM for the community alone, we were able to determine which organisms increased or decreased in normalized abundance upon treatment (Figure 3.4C). Each plot also contains a dotted gray line, representing the line expected if there are no changes between the communities (x = y), and a blue line with shaded gray area, representing a linear regression of the data and a 95% confidence interval (CI). Points within the CI were considered to not change significantly between conditions.

Crt (0.1%) applied at 0h caused many changes in community composition, although only the change in *S. aureus* places it outside the 95% CI. In contrast, when Crt (0.1%) was applied at 24h, the only community change observed was an increase in *C. acnes* RPKM. Remarkably, this increase in *C. acnes* occurred despite the aerobic growth conditions. We tested the growth of *C. acnes* alone in the same aerobic conditions and

saw no growth, as expected (Figure 3.4D). RL (0.5%) application also caused changes in community RPKM composition, most notably a decrease in *C. acnes* and *S. aureus* and an increase in *S. warneri.* The same changes were observed when applied at 0h and 24h. The composition changes observed with RL were similar to the changes observed with SLS and SLES (Figure 3.5).

To confirm the statistical significance of these noted changes in community RPKM, we tested for differential abundance using DESeq2[278]. DESeq2 analyzes raw sequencing reads to test for differential abundance using a negative binomial distribution and reports the $\log_2$ fold-change in RPKM between tested conditions (in this case, creatine vs control communities or rhamnolipid vs control communities) and a p-value for each fold-change. Analyzing these results in a volcano plot showed that the *C. acnes* was approximately 4-fold more abundant in communities grown with creatine (Wald test, $p = 0.033$) (Figure 3.4E). *C. afermentans* was also identified as significantly more abundant in creatine samples, by approximately 2-fold (Wald test, $p = 0.002$). In contrast, *S. aureus* and *C. acnes* were approximately 6-fold less abundant in rhamnolipid samples, while *S. warneri* and *S. hominis* were 2-3 fold more abundant.

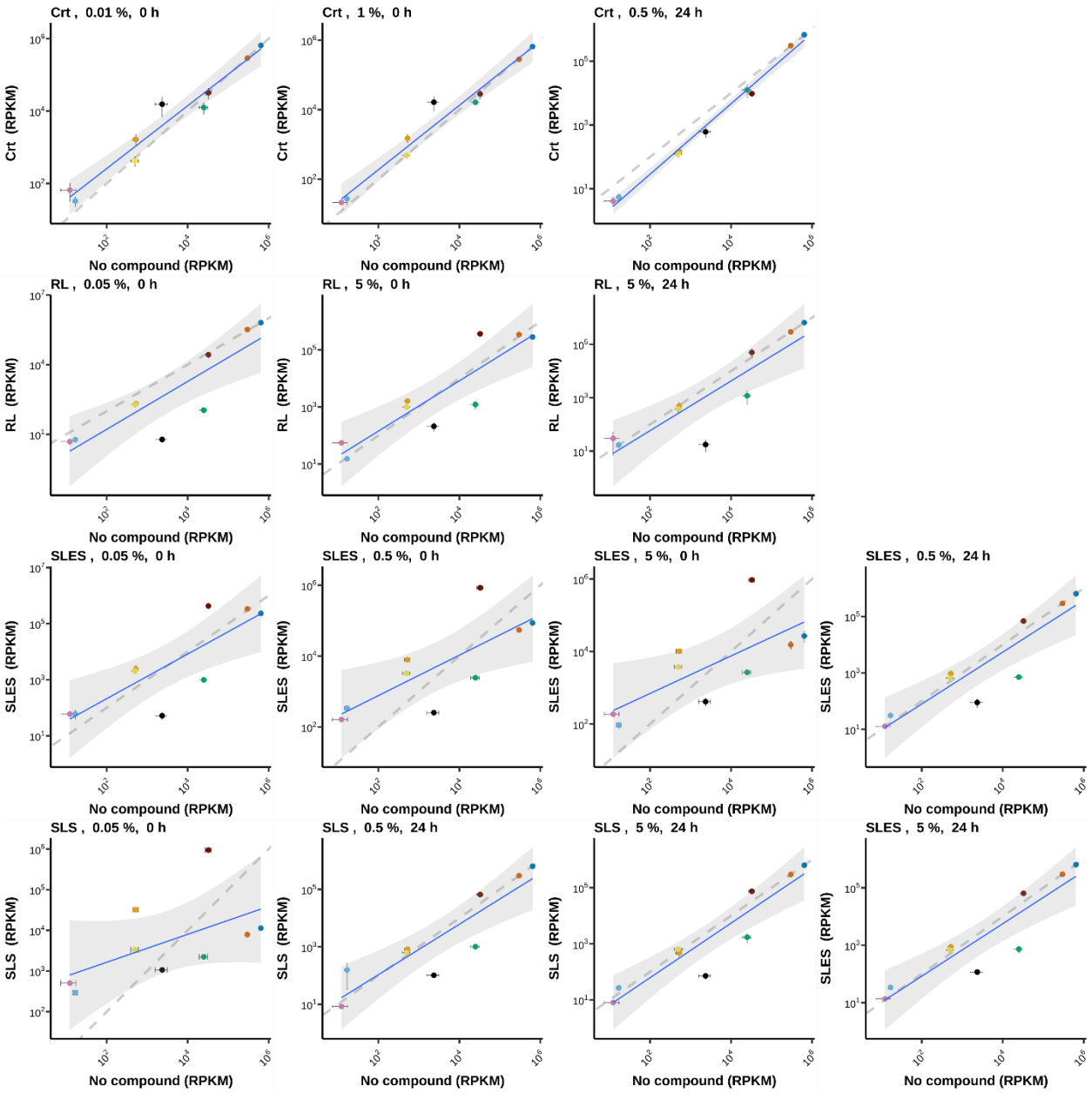

Figure 3.5 Supplement to Figure 3.4. Changes in community composition in the presence of skin product compounds. RPKM of the compound, concentration, and time of compound addition (as indicated by each plot title) is plotted against RPKM of the community alone. The gray dotted line represents no change between communities (x = y). The blue line represents a linear regression of the community comparison, with a 95% confidence interval indicated by the shaded gray area. RPKM is averaged between the 4 replicates for each condition, with error bars representing the standard error of the mean.

3.4 Discussion

The skin microbiome is enormously important for skin health but extremely difficult to study effectively. In this study, we developed a model synthetic skin community and optimized its reproducibility, composition, and diversity in our *in vitro* system. We then used this community to test the effect of four compounds commonly found in cosmetics products on *in vitro* community growth and composition. Of the nine starting microbes, eight can be reliably identified in all experiments through shotgun metagenomic sequencing. *C. acnes* grew to a large proportion of the community in anaerobic conditions, but surprisingly it was also able to grow (to a smaller proportion) in fully aerobic conditions when mixed with other members of the community, despite the presence of oxygen and the lack of hemin-Vitamin K supplementation usually required. We hypothesize that the non-shaking conditions under which the communities were grown allowed the microbes to form an oxygen gradient within each well, with less oxygen at the bottom of the well. *C. acnes*, as an aerotolerant anaerobe, could then have been able to grow at the bottom of each well. The community setting likely provided the supplemental nutrients that have to be provided exogenously when *C. acnes* is grown in isolation.

Unlike previous findings that growing communities in nutrient-limited conditions can increase alpha-diversity, we achieved highest alpha-diversity growing our community in the complex rich growth medium of undiluted BHI. We also found that the amount of *S. aureus* in the community could be changed by adjusting the starting inoculum proportions. *S. aureus* is a common member of the skin microbiome, but its presence and an imbalance of *S. aureus* and *S. epidermidis* has been associated with disease such as

atopic dermatitis[189,279]. We therefore decided to pursue further experiments with the GCS skin community, which contained a mid-level amount of *S. aureus*.

SLS, SLES, and RL are molecules included in skin products for their detergent/surfactant properties, in order of decreasing harshness on skin. Treatment of the skin community with the detergent SLS prevented all microbial growth even in very small doses, as expected from previous work on the harsh effects of this detergent (refs needed). Treatment with SLES also inhibited community growth in our *in vitro* setting, although to a lesser extent than SLS. This indicates that although SLES is a “gentler” compound than SLS, it likely still has an inhibitory effect on skin microbe growth. Rhamnolipid also inhibited community growth, although to an even lesser extent than SLES. All three of these compounds caused similar changes in community composition profiles (Figure 3.4C, Figure 3.5), most notably a decrease in the proportion of *S. aureus* and *C. acnes* and increase in *S. warneri.*

Strikingly, treatment with creatine increased the RPKM of *C. acnes*. *C. acnes* can be both a commensal and pathogenic member of the skin community, depending on the virulence factors carried by an individual strain[279,280]. This effect on *C. acnes* could play a role in the advertised benefits of creatine in skin care products. Further investigations are needed to confirm the health effect and mechanism of creatine treatment on skin health and the microbiome.

In summary, the model synthetic skin community presented here can serve as an efficient and high-throughput first-pass system to get an idea of the effect of compounds on the skin microbiome. Promising compounds can then be further investigated through

more developed *ex vivo* skin and/or animal models to further elucidate their impact on the skin microbiome.

3.5 Materials and Methods

3.5.1 Isolate growth conditions

All strains were purchased from ATCC. Strains were streaked out on Brain-Heart Infusion (BHI; Millipore Sigma 53286) agar plates prior to making glycerol stocks to confirm purity of the individual organisms. Individual strains were cultured in sterile BHI broth at 37 C, without shaking. 1X BHI was made as directed by manufacturer instructions (37 g BHI powder in 1 L water). 0.1X and 0.2X BHI were made by diluting 1X BHI with sterile water. For anaerobic conditions, BHI broth was anoxified by bubbling with N2 and CO2, then the container was sealed and the headspace exchanged with N2 and CO2. L-cysteine (Sigma Aldrich 168149) was added to final concentration 2 mM directly before culturing. For *C. acnes* cultures, hemin and vitamin K (Spectrum Chemical Mfg Corp, 743-23178) were added in a 1:100 dilution from the sterile stock directly before culturing.

3.5.2 Community assembly with CellenONE printer

Individual strains were diluted in BHI to an OD600 of 0.07 after subtracting the blank reading. This OD was confirmed by eye to have 4-5 cells/drop using the CellenONE camera. Aerobic optical density readings at 600nm, to normalize isolates and monitor community growth, were taken with a Molecular Devices SpectraMax M3 Multi-Mode Microplate Reader (VWR, cat # 89429-536). The diluted strains were loaded into a 384-well “probe” plate, one strain per well. The CellenONE X1 liquid printer (SCIENION US Inc., Phoenix, AZ) was programmed to pick up 30 uL from a well of the probe plate and dispense the appropriate number of drops (see Table 3.1) in the appropriate wells of a

96-well “target” plate, which was preloaded with 200 uL BHI/well. Droplet integrity was confirmed before and after each spotting run using the droplet camera and automated droplet detection. The PDC was cleaned between isolates by flushing the PDC interior with 0.5mL water. 200 drops of BHI were added to negative control wells as the last step in each experimental setup, to ensure no contamination occurred due to incomplete flushing of the PDC between strains.

3.5.3 Community growth conditions

Communities were grown in 200 uL of BHI broth in 96-well plates, 37 C, without shaking. To prevent condensation, each plate lid was coated with 3mL of an aqueous solution with 20% ethanol and 0.01% Triton X-100 (Sigma, cat # X100-100ML). Excess liquid was removed after 30sec and the lid was allowed to air-dry for 30min under a UV light for sterilization. Also, to prevent condensation, plates were set on 4 100mm-diameter Petri dishes (2 stacks of 2 dishes) filled with ~20mL water each to generate a humid environment around the plates.

Community plates grown anaerobically were incubated in a vinyl anaerobic chamber (Coy Lab Products) with an atmosphere of N2/CO2/H2 (85/10/5%). Plates were maintained at 37 °C and underwent OD600 readings in a Molecular Devices SpectraMax i3 spectrophotometer with a StakMax Microplate Handling System.

3.5.4 Community growth with cosmetic compounds

SLS, SLES, RL, and creatine compounds were obtained from Evonik Industries (https://corporate.evonik.com/en). For compounds added at time of inoculation, compounds were diluted to the indicated concentration (*w/v*) in 1X BHI and loaded into the target plate prior to community spotting, 150 uL/well. Communities receiving

compounds at 24 hr post-inoculation were spotted into plain 1X BHI. For compounds added at 24 hr post-inoculation, compounds were diluted to 4X the indicated concentration in 1X BHI. 50 uL of 4X compound was then added to the appropriate wells, bringing the well volume to 200 uL. 50 uL of plain BHI was added to communities that received compounds at time of inoculation. All compound solutions were sterilized by syringe-filtering across a 0.22 um filter before addition. Community plates were grown aerobically for 3 days. Plates were then stored at -20 °C until processing for sequencing.

3.5.5 Shotgun metagenomics library preparation and sequencing

DNA was extracted from community samples using a Qiagen DNeasy PowerSoil Pro Kit (Qiagen 47016) according to manufacturer's instructions with the following noted change. Samples were heated for 10 min at 100 °C after addition of lysis buffer and prior to vortexing. Following extraction DNA was quantified with Qubit dsDNA, high sensitivity (ThermoFisher Q32851) and normalized to 0.2 ng/uL. Shotgun metagenomic sequencing libraries were prepared using the Nextera XT DNA Library kit with 1 ng DNA input, according to manufacturer's instructions (Illumina FC-131-1096 and FC-131-2001). Libraries were quantified using Qubit as above and normalized to 2 ng/uL for sequencing, then sequenced on an Illumina MiSeq platform with a paired-end 150 V2 kit (Figure 3.2 and 3 data) or a paired-end 100 V2 kit (Figure 3.4-3.5 data).

3.5.6 Metagenomics sequencing analysis

Reads from raw FASTQ files were processed with Trimmomatic (v0.36) to remove adapters and trim low-quality base calls using the parameters "ILLUMINACLIP:NexteraPE-PE.fa:2:30:10 LEADING:10 TRAILING:10 SLIDINGWINDOW:4:15 MINLEN:36". Trimmed reads were first aligned to the

minikraken2 database to exclude possible contamination from non-community organisms. Following this, trimmed reads were aligned to a custom database of community strain genomes using bowtie2 (v2.2.3) using default settings and read counts were transformed into RPKM. Alpha- and beta-diversity was calculated in phyloseq. Beta-diversity plots were generated using phyloseq, and beta-diversity significance testing was done in R with the package vegan. Volcano plots were generated in base R (v4.3.0) using data from DESeq2[278]. All other plots were generated using GraphPad Prism 8 software. Code used to process and analyze sequencing data can be found on Github (https://github.com/jkccoker/Skin_synthetic_community/tree/main).

3.6 Acknowledgements

Chapter 3, in full, is being prepared as a manuscript for submission for publication of the material. Coker J, Thriuppathy D, Flores-Ramos S, Marotz C, Tjuanta M, Zengler K. A model synthetic skin microbial community allows investigation of cosmetics chemicals and the skin microbiome. *In preparation.* The dissertation author is the primary investigator and author of this material.

We thank Peter Lersch and Tobias Blattert for their invaluable input and advice about the experiments reported here.

Chapter 4: Removal of the endothelial non-human sialic acid Neu5Gc reduces atherosclerosis

4.1 Abstract

Cardiovascular disease (CVD) remains the leading cause of death worldwide, despite decades of research and hundreds of drugs developed to combat it. Red meat consumption is a major risk factor for atherosclerosis, the most common cause of CVD in humans. Red meat is heavily enriched in the non-human sialic acid *N*-glycolylneuraminic acid (Neu5Gc), which can be recycled by human enzymes to place Neu5Gc on our own glycoconjugates. This Neu5Gc is enriched in the endothelium and invokes an inflammatory response known as xenosialitis due to anti-Neu5Gc antibodies present in all people. This inflammatory response significantly promotes atherosclerosis development in a humanized mouse model with Neu5Gc-feeding and induction of anti-Neu5Gc antibodies, recapitulating the human condition. The aim of this study is to investigate the effect of removing endothelial Neu5Gc after consumption of a Neu5Gc-rich diet in a mouse model. Removal of Neu5Gc with a Neu5Gc-preferential sialidase is expected to reduce endothelial inflammatory responses and therefore decrease atherosclerosis development. Here we show the Neu5Gc-preferential Sialidase26 (Sia26) can be used to effectively remove Neu5Gc from the cell surface *in vitro* and *in vivo*. We also establish intravenous injection as the optimal route of Sia26 delivery in this system and show significantly decreased aortic Neu5Gc following Sia26 injection, with sialic acid repopulation 24-48 hours after injection. Studies are currently ongoing to determine the efficacy of long-term injection of Sia26 to reduce atherosclerosis in this model. If successful, this will suggest an exciting new approach to atherosclerosis treatment in populations with significant red meat consumption.

4.2 Introduction

Red meat consumption has long been linked to an increased incidence of several diseases, including cancer[281] and cardiovascular disease (CVD), the leading cause of death worldwide[282,283]. In humans, CVD events are primarily caused by complications of atherosclerosis, the narrowing of arteries from plaque buildup in artery walls[284]. Surprisingly, non-human mammals with risk factor profiles similar to humans only rarely develop CVD due to atherosclerosis, including non-human primates and carnivores with red-meat heavy diets[285–287]. Atherogenesis is a multifactorial process, driven by a mix of genetic, lifestyle, and physiologic factors[288], but the human-specific link between CVD and read meat consumption remains an unanswered question[289].

The evolutionary loss of the CMP-N-acetylneuraminic acid hydroxylase (CMAH) enzyme in hominins 2-3 million years ago rendered humans unable to produce the sialic acid *N*-glycoylneuraminic acid (Neu5Gc)[286,290]. Sialic acids (Sia) act as the terminal carbohydrate on most extracellular glycoconjugates[291,292] and are essential for numerous cellular processes such as cell adhesion, immune system signaling, embryogenesis, and brain development[292–294]. The loss of CMAH means humans can only produce *N*-acetylneuraminic acid (Neu5Ac), in contrast to most mammals that can produce both Neu5Ac and Neu5Gc. However, small amounts of Neu5Gc are found in human tissues due to incorporation from foods containing Neu5Gc, particularly red meat[295–297].

The Neu5Gc in human tissues has been implicated in many immune-related conditions due to anti-Neu5Gc antibodies that all humans possess[298–300]. Anti-Neu5Gc antibodies have long been known to be involved in acute immune reactions,

such as serum sickness and xenotransplant rejection[301–303], and have more recently been associated with chronic inflammatory diseases such as cancer[297,304–307] and atherosclerosis[308,309]. A *Cmah*$^{-/-}$ mouse model of atherosclerosis in a *Ldlr*$^{-/-}$ background showed that feeding a Neu5Gc-containing diet to animals immunized against Neu5Gc-containing glycans led to a significant 3-fold increase in atherosclerosis lesion volume and 5-fold increase in necrotic core size, compared to mice immunized against Neu5Ac or Neu5Gc-immunized mice without Neu5Gc feeding[308]. Furthermore, a second study showed that the effect of dietary Neu5Gc on atherosclerosis can be attenuated by feeding with Neu5Ac, to compete with the Neu5Gc for glycoconjugate incorporation[309]. However, these studies did not address if removal of Neu5Gc after it has been incorporated into endothelial glycoconjugates can attenuate atherosclerosis development.

In this study, we investigate the potential of a Neu5Gc-prefential sialidase, Sialidase26 (Sia26)[310], to attenuate atherosclerosis by removing Neu5Gc from endothelial glycans. Sia26 is a microbial sialidase isolated from the gut microbiome of *Cmah*$^{-/-}$ mice on a Neu5Gc-rich diet. We characterize the ability of Sia26 to remove cell-surface Neu5Gc both *in vitro* and *in vivo* and optimize Sia26 dosing strategy in the *Cmah*$^{-/-}$*Ldlr*$^{-/-}$ mouse model. Studies are currently ongoing to investigate the ability of Sia26 to attenuate atherosclerosis with regular injections in mice on a Neu5Gc-rich diet. This experimental system models treatment of humans to reduce atherogenesis after consuming a red meat-heavy diet. These studies investigate an exciting new avenue of atherosclerosis treatment designed to help individuals with red meat in their diets.

4.3 Results

4.3.1 Sialidase26 removes sialic acids *in vitro* and *in vivo*

All previous work characterizing Sia26 activity was done *in vitro*. We first confirmed the Gc-preferential activity of Sia26 using the same assay reported in Zaramela et al[310] (Figure 4.1A). We next investigated whether Sia26 could remove Neu5Gc from mammalian cells in an *in vitro* cell culture system. Murine embryonic fibroblasts were treated with increasing amounts of Sia26 (0.1-1 µg) or heat-inactivated Sia26 (1 µg) for 30 min. Treatment with Sia26 decreased cell-surface Neu5Gc in a dose-dependent manner, with 1 µg removing about 25% (Figure 4.1B). The amount of cell-surface sialic acid does not decrease linearly with treatment dose, which could indicate that not all sialic acids are accessible to the enzyme in this system.

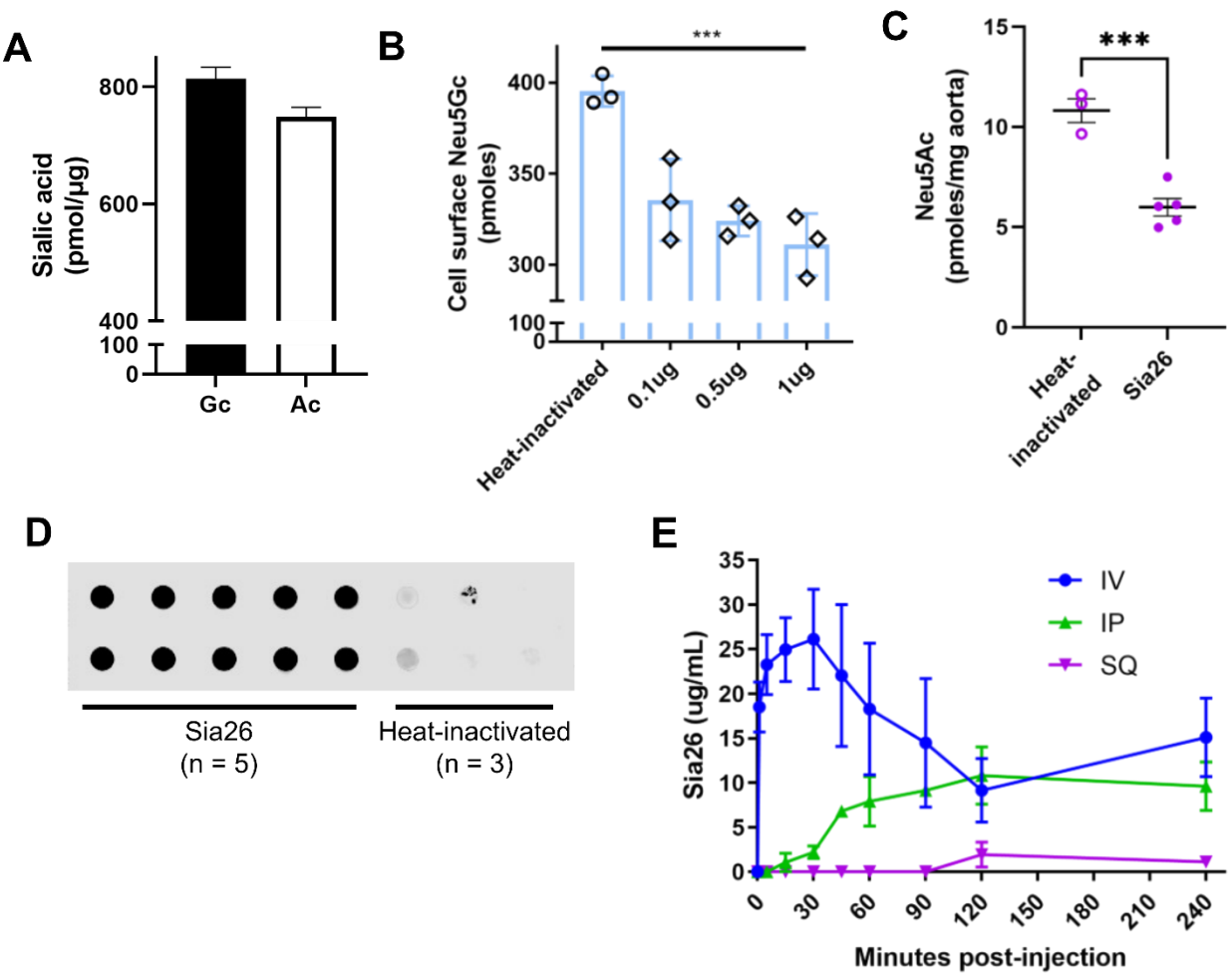

Figure 4.1 *In vitro* and *in vivo* removal of sialic acids. A) Sia26 *in vitro* activity assay using 0.5ug. A mix of Ldlr-/- and Cmah-/-Ldlr-/- mouse plasma with similar amounts of bound Neu5Ac/Neu5Gc was used as substrate (n = 3 independent replicates). B) Sia26 release of cell-surface Neu5Gc. Cultured MEF cells were treated with increasing amounts of Sia26 for 2hr, then washed and treated with trypsin (n = 3 independent replicates). The trypsin supernatant was collected and analyzed for Neu5Gc content. Heat-inactivated cells were treated with 5ug Sia26 incubated at 100 °C for 10min. C) Sia26 release of *in vivo* aortic sialic acid. *Cmah*$^{-/-}$*Ldlr*$^{-/-}$ mice were injected IV with 50ug of Sia26. The thoracic aorta was collected 2hr later and analyzed for sialic acid content (n = 3-5 each). D) Example of a dot blot for Sia26 from mouse plasma samples. E) Sia26 plasma clearance following injection. *Cmah*$^{-/-}$*Ldlr*$^{-/-}$ mice were injected with 50ug Sia26 via the IV, IP, or SQ route (n = 3 each). Plasma samples were collected at time of injection and out to 240min post-injection. A control group of mice was injected with 50ug heat-inactivated Sia26 IV; the average signal from this group at each time point was subtracted from the experimental groups.

We next sought to determine if Sia26 would have a similar effect on *in vivo* endothelial sialic acid as in the *in vitro* cell culture system. *Cmah*$^{-/-}$*Ldlr*$^{-/-}$ mice were injected intravenously with 50 µg active or heat-inactivated Sia26; the thoracic aorta was isolated 2 hr post-injection and analyzed for sialic acid content. Sia26 acutely reduced aortic sialic acid by about 50%, a greater effect than observed in the cell culture system (although the dose was also much larger) (Figure 4.1C). In this experiment the mice were not fed a Gc-enriched diet, so no Neu5Gc was detected in the endothelium. These studies show that Sia26 can remove sialic acids from the cell surface and from the endothelium in particular, as would be required for removing endothelial Neu5Gc to prevent xenosialitis.

4.3.2 Intravenous injection provides optimal Sia26 dosing strategy

To determine the best way to administer Sia26 to mice, we injected WT mice with 50 µg Sia26 intravenously (IV), intraperitoneally (IP), or subcutaneously (SQ). Plasma samples were collected at 1, 5, 15, 30, 45, 60, 90, 120, and 240 min after injection. Sia26 signal was determined via dot blotting and quantified by comparing to a standard curve of purified protein; an example blot is shown in Figure 4.1D. Control mice were injected IV with heat-inactivated enzyme, and the resulting background signal was subtracted from the experimental data. As expected, results showed that IV injection produces the highest peak levels of Sia26 in the blood, with peak levels detected on average at 45 min. However, protein was detectable in the blood out to 240 min. IP and SQ injection showed significantly lower levels of protein in circulation. We therefore decided to pursue all future experiments with IV injections.

4.3.3 Sia26 removes endothelial Neu5Gc in a dose-dependent manner

We next investigated the appropriate dose of Sia26 to acutely remove Neu5Gc from the aortic endothelium. WT mice were injected with doses from 3-25 µg active Sia26 or 25ug of heat-inactivated Sia26 (“0 µg”, control condition). The thoracic aorta was collected 2 hr post-injection and analyzed for sialic acid content. Sia26 acutely removed sialic acids from the aorta in a dose-dependent manner, with up to 15 pmol of Neu5Gc removed per microgram aorta (Figure 4.2A). The maximum removal achieved with the 12 µg dose; there was no increase in sialic acid removal between 12 and 25 µg. Furthermore, Sia26 preferentially removed aortic Neu5Gc over Neu5Ac (Figure 4.2B). This finding supports the idea that Sia26 displays preferential Neu5Gc activity within the organism, as well as in our *in vitro* assays.

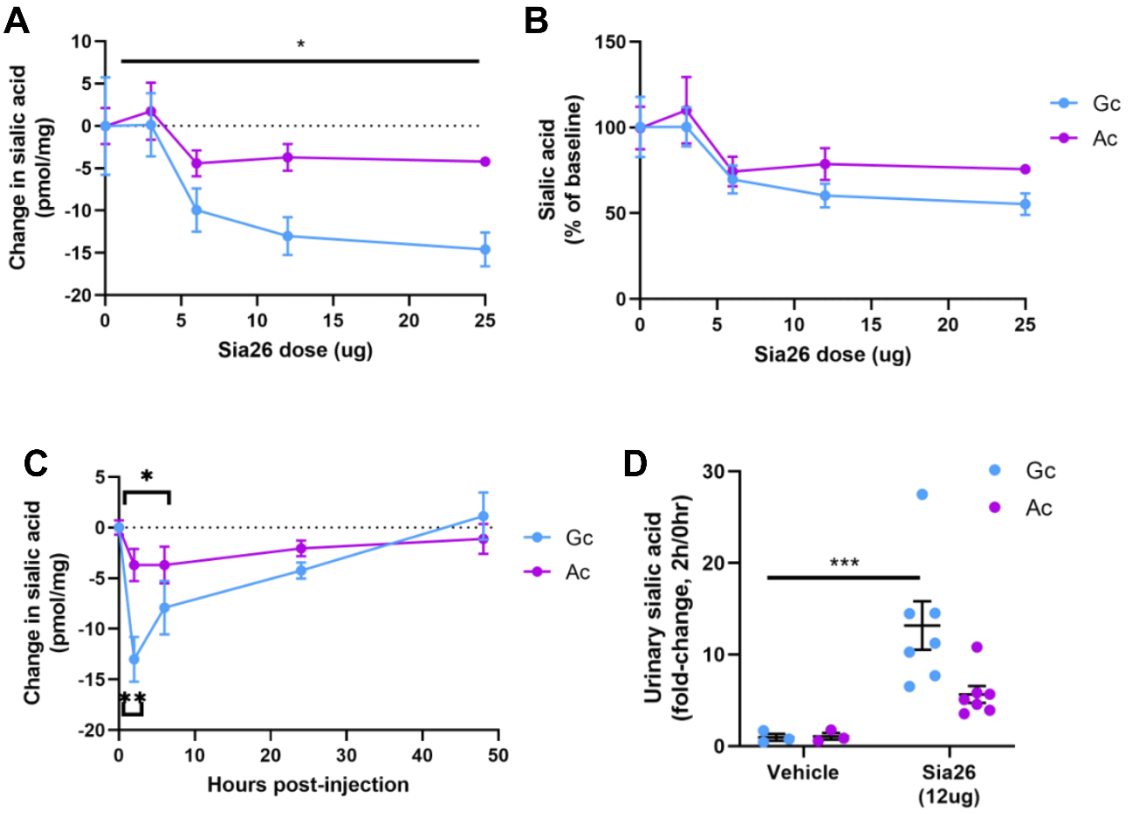

Figure 4.2 Neu5Gc-preferential activity of Sia26 in vivo. A) Sia26 release of aortic sialic acid at increasing doses (pmol/mg aorta). WT mice were injected IV with increasing doses of Sia26 (n = 3 each). The thoracic aorta was isolated 2hr post-injection and analyzed for sialic acid content. B) Sia26 release of aortic sialic acid at increasing doses (% of 0ug control group). C) Aortic sialic acid repopulation over time. WT mice were injected IV with 12ug Sia26 (n = 3 each). The thoracic aorta was isolated at 2, 6, 24, or 48hr post-injection and analyzed for sialic acid content. D) Urinary sialic acid levels following Sia26 injection. WT mice were injected with 12ug Sia26 (n = 7) or vehicle (n = 3). Urine samples were collected from mice before injection (0hr) and 2hr post-injection. Urinary sialic acid is expressed as fold-change for each mouse between 2hr and 0hr.

We also wished to determine how much time was required for aortic sialic acid levels to return to baseline levels following Sia26 treatment. WT mice were injected with 12 µg Sia26 and the thoracic aorta was collected at 2, 6, 24, and 48 hr post-injection. Sialic acid levels were significantly lower at the 2- and 6-hr time points, although the level had already begun to return to baseline between 2 and 6 hr (Figure 4.2D). Neu5Gc levels were still below baseline at 24 hr, although the difference was not significant. Levels had fully returned to baseline by 48 hr post-injection. Using this information, we decided to inject mice twice a week with Sia26 in the long-term atherosclerosis experiments. This experiment was repeated in *Cmah*$^{-/-}$*Ldlr*$^{-/-}$ mice on a Neu5Gc-rich diet for 4 weeks, but aortic Neu5Gc was undetectable in all samples through HPLC (data not shown). The presence of aortic Neu5Gc in this model has been well-established after 3 weeks of Neu5Gc feeding with histology[308], indicating that HPLC of the whole aorta is not sensitive enough to detect the small levels of Neu5Gc present in this model.

4.3.4 Sialic acid released by Sia26 is excreted renally

Previous work has shown the free sialic acids in circulation are rapidly excreted by the kidneys[295,296,311]. We therefore measured free sialic acid levels in the urine of mice injected with 12 µg of active Sia26 or vehicle. Urine was collected before injection (0 hr) and 2 hr post-injection for each mouse. Urinary sialic acid was significantly increased following Sia26 injection, with on average 12-fold more Neu5Gc and 6-fold more Neu5Ac in the urine for mice receiving active enzyme (Figure 4.2E). Urinary sialic acid was not increased in mice that received the vehicle injection.

4.4 Discussion

Neu5Gc is an inevitable presence in the average human diet. Many people will not remove Neu5Gc-rich foods, such as red meat and certain dairy products[297], from their diets. Indeed, red meat and dairy serve as important sources of protein and iron or calcium for much of the world's population. The consumption of high levels of Neu5Ac at the same time as Neu5Gc can seemingly prevent Neu5Gc incorporation in host glycoconjugates[309]. However, coordinating dietary sialic acid levels like this is not straight-forward because most foods rich in Neu5Gc are not correspondingly rich in Neu5Ac[295,297]. Additionally, the sialic acids must presumably be consumed at the same time for Neu5Ac to effectively compete with Neu5Gc for absorption and glycoconjugate incorporation. This study therefore sought to investigate the effect of removing endothelial Neu5Gc after glycoconjugate incorporation, circumventing the need for balancing dietary sialic acid intake.

Taking advantage of the Neu5Gc-preferential sialidase Sia26, this study first characterized the ability of Sia26 to release Neu5Gc from the cell surface. Previous work with Sia26 examined its overall activity and substrate preference[310] but did not examine its efficacy in an *in vivo* cell surface setting. Sia26 was able to release Neu5Gc effectively from the cell surface in an *in vitro* cell culture setting. It was also able to release Neu5Gc effectively from aortic endothelium. Although the entire aorta was analyzed for sialic acid quantification, sialic acids are localized almost exclusively to glycoconjugates on the cell surface[293], indicating that the differences detected are overwhelmingly due to cell-surface sialic acid. Furthermore, the Neu5Gc-preference was even more pronounced *in vivo* (Figure 4.2A-B) than detected in the *in vitro* activity assay (Figure 4.1A). This could

indicate there are conditions or factors inside the host body that support optimal Sia26 activity on Neu5Gc.

This study also investigated how quickly aortic sialic acid is repopulated following IV injections of Sia26 in mice. Aortic sialic acid was acutely decreased following injection and gradually increased, returning to baseline between 24 and 48 hr post-injection. Endothelial sialic acid repopulation could be achieved by two possible mechanisms: turnover of cell-surface proteins, resulting in new glycosylated proteins; or sialylation of existing glycoconjugates by extracellular sialyltransferases, a process known as extrinsic sialylation[312,313]. Either or both mechanisms could be driving aortic re-sialylation in this model. The relatively low turnover rate of endothelial cells[314] and direct proximity of the endothelial glycocalyx to the blood could indicate that blood-borne sialyltransferases are more likely to contribute to aortic re-sialylation. However, many more experiments would be needed to investigate this hypothesis.

The effectiveness of Sia26 at removing aortic Neu5Gc and lack of acute adverse effects in the mice (data not shown) suggest that long-term treatment with Sia26 could reduce atherosclerosis development by regularly removing endothelial Neu5Gc. Ongoing follow-up studies to this work will address this question by injecting *Cmah*$^{-/-}$*Ldlr*$^{-/-}$ mice on an Neu5Gc-rich diet with active or heat-inactivated Sia26 twice a week for four weeks. A comparison between the active and heat-inactivated enzyme groups will determine if endothelial removal of Neu5Gc results in decreased atherosclerosis plaque development. If successful, this work would provide a new therapeutic strategy to consider for cases of human CVD driven at least partly by dietary red meat.

4.5 Materials and Methods

4.5.1 Ethics Statement

The proposed use of mice in this project was approved by the University of California San Diego (UCSD) Animal Subjects Committee. All procedures were approved by the Animal Care Program and Institutional Animal Care and Use Committee, UCSD. Human and macaque RBCs were purchased from BioIVT (https://bioivt.com/).

4.5.2 Mice and Cell Culture

Cmah$^{-/-}$*Ldlr*$^{-/-}$ mice were generated as described previously[308] in a congenic C57BL/6 background and maintained in the UCSD vivarium according to Institutional Review Board guidelines for the care and use of laboratory animals. All animals were fully back-crossed and maintained on a 12-h light cycle and fed water and standard rodent chow for ad libitum consumption. Animals used in experiments were age-matched and placed on a Neu5Gc-rich soy-based HFD containing 20% anhydrous milk fat, 0.2% cholesterol, and 0.25mg Neu5Gc per gram of chow or a Neu5Ac-rich soy-based HFD containing 0.25mg Neu5Ac per gram of chow (custom diets from Dyets, Inc.). Neu5Gc-rich chow and Neu5Gc-rich chow was made by adding purified porcine submaxillary mucin (PSM) and edible bird's nest (EBN) (Golden Nest, Inc.) as previously described[297]. The amount of Neu5Gc and Neu5Ac in the PSM and EBN was determined by HPLC as described below.

Murine embryonic fibroblast (MEF) cells were grown in Gibco Dulbecco's Modified Eagle Medium (DMEM) with 10% FBS and 1% penicillin/streptomycin. For sialidase treatment, 5x10e4 cells/well were seeded into 12-well plates. The following day cells were washed 3x in DMEM without FBS or pen/strep. Purified Sialidase26 was added to wells

with 1mL DMEM and cells were incubated at 37 °C for 2hr. Cells were then washed once with DMEM and treated with 0.25% trypsin/EDTA (Gibco™ 25200056). The trypsinized sample was collected and spun down at 500 rpm for 5 min to pellet cells. The supernatant containing cell-surface proteins was removed and frozen at -80 C. Samples were then lyophilized on a Labconco FreeZone Plus 4.5 L Cascade Benchtop Freeze Dry System, resuspended in 100uL H2O, and processed for HPLC quantification as described below.

4.5.3 *In vitro* sialidase activity assay

0.5ug of Sialidase26 was incubated with equal amount of human-like *Cmah*$^{-/-}$*Ldlr*$^{-/-}$ mouse serum and *Ldlr*$^{-/-}$ mouse serum for 1 hour at 37 °C. An additional 0.5 µg of each enzyme was inactivated by heat for 10 minutes at 95 °C. The samples were kept at −20 °C until derivatization and analyzed by HPLC as described below.

4.5.4 *In vivo* sialidase detection

Injected sialidase was detected in plasma samples with an anti-6xHis antibody through dot-blotting. Plasma samples were diluted 1:5 in PBS and 10uL was dotted on nitrocellulose membrane (BioRad 162-0113) using a Bio-Dot vacuum blotting apparatus (BioRad 1706545). The membrane was blocked with fish serum blocking buffer (Thermo Scientific 37527) for 30min, then treated with a goat anti-6xHis antibody (1:2500, Invitrogen MA1-21315-A488) in TBST for 30min. Following 3x3min washes in TBST the membrane was treated with a donkey anti-goat secondary (1:14000, Licor IRDye 680LT, 926-68023) in TBST for 30min, followed by 3 more washes. The membrane was imaged using a Licor Odyssey Infrared Imager. Image intensity was measured with ImageJ and quantified by comparison to a standard curve of purified Sia26.

4.5.5 Neu5Gc and control immunization

Pooled macaque and human RBC membrane ghosts were prepared as described previously[315]. RBC ghosts were incubated at 100 °C for 10 min prior to injection to kill any potential microbial organisms. *Cmah*$^{-/-}$*Ldlr*$^{-/-}$ male and female mice were immunized as described previously[315]. Briefly, mice were injected once per week for three weeks via intraperitoneal injection with 100uL of 1mg/mL macaque RBC ghosts (Neu5Gc: 1.71 nmol/uL, Neu5Ac: 0.093 nmol/uL) or control human RBC ghosts (Neu5Gc: undetectable, Neu5Ac: 1.84 nmol/uL). The immunogen was mixed with an equal volume of complete Freund's adjuvant (ThermoFisher 77145) for the first week and an equal volume of incomplete Freund's adjuvant (ThermoFisher 77140) for the subsequent weeks.

4.5.6 Serum lipoprotein, lipid, and inflammatory cytokine analysis

Blood samples were obtained by mandibular plexus bleeding and cardiac puncture from mice fasted for 5h. Plasma lipoproteins in 25-uL pooled samples were separated by size-exclusion chromatography using a polyethylene filter column (Sigma-Aldrich). Cholesterol and triglyceride levels in whole plasma and in separated lipoprotein fractions were measured by enzymatic kits (Sekisui). Multiplex inflammatory cytokine levels were measured with Proinflammatory Panel 1 (mouse) kits (Meso Scale Diagnostics, LLC).

4.5.7 Quantification of sialic acid by HPLC in cell culture, aorta, plasma, and urine

To analyze total sialic acid (cell culture, aorta, plasma), aqueous samples were acid hydrolyzed with glacial acetic acid (2M final in total volume 200 µL) for 3 hours at 80 °C to remove terminal Sias. This step was not done when analyzing free sialic acid (plasma, urine). Samples were spin-filtered (Millipore Sigma Amicon Ultra-0.5 Centrifugal Filter Unit; cat No. UFC5010BK) to remove cellular debris. Free sialic acids were then

derivatized with DMB as described previously[316]. The DMB reagent was made as follows: 14 mM DMB (1,2-diamino-4,5-methylenedioxybenzene, Sigma D4787), 18 mM sodium hydrosulfite (Sigma 157953), 1.0 M 2-mercaptoethanol (Sigma M3148), and 40 mM trifluoroacetic acid (Sigma T6508), incubated with samples at 50 °C for 2.5 h. DMB-derivatized sialic acids were analyzed on a Dionex Ultra3000 HPLC System using a Phenomenex Gemini 5µ C18 250 × 4.6-mm HPLC column, eluted in isocratic mode with 85% water, 7% methanol, and 8% acetonitrile and quantified by comparison to Neu5Ac (Nacalai) and Neu5Gc (Inalco) standards.

4.5.8 Expression of Sialidase26 recombinant protein

Sialidase26 DNA sequence was ordered from Integrated DNA Technologies (IDT), subcloned into a pET19b expression vector with a C-terminal 10×His tag and N-terminal truncation to remove any signal peptide sequence (predicted by SignalP 4.1, CBS), and transformed into BL21(DE3) E. coli (MilliporeSigma) using established heat-shock methods. Cells were grown to OD 0.6-0.8 (OD 600) in multiple 1 L cultures at 37 °C and induced overnight at 25 °C with 1 mM isopropyl-β-D-1-thiogalactopyranoside (IPTG). Harvested cells were resuspended in lysis buffer (50 mM HEPES pH 8.0, 50 mM NaCl, and 1 mM TCEP (tris(2-carboxyethyl)phosphine hydrochloride))) with DNaseI and hen egg white lysozyme, lysed with a TS-Series cell disruptor (Constant Systems, Inc.) at 15 KPSI (Kilo-Pound per Square Inch), and spun for 45 minutes at 186,000×g with a Ti45 ultracentrifugation rotor (Beckman Coulter, Inc.) to remove cell debris. Purification was performed as below and based on purification of a putative Bacteroides neuraminidase as provided by the Protein Structure Initiative (BACCAC_01090, Joint Center for Structural Genomics, to be published), with modifications to imidazole stringency based

on the sialidase purified. Supernatant was loaded on a 5-mL HisTrap Ni affinity column (nickel-charged columns for high resolution histidine-tagged protein purification) on an Akta Explorer purification system (GE Healthcare Life Sciences) with 20-40 mM imidazole added, washed with Running Buffer (50 mM HEPES pH 8.0, 300 mM NaCl, 40-60 mM imidazole, 10% glycerol, and 1 mM TCEP), and eluted with Elution Buffer (20 mM HEPES pH 8.0, 300 mM imidazole, 10% glycerol, and 1 mM TCEP). Samples were concentrated using 10-30 kDa Amicon centrifugal filters (MilliporeSigma) at 1500×g to 1 mL and desalted over a 5-mL. Desalting column using the Akta system into Desalting Buffer (20 mM HEPES pH 8.0, 200 mM NaCl). Resulting protein sample was diluted as needed for functional studies.

4.5.9 Statistical analyses

All data were analyzed by Student's t-test, 1-way ANOVA, or 2-way ANOVA and presented as mean +/- SEM. Statistical analyses were performed using Prism (v8, GraphPad Software).

4.6 Acknowledgements

Chapter 4, in full, is being prepared as a manuscript for submission for publication of the material. Coker J, Secrest P, Rees S, Quinnell D, Glonek N, Rosete N, Zaramela L, Chang G, Gordts PLSM, Zengler K. Removal of the endothelial non-human sialic acid Neu5Gc reduces atherosclerosis. *In preparation.* The dissertation author is the primary investigator and author of this material.

Chapter 5: Concluding Remarks

5.1 Project summary

Microbiomes are present in almost every environment on Earth, even regions once through unable to support life such as the ocean floor or dormant volcanos[317]. The controlled study of such complicated communities comes with its own extreme challenges. The laboratory is a poor replacement for the world outside, with many microbes that thrive in nature unable to grow in research settings. Natural systems are also incredibly intricate and interconnected, and we often struggle to identify and reproduce the most important conditions for community development. Given these issues, *in vitro* microbial communities are often difficult to reproduce and less diverse than natural communities. We are still searching for the most effective methods to study the dynamics of these communities that are imperative to human life.

The work presented in this dissertation aims to develop methods to address these issues, and beyond that to demonstrate how discoveries from microbial communities can be used to improve human health. A system was developed for the precise and automated assembly of synthetic soil and skin microbial communities, allowing the high-throughput assembly of reproducible *in vitro* communities for controlled studies. This system allowed for the investigation of community dynamics through minute adjustments in starting ratios and easy removal of individual organisms, revealing that some microbes play a driving role in community development while others can be removed without substantially altering the final community composition. Such synthetic communities can also be used to predict what will happen in natural communities when conditions change, as shown with the significant changes in skin community composition when treated with compounds commonly found in skin cosmetics.

Despite the difficulties of microbiome research, the discoveries made in this field are often surprising and deeply impactful. Microbes frequently contain proteins with capabilities scientists have only dreamed of, and certainly cannot engineer yet. Such is the case with a microbial enzyme isolated from the gut microbiome, the first published sialidase to preferentially act on the inflammatory sialic acid Neu5Gc instead of the more common Neu5Ac[310]. Here this sialidase was applied to remove Neu5Gc from endothelial glycoconjugates, to investigate its potential to treat cardiovascular disease related to red meat consumption. The application of discoveries from the microbial level of a metaorganism to impact the health and development of the host is at the heart of this dissertation and all microbiome research.

5.2 Future directions in the microbiome landscape

From a certain perspective, all fundamental biological research uses models to explain natural phenomena. Researchers go through countless iterations of constructing a model, which can be as varied as a simple hypothesis or a complex computational algorithm. They then modify and refine that model based on experimental data. This process has occurred for decades for the most well-studied biological systems, such as the organism *Escherichia coli* or biochemical processes like DNA replication. Their models have gotten so accurate, they are now accepted as fact. However, this process is still in its infancy for microbial communities.

Models of natural microbial communities will, by definition of a model, fail to capture every aspect of the community. Current *in vitro* models still struggle with fundamentals such as diversity and stability that are achieved effortlessly in nature. The research presented in this dissertation provides methods for improving diversity, stability,

and reproducibility in soil and skin community models, seeking to improve these models so they can be one day be as reliable as our understanding of *E. coli*. However, much work remains before this point. In the immediate future, developing models for other environments, such as ocean or vaginal microbiota, would spread these findings to other areas of microbiome research. Additionally, comparing changes observed in these *in vitro* models against *in vivo* communities subjected to the same interventions would allow validation and fine-tuning of these models.

The field of gut microbiome research in particular could benefit from development of a model *in vitro* gut community. The gut microbiome is one of the most well-studied microbiomes, both for its importance in human health and development and the relative ease of collecting samples for sequencing. Many synthetic gut microbial systems already exist, as discussed in previous chapters (see page 37 specifically). However, most of these models are developed with the express purpose of inoculating a defined community into an *in vivo* model. This approach addresses questions of host-microbe interactions, but it does not allow for investigations into community dynamics, specifically microbe-microbe interactions within the community. As demonstrated in this dissertation, an *in vitro* model community can be used to determine the role of individual microbes in establishing community diversity or to test the effect of specific interventions on major community players. A model gut community, designed to recapitulate natural diversity and stability but grown *in vitro*, would support a wide variety of studies to tease apart the role of individual microbes within the gut.

A model such as this would also provide an opportunity to test the effect of interventions like Sia26 before moving to *in vivo* models. Sia26 was isolated from the gut

microbiome. The research presented here uses this gut microbial enzyme in host circulation to release Neu5Gc after endothelial incorporation, as a proof of concept for the benefits of removing Neu5Gc. However, Sia26 could also be applied in the gut to release Neu5Gc from ingested food before it even reaches circulation, thereby preventing endothelial incorporation from ever occurring. Delivering an active enzyme to the gastrointestinal tract presents several challenges, most notably getting the enzyme past the stomach without denaturation, but enrichment of a living microbe producing Sia26 would subvert many of these challenges. However, long-term enrichment of an organism in an established gut microbiome is notoriously difficult. With an *in vitro* model gut community, we could quickly and cheaply test many microbes and conditions, narrowing down the approaches most likely to succeed *in vivo*. Similar studies can be carried out with all types of *in vitro* model communities, as demonstrated here with the skin and soil communities. These models can also serve as an important first check on the community effect of adding microbes engineered to produce certain proteins or metabolites[183], before moving to *in vivo* models.

Our understanding of the human metaorganism and the outsize role the microbial world plays in human life is changing with astounding rapidity. As research in this field explodes, we need reliable model community systems to test and refine our hypotheses *in vitro*. The process of establishing new model systems is arduous, but the research in this dissertation is driven by the belief that the benefits for future microbiome research will be well worth the present input of time and effort.

REFERENCES

1. Bosch TCG, McFall-Ngai MJ. Metaorganisms as the new frontier. Vol. 114, Zoology. 2011. p. 185–90.

2. Turnbaugh PJ, Ley RE, Hamady M, Fraser-Liggett CM, Knight R, Gordon JI. The Human Microbiome Project. Nature. 2007;449(7164):804–10.

3. Knight R, Callewaert C, Marotz C, Hyde ER, Debelius JW, McDonald D, Sogin ML. The Microbiome and Human Biology. Annual Review of Genomics and Human Genetics. 2017;18(1):65–86.

4. Kamada N, Kim YG, Sham HP, Vallance BA, Puente JL, Martens EC, Núñez G. Regulated virulence controls the ability of a pathogen to compete with the gut microbiota. Science (1979). 2012;336(6086):1325–9.

5. Macfarlane GT, Macfarlane S. Bacteria, Colonic Fermentation, and Gastrointestinal Health. J AOAC Int. 2012;95(1):50–60.

6. Smits SA, Leach J, Sonnenburg ED, Gonzalez CG, Lichtman JS, Reid G, Knight R, Manjurano A, Changalucha J, Elias JE, Dominguez-Bello MG, Sonnenburg JL. Seasonal cycling in the gut microbiome of the Hadza hunter-gatherers of Tanzania. Science (1979). 2017;357(6353):802–5.

7. Ley RE, Turnbaugh PJ, Klein S, Gordon JI. Human gut microbes associated with obesity. Nature. 2006;444(7122):1022–3.

8. Rothschild D, Weissbrod O, Barkan E, Kurilshikov A, Korem T, Zeevi D, Costea PI, Godneva A, Kalka IN, Bar N, Shilo S, Lador D, Vila AV, Zmora N, Pevsner-Fischer M, Israeli D, Kosower N, Malka G, Wolf BC, Avnit-Sagi T, Lotan-Pompan M, Weinberger A, Halpern Z, Carmi S, Fu J, Wijmenga C, Zhernakova A, Elinav E, Segal E. Environment dominates over host genetics in shaping human gut microbiota. Nature. 2018;555(7695):210–5.

9. De Filippo C, Cavalieri D, Di Paola M, Ramazzotti M, Poullet JB, Massart S, Collini S, Pieraccini G, Lionetti P. Impact of diet in shaping gut microbiota revealed by a comparative study in children from Europe and rural Africa. PNAS. 2010;107(33):14691–6.

10. Carmody RN, Bisanz JE, Bowen BP, Maurice CF, Lyalina S, Louie KB, Treen D, Chadaideh KS, Maini Rekdal V, Bess EN, Spanogiannopoulos P, Ang QY, Bauer KC, Balon TW, Pollard KS, Northen TR, Turnbaugh PJ. Cooking shapes the structure and function of the gut microbiome. Nature Microbiology. 2019;4(12):2052–63.

11. Koropatkin NM, Cameron E a, Martens EC. How Glycan Metabolism Shapes the Human Gut Microbiota. Nat Rev Microbiol. 2014;10(5):323–35.

12. Varki A, Cummings RD, Aebi M, Packer NH, Seeberger PH, Esko JD, Stanley P, Hart G, Darvill A, Kinoshita T, Prestegard JJ, Schnaar RL, Freeze HH, Marth JD, Bertozzi CR, Etzler ME, Frank M, Vliegenthart JFG, Lütteke T, Perez S, Bolton E, Rudd P, Paulson J, Kanehisa M, Toukach P, Aoki-Kinoshita KF, Dell A, Narimatsu H, York W, Taniguchi N, Kornfeld S. Symbol nomenclature for graphical representations of glycans. Glycobiology. 2015;25(12):1323–4.

13. Neelamegham S, Aoki-Kinoshita K, Bolton E, Frank M, Lisacek F, Lütteke T, O'Boyle N, Packer NH, Stanley P, Toukach P, Varki A, Woods RJ. Updates to the Symbol Nomenclature for Glycans guidelines. Glycobiology. 2019;29(9):620–4.

14. Walker AW, Ince J, Duncan SH, Webster LM, Holtrop G, Ze X, Brown D, Stares MD, Scott P, Bergerat A, Louis P, McIntosh F, Johnstone AM, Lobley GE, Parkhill J, Flint HJ. Dominant and diet-responsive groups of bacteria within the human colonic microbiota. ISME Journal. 2011;5(2):220–30.

15. David LA, Maurice CF, Carmody RN, Gootenberg DB, Button JE, Wolfe BE, Ling A V., Devlin AS, Varma Y, Fischbach MA, Biddinger SB, Dutton RJ, Turnbaugh PJ. Diet rapidly and reproducibly alters the human gut microbiome. Nature. 2014;505(7484):559–63.

16. Salonen A, Lahti L, Salojärvi J, Holtrop G, Korpela K, Duncan SH, Date P, Farquharson F, Johnstone AM, Lobley GE, Louis P, Flint HJ, De Vos WM. Impact of diet and individual variation on intestinal microbiota composition and fermentation products in obese men. ISME Journal. 2014;8(11):2218–30.

17. Duncan SH, Belenguer A, Holtrop G, Johnstone AM, Flint HJ, Lobley GE. Reduced dietary intake of carbohydrates by obese subjects results in decreased concentrations of butyrate and butyrate-producing bacteria in feces. Applied and Environmental Microbiology. 2007;73(4):1073–8.

18. Kolodziejczyk AA, Zheng D, Elinav E. Diet–microbiota interactions and personalized nutrition. Nature Reviews Microbiology. 2019;17(12):742–53.

19. Wu GD, Chen J, Hoffmann C, Bittinger K, Chen YY, Keilbaugh SA, Bewtra M, Knights D, Walters WA, Knight R, Sinha R, Gilroy E, Gupta K, Baldassano, Wu R, D G, Chen J, Hoffmann C, Bittinger K, Chen YY, Keilbaugh SA, Bewtra M, Knights D, Walters WA, Knight R, Sinha R, Gilroy E, Gupta K, Baldassano R, Nessel L, Li H, Bushman FD, Lewis JD. Linking Long-Term Dietary Patterns with Gut Microbial Enterotypes. Science (1979). 2011;105–9.

20. Louis P, Hold GL, Flint HJ. The gut microbiota, bacterial metabolites and colorectal cancer. Nature Reviews Microbiology. 2014;12(10):661–72.

21. Yatsunenko T, Rey FE, Manary MJ, Trehan I, Dominguez-Bello MG, Contreras M, Magris M, Hidalgo G, Baldassano RN, Anokhin AP, Heath AC, Warner B, Reeder J, Kuczynski J, Caporaso JG, Lozupone CA, Lauber C, Clemente JC, Knights D,

Knight R, Gordon JI. Human gut microbiome viewed across age and geography. Nature. 2012;486(7402):222–7.

22. Le Chatelier E, Nielsen T, Qin J, Prifti E, Hildebrand F, Falony G, Almeida M, Arumugam M, Batto JM, Kennedy S, Leonard P, Li J, Burgdorf K, Grarup N, Jørgensen T, Brandslund I, Nielsen HB, Juncker AS, Bertalan M, Levenez F, Pons N, Rasmussen S, Sunagawa S, Tap J, Tims S, Zoetendal EG, Brunak S, Clément K, Doré J, Kleerebezem M, Kristiansen K, Renault P, Sicheritz-Ponten T, De Vos WM, Zucker JD, Raes J, Hansen T, Bork P, Wang J, Ehrlich SD, Pedersen O, Guedon E, Delorme C, Layec S, Khaci G, Van De Guchte M, Vandemeulebrouck G, Jamet A, Dervyn R, Sanchez N, Maguin E, Haimet F, Winogradski Y, Cultrone A, Leclerc M, Juste C, Blottière H, Pelletier E, Lepaslier D, Artiguenave F, Bruls T, Weissenbach J, Turner K, Parkhill J, Antolin M, Manichanh C, Casellas F, Boruel N, Varela E, Torrejon A, Guarner F, Denariaz G, Derrien M, Van Hylckama Vlieg JET, Veiga P, Oozeer R, Knol J, Rescigno M, Brechot C, M'Rini C, Mérieux A, Yamada T. Richness of human gut microbiome correlates with metabolic markers. Nature. 2013;500(7464):541–6.

23. Vangay P, Johnson AJ, Ward TL, Al-Ghalith GA, Shields-Cutler RR, Hillmann BM, Lucas SK, Beura LK, Thompson EA, Till LM, Batres R, Paw B, Pergament SL, Saenyakul P, Xiong M, Kim AD, Kim G, Masopust D, Martens EC, Angkurawaranon C, McGready R, Kashyap PC, Culhane-Pera KA, Knights D. US Immigration Westernizes the Human Gut Microbiome. Cell. 2018;175(4):962-972.e10.

24. Baxter NT, Schmidt AW, Venkataraman A, Kim KS, Waldron C, Schmidt TM. Dynamics of human gut microbiota and short-chain fatty acids in response to dietary interventions with three fermentable fibers. mBio. 2019;10(1):1–13.

25. Eswaran S, Muir J, Chey WD. Fiber and Functional Gastrointestinal Disorders. Am J Gastroenterol. 2013;108:718–27.

26. Den Besten G, Van Eunen K, Groen AK, Venema K, Reijngoud DJ, Bakker BM. The role of short-chain fatty acids in the interplay between diet, gut microbiota, and host energy metabolism. Journal of Lipid Research. 2013;54(9):2325–40.

27. Roy CC, Kien CL, Bouthillier L, Levy E. Short-chain fatty acids: ready for prime time? Nutrition in Clinical Practice. 2006;21(4):351–66.

28. Cummings JH, Pomare EW, Branch WJ, Naylor CPE, MacFarlane GT. Short chain fatty acids in human large intestine, portal, hepatic and venous blood. Gut. 1987;28:1221–7.

29. Bloemen JG, Venema K, van de Poll MC, Olde Damink SW, Buurman WA, Dejong CH. Short chain fatty acids exchange across the gut and liver in humans measured at surgery. Clinical Nutrition. 2009;28(6):657–61.

30. Dalile B, Van Oudenhove L, Vervliet B, Verbeke K. The role of short-chain fatty acids in microbiota–gut–brain communication. Nature Reviews Gastroenterology and Hepatology. 2019;16(8):461–78.

31. Chang P V., Hao L, Offermanns S, Medzhitov R. The microbial metabolite butyrate regulates intestinal macrophage function via histone deacetylase inhibition. Proc Natl Acad Sci U S A. 2014;111(6):2247–52.

32. Maslowski KM, Vieira AT, Ng A, Kranich J, Sierro F, Di Yu, Schilter HC, Rolph MS, MacKay F, Artis D, Xavier RJ, Teixeira MM, MacKay CR. Regulation of inflammatory responses by gut microbiota and chemoattractant receptor GPR43. Nature. 2009;461(7268):1282–6.

33. Smith PM, Howitt MR, Panikov N, Michaud M, Gallini CA, Bohlooly-y M, Glickman JN, Garrett WS. The Microbial Metabolites, Short-Chain Fatty Acids, Regulate Colonic Treg Cell Homeostatsis. Science (1979). 2013;341(August):569–74.

34. Sina C, Gavrilova O, Förster M, Till A, Derer S, Hildebrand F, Raabe B, Chalaris A, Scheller J, Rehmann A, Franke A, Ott S, Häsler R, Nikolaus S, Fölsch UR, Rose-John S, Jiang HP, Li J, Schreiber S, Rosenstiel P. G Protein-Coupled Receptor 43 Is Essential for Neutrophil Recruitment during Intestinal Inflammation. The Journal of Immunology. 2009;183(11):7514–22.

35. Haase S, Haghikia A, Wilck N, Müller DN, Linker RA. Impacts of microbiome metabolites on immune regulation and autoimmunity. Immunology. 2018.

36. Singh N, Thangaraju M, Prasad PD, Martin PM, Lambert NA, Boettger T, Offermanns S, Ganapathy V. Blockade of dendritic cell development by bacterial fermentation products butyrate and propionate through a transporter (Slc5a8)-dependent inhibition of histone deacetylases. Journal of Biological Chemistry. 2010;285(36):27601–8.

37. Trompette A, Gollwitzer ES, Yadava K, Sichelstiel AK, Sprenger N, Ngom-Bru C, Blanchard C, Junt T, Nicod LP, Harris NL, Marsland BJ. Gut microbiota metabolism of dietary fiber influences allergic airway disease and hematopoiesis. Nature Medicine. 2014;20(2):159–66.

38. Fukuda S, Toh H, Hase K, Oshima K, Nakanishi Y, Yoshimura K, Tobe T, Clarke JM, Topping DL, Suzuki T, Taylor TD, Itoh K, Kikuchi J, Morita H, Hattori M, Ohno H. Bifidobacteria can protect from enteropathogenic infection through production of acetate. Nature. 2011;469(7331):543–9.

39. Desai MS, Seekatz AM, Koropatkin NM, Kamada N, Hickey CA, Wolter M, Pudlo NA, Kitamoto S, Terrapon N, Muller A, Young VB, Henrissat B, Wilmes P, Stappenbeck TS, Núñez G, Martens EC. A Dietary Fiber-Deprived Gut Microbiota Degrades the Colonic Mucus Barrier and Enhances Pathogen Susceptibility. Cell. 2016;167(5):1339-1353.e21.

40. Peters BA, Dominianni C, Shapiro JA, Church TR, Wu J, Miller G, Yuen E, Freiman H, Lustbader I, Salik J, Friedlander C, Hayes RB, Ahn J. The gut microbiota in conventional and serrated precursors of colorectal cancer. Microbiome. 2016;4(1):69.

41. Dai Z, Coker OO, Nakatsu G, Wu WKK, Zhao L, Chen Z, Chan FKL, Kristiansen K, Sung JJY, Wong SH, Yu J. Multi-cohort analysis of colorectal cancer metagenome identified altered bacteria across populations and universal bacterial markers. Microbiome. 2018;6(1):70.

42. Aune D, Keum N, Giovannucci E, Fadnes LT, Boffetta P, Greenwood DC, Tonstad S, Vatten LJ, Riboli E, Norat T. Whole grain consumption and risk of cardiovascular disease, cancer, and all cause and cause specific mortality: Systematic review and dose-response meta-analysis of prospective studies. BMJ (Online). 2016;353:1–14.

43. Chen HM, Yu YN, Wang JL, Lin YW, Kong X, Yang CQ, Yang L, Liu ZJ, Yuan YZ, Liu F, Wu JX, Zhong L, Fang DC, Zou W, Fang JY. Decreased dietary fiber intake and structural alteration of gut microbiota in patients with advanced colorectal adenoma. American Journal of Clinical Nutrition. 2013;97(5):1044–52.

44. Singh V, Yeoh BS, Chassaing B, Xiao X, Saha P, Aguilera Olvera R, Lapek JD, Zhang L, Wang WB, Hao S, Flythe MD, Gonzalez DJ, Cani PD, Conejo-Garcia JR, Xiong N, Kennett MJ, Joe B, Patterson AD, Gewirtz AT, Vijay-Kumar M. Dysregulated Microbial Fermentation of Soluble Fiber Induces Cholestatic Liver Cancer. Cell. 2018;175(3):679-694.e22.

45. Golonka RM, Yeoh BS, Vijay-Kumar M. Dietary Additives and Supplements Revisited: the Fewer, the Safer for Gut and Liver Health. Current Pharmacology Reports. 2019;5(4):303–16.

46. Makki K, Deehan EC, Walter J, Bäckhed F. The Impact of Dietary Fiber on Gut Microbiota in Host Health and Disease. Cell Host and Microbe. 2018;23(6):705–15.

47. Townsend GE, Han W, Schwalm ND, Raghavan V, Barry NA, Goodman AL, Groisman EA. Dietary sugar silences a colonization factor in a mammalian gut symbiont. Proc Natl Acad Sci U S A. 2019;116(1):233–8.

48. Abdelmalek MF, Suzuki A, Guy C, Unalp-Arida A, Colvin R, Johnson RJ, Diehl AM. Increased fructose consumption is associated with fibrosis severity in patients with NAFLD. Hepatology. 2010;51(6):1961–71.

49. Alwahsh SM, Xu M, Seyhan HA, Ahmad S, Mihm S, Ramadori G, Schultze FC. Diet high in fructose leads to an overexpression of lipocalin-2 in rat fatty liver. World Journal of Gastroenterology. 2014;20(7):1807–21.

50. Sellmann C, Priebs J, Landmann M, Degen C, Engstler AJ, Jin CJ, Gärttner S, Spruss A, Huber O, Bergheim I. Diets rich in fructose, fat or fructose and fat alter

intestinal barrier function and lead to the development of nonalcoholic fatty liver disease over time. Journal of Nutritional Biochemistry. 2015;26(11):1183–92.

51. Le Roy T, Llopis M, Lepage P, Bruneau A, Rabot S, Bevilacqua C, Martin P, Philippe C, Walker F, Bado A, Perlemuter G, Cassard-Doulcier AM, Gérard P. Intestinal microbiota determines development of non-alcoholic fatty liver disease in mice. Gut. 2013;62(12):1787–94.

52. Jegatheesan P, Beutheu S, Ventura G, Sarfati G, Nubret E, Kapel N, Waligora-Dupriet AJ, Bergheim I, Cynober L, De-Bandt JP. Effect of specific amino acids on hepatic lipid metabolism in fructose-induced non-alcoholic fatty liver disease. Clinical Nutrition. 2016;35(1):175–82.

53. Ritze Y, Bárdos G, Claus A, Ehrmann V, Bergheim I, Schwiertz A, Bischoff SC. Lactobacillus rhamnosus GG Protects against non-alcoholic fatty liver disease in mice. PLoS ONE. 2014;9(1):1–9.

54. Boursier J, Mueller O, Barret M, Machado M, Fizanne L, Araujo-Perez F, Guy CD, Seed PC, Rawls JF, David LA, Hunault G, Oberti F, Calès P, Diehl AM. The severity of nonalcoholic fatty liver disease is associated with gut dysbiosis and shift in the metabolic function of the gut microbiota. Hepatology. 2016;63(3):764–75.

55. Sonnenburg JL, Xu J, Leip DD, Chen CH, Westover BP, Weatherford J, Buhler JD, Gordon JI. Glycan foraging in vivo by an intestine-adapted bacterial symbiont. Science (1979). 2005;307(5717):1955–9.

56. Atuma C, Strugala V, Allen A, Holm L. The adherent gastrointestinal mucus gel layer: Thickness and physical state in vivo. American Journal of Physiology - Gastrointestinal and Liver Physiology. 2001;280(5 43-5):922–9.

57. Baeckstrom D, Hansson GC, Nilsson O, Johansson C, Gendler SJ, Lindholm L. Purification and characterization of a membrane-bound and a secreted mucin-type glycoprotein carrying the carcinoma-associated sialyl-Lea epitope on distinct core proteins. Journal of Biological Chemistry. 1991;266(32):21537–47.

58. Johansson MEV, Phillipson M, Petersson J, Velcich A, Holm L, Hansson GC. The inner of the two Muc2 mucin-dependent mucus layers in colon is devoid of bacteria. Proc Natl Acad Sci U S A. 2008;105(39):15064–9.

59. Norin KE, Gustafsson BE, Lindblad BS, Midtvedt T. The Establishment of Some Microflora Associated Biochemical Characteristics in Feces from Children during the First Years of Life. Acta Pædiatrica. 1985;74(2):207–12.

60. Tailford LE, Crost EH, Kavanaugh D, Juge N. Mucin glycan foraging in the human gut microbiome. Front Genet. 2015;6(81).

61. McDonald D, Hyde E, Debelius JW, Morton JT, Gonzalez A, Ackermann G, Aksenov AA, Behsaz B, Brennan C, Chen Y, Goldasich LD, Dorrestein PC, Dunn

RR, Fahimipour AK, Gaffney J, Gilbert JA, Gogul G, Green JL, Hugenholtz P, Humphrey G, Huttenhower C, Jackson MA, Janssen S, Jeste D V, Jiang L, Kelley ST, Knights D, Kosciolek T, Ladau J, Leach J, Marotz C, Meleshko D, Melnik A V, Metcalf JL, Mohimani H, Montassier E, Rahnavard G, Robbins-pianka A, Sangwan N, Shorenstein J, Smarr L, Vázquez-baeza Y, Vrbanac A, Wischmeyer P, Wolfe E, Zhu Q, Gut A, Jt M, Gonzalez A, Ackermann G, Behsaz B, Brennan C, Chen Y, Goldasich L, Pc D, Rr D, Jl G, Hugenholtz P, Humphrey G, Huttenhower C, Ma J, Janssen S, Jiang L, St K, Knights D, Kosciolek T. American Gut : an Open Platform for Citizen Science. 2018;3(3):1–28.

62. Earle KA, Billings G, Sigal M, Lichtman JS, Hansson GC, Elias JE, Amieva MR, Huang KC, Sonnenburg JL. Quantitative Imaging of Gut Microbiota Spatial Organization. Cell Host Microbe. 2015;18(4):478–88.

63. Earley H, Lennon G, Balfe Á, Coffey JC, Winter DC, O'Connell PR. The abundance of Akkermansia muciniphila and its relationship with sulphated colonic mucins in health and ulcerative colitis. Scientific Reports. 2019;9(1):1–9.

64. Png CW, Lindén SK, Gilshenan KS, Zoetendal EG, McSweeney CS, Sly LI, McGuckin MA, Florin THJ. Mucolytic bacteria with increased prevalence in IBD mucosa augment in vitro utilization of mucin by other bacteria. American Journal of Gastroenterology. 2010;105(11):2420–8.

65. Fu J, Wei B, Wen T, Johansson ME V, Liu X, Bradford E, Thomsson K a, Mcgee S, Mansour L, Tong M, Mcdaniel JM, Sferra TJ, Turner J, Chen H, Hansson GC, Braun J, Xia L. Loss of intestinal core 1–derived O-glycans causes spontaneous colitis in mice. J Clin Invest. 2011;121(4):1657–66.

66. Holmn Larsson JM, Karlsson H, Graberg Crespo J, Johansson ME, Eklund L, Sjovall H, Hansson GC. Altered O-glycsoylation profile of MUC2 mucin occurs in active ulcerative colitis and is associated with increased inflammation. Inflamm Bowel Dis. 2011;17(11):2299–307.

67. Johansson MEV, Gustafsson JK, Holmen-Larsson J, Jabbar KS, Xia L, Xu H, Ghishan FK, Carvalho FA, Gewirtz AT, Sjovall H, Hansson GC. Bacteria penetrate the normally impenetrable inner colon mucus layer in both murine colitis models and patients with ulcerative colitis. Gut. 2014;63(2):281–91.

68. Schroeder BO, Birchenough GMH, Ståhlman M, Arike L, Johansson ME V, Hansson GC, Bäckhed F. Bifidobacteria or fiber protect against diet-induced microbiota-mediated colonic mucus deterioration HHS Public Access The defects can be prevented by application of a probiotic bifidobacteria or the prebiotic fiber inulin. Cell Host Microbe. 2018;23(1):27–40.

69. Yamada T, Hino S, Iijima H, Genda T, Aoki R, Nagata R, Han KH, Hirota M, Kinashi Y, Oguchi H, Suda W, Furusawa Y, Fujimura Y, Kunisawa J, Hattori M, Fukushima M, Morita T, Hase K. Mucin O-glycans facilitate symbiosynthesis to maintain gut immune homeostasis. EBioMedicine. 2019;48:513–25.

70. Harig JM, Soergel KH, Komorowski RA, Wood CM. Treatment of diversion colitis with short-chain-fatty acid irrigation. N Engl J Med. 1989;320(1):23–8.

71. Scheppach W, Sommer H, Kirchner T, Paganelli GM, Bartram P, Christl S, Richter F, Dusel G, Kasper H. Effect of butyrate enemas on the colonic mucosa in distal ulcerative colitis. Gastroenterology. 1992;103(1):51–6.

72. Angata T, Varki A. Chemical diversity in the sialic acids and related α-keto acids: An evolutionary perspective. Chemical Reviews. 2002;102(2):439–69.

73. Varki A. Sialic acids in human health and disease. Trends Mol Med. 2008;14(8):351–60.

74. Vimr ER, Kalivoda KA, Deszo EL, Steenbergen SM. Diversity of Microbial Sialic Acid Metabolism. Microbiology and Molecular Biology Reviews. 2004;68(1):132–53.

75. Schwarzkopf M, Knobeloch K, Rohde E, Hinderlich S, Wiechens N, Lucka L, Horak I, Reutter W, Horstkorte R. Sialylation is essential for early development in mice. Proc Natl Acad Sci USA. 2002;99(8):5267–70.

76. Schoop HJ, Schauer R, Faillard H. [On the biosynthesis of N-glycolylneuraminic acid. Oxidative formation of N-glycolylneuraminic acid from N-acetylneuraminic acid]. Hoppe Seylers Z Physiol Chem. 1969;350(2):155–62.

77. Schauer R. [Biosynthesis of N-glycoloylneuraminic acid by an ascorbic acid- or NADP-dependent N-acetyl hydroxylating “N-acetylneuraminate: O2-oxidoreductase” in homogenates of porcine submaxillary gland]. Hoppe Seylers Z Physiol Chem. 1970;351(7):783–91.

78. Hayakawa T, Satta Y, Gagneux P, Varki A, Takahata N. Alu-mediated inactivation of the human CMP-N-acetylneuraminic acid hydroxylase gene. Proc Natl Acad Sci U S A. 2001;98(20):11399–404.

79. Padler-Karavani V, Yu H, Cao H, Chokhawala H, Karp F, Varki N, Chen X, Varki A. Diversity in specificity, abundance, and composition of anti-Neu5Gc antibodies in normal humans: Potential implications for disease. Glycobiology. 2008;18(10):818–30.

80. Paul A, Padler-Karavani V. Evolution of sialic acids: Implications in xenotransplant biology. Xenotransplantation. 2018;25(8):e12424.

81. Banda K, Gregg CJ, Chow R, Varki NM, Varki A. Metabolism of Vertebrate Amino Sugars with N-Glycolyl Groups: mechanisms underlying gastrointestinal incorporation of the non-human sialic acid xeno-autoantigen N-glycolylneuraminic acid. J Biol Chem. 2012;287(34):28852–64.

82. Bergfeld AK, Pearce OM, Diaz SL, Pham T, Varki A. Metabolism of Vertebrate Amino Sugars with N-Glycolyl Groups: elucidating the intracellular fate of the non-human sialic acid N-glycolylneuraminic acid. J Biol Chem. 2012;287(34):28865–81.

83. Dhar C, Sasmal A, Varki A. From “Serum Sickness” to “Xenosialitis”: Past, Present, and Future Significance of the Non-human Sialic Acid Neu5Gc. Front Immunol. 2019;10:807.

84. Wang B, Brand-Miller J. The role and potential of sialic acid in human nutrition. Eur J Clin Nutr. 2003;57:1351–69.

85. Guo S, Tian H, Dong R, Yang N, Zhang Y, Yao S, Li Y, Zhou Y, Si Y, Qin S. Exogenous supplement of N-acetylneuraminic acid ameliorates atherosclerosis in apolipoprotein E-deficient mice. Atherosclerosis. 2016;251:183–91.

86. Samraj AN, Pearce OMT, Laubli H, Crittenden AN, Bergfeld AK, Banda K, Gregg CJ, Bingman AE, Secrest P, Diaz SL, Varki NM, Varki A. A red meat-derived glycan promotes inflammation and cancer progression. Proc Natl Acad Sci USA. 2015;112(2):542–7.

87. Kawanishi K, Dhar C, Do R, Varki N, Gordts PLSM, Varki A. Human Species-Specific Loss of CMP-N-acetylneuraminic Acid Hydroxylase Accelerates Atherosclerosis via Intrinsic and Extrinsic Mechanisms. Proc Natl Acad Sci USA. 2019;116(32).

88. Brigham C, Caughlan R, Gallegos R, Dallas MB, Godoy VG, Malamy MH. Sialic Acid (N-acetyl Neuraminic Acid) Utilization by Bacteroides Fragilis Requires a Novel N-acetyl Mannosamine Epimerase. J Bacteriol. 2009;191(11):3629–38.

89. Newstead SL, Potter JA, Wilson JC, Xu G, Chien CH, Watts AG, Withers SG, Taylor GL. The structure of Clostridium perfringens NanI sialidase and its catalytic intermediates. Journal of Biological Chemistry. 2008;283(14):9080–8.

90. Egan M, Motherway MO, Ventura M, van Sinderen D. Metabolism of Sialic Acid by Bifidobacterium Breve UCC2003. Appl Environ Microbiol. 2014;80(14):4414–26.

91. Nilsson I, Prathapam R, Grove K, Lapointe G, Six DA. The sialic acid transporter NanT is necessary and sufficient for uptake of 3-deoxy-d-manno-oct-2-ulosonic acid (Kdo) and its azido analog in Escherichia coli. Molecular Microbiology. 2018;110(2):204–18.

92. Kiyohara M, Tanigawa K, Chaiwangsri T, Katayama T, Ashida H, Yamamoto K. An exo-alpha-Sialidase from bifidobacteria involved in the degradation of sialyloligosaccharides in human milk and intestinal glycoconjugates. Glycobiology. 2011;21(4):437–47.

93. Park KH, Kim MG, Ahn HJ, Lee DH, Kim JH, Kim YW, Woo EJ. Structural and biochemical characterization of the broad substrate specificity of Bacteroides

thetaiotaomicron commensal sialidase. Biochimica et Biophysica Acta - Proteins and Proteomics. 2013;1834(8):1510–9.

94. Post DMB, Mungur R, Gibson BW, Munson RS. Identification of a novel sialic acid transporter in Haemophilus ducreyi. Infection and Immunity. 2005;73(10):6727–35.

95. Severi E, Hosie AHF, Hawkhead JA, Thomas GH. Characterization of a novel sialic acid transporter of the sodium solute symporter (SSS) family and in vivo comparison with known bacterial sialic acid transporters. FEMS Microbiology Letters. 2010;304(1):47–54.

96. Mulligan C, Leech AP, Kelly DJ, Thomas GH. The membrane proteins SiaQ and SiaM form an essential stoichiometric complex in the sialic acid tripartite ATP-independent periplasmic (TRAP) transporter SiaPQM (VC1777-1779) from Vibrio cholerae. Journal of Biological Chemistry. 2012;287(5):3598–608.

97. Severi E, Hood DW, Thomas GH. Sialic acid utilization by bacterial pathogens. Microbiology (N Y). 2007;153(9).

98. Mahajan VS, Pillai S. Sialic acids and autoimmune disease. Immunol Rev. 2016;169(1):145–61.

99. Macauley MS, Crocker PR, Paulson JC. Siglec-mediated regulation of immune cell function in disease. Nat Rev Immunol. 2014;14:653–66.

100. Haines-Menges BL, Whitaker WB, Lubin JB, Boyd EF. Host Sialic Acids: A delicacy for the pathogen with discerning taste. Microbiol Spectr. 2015;3(4).

101. Plumbridge J, Vimr E. Convergent Pathways for Utilization of the Amino Sugars N-acetylglucosamine, N-acetylmannosamine, and N-acetylneuraminic Acid by Escerichia Coli. J Bacteriol. 1999;181(1):47–54.

102. Chang DE, Smalley DJ, Tucker DL, Leatham MP, Norris WE, Stevenson SJ, Anderson AB, Grissom JE, Laux DC, Cohen PS, Conway T. Carbon Nutrition of Escherichia Coli in the Mouse Intestine. Proc Natl Acad Sci USA. 2004;101(19):7427–37.

103. Hopkins AP, Hawkhead JA, Thomas GH. Transport and catabolism of the sialic acids N-glycolylneuraminic acid and 3-keto-3-deoxy-d-glycero-d-galactonononic acid by Escherichia coli K-12. FEMS Microbiology Letters. 2013;347(1):14–22.

104. Almagro-Moreno S, Boyd EF. Insights into the evolution of sialic acid catabolism among bacteria. BMC Evol Biol. 2009;9(118).

105. Marcobal AM, Barboza M, Sonnenburg ED, Pudlo N, Martens EC, Desai P, Lebrilla CB, Weimer BC, Mills DA, German JB, Sonnenburg JL. Bacteroides in the Infant Gut Consume Milk Oligosaccharides via Mucus-Utilization Pathways. Cell Host Microbe. 2011;10(5):507–14.

106. Sebaihia M, Wren BW, Mullany P, Fairweather NF, Minton N, Stabler R, Thomson NR, Roberts AP, Cerdeno-Tarraga AM, Wang H, Holden MT, Wright A, Churcher C, Quail MA, Baker S, Bason N, Brooks K, Chillingworth T, Cronin A, Davis P, Dowd L, Fraser A, Feltwell T, Hance Z, Holroyd S, Jagels K, Moule S, Mungall K, Price C, Rabbinowitsch E, Sharp S, Simmonds M, Stevens K, Unwin L, Whithead S, Dupuy B, Dougan G, Barrell B, Parkhill J. The multidrug-resistant human pathogen Clostridium difficile has a highly mobile, mosaic genome. Nat Genetics. 2006;38:779–86.

107. Rodionov DA, Arzamasov AA, Khoroshkin MS, Iablokov SN, Leyn SA, Peterson SN, Novichkov PS, Osterman AL. Micronutrient requirements and sharing capabilities of the human gut microbiome. Frontiers in Microbiology. 2019;10(JUN):1–22.

108. Overbeek R, Olson R, Pusch GD, Olsen GJ, Davis JJ, Disz T, Edwards RA, Gerdes S, Parrello B, Shukla M, Vonstein V, Wattam AR, Xia F, Stevens R. The SEED and the Rapid Annotation of microbial genomes using Subsystems Technology (RAST). Nucleic Acids Research. 2014;42(D1):206–14.

109. Rakoff-Nahoum S, Coyne MJ, Comstock LE. An Ecological Network of Polysaccharide Utilization Among Human Intestinal Symbionts. Curr Biol. 2014;24(1):40–9.

110. Ng KM, Ferreyra JA, Higginbottom SK, Lynch JB, Kashyap PC, Gopinath S, Naidu N, Choudhury B, Weimer BC, Monack DM, Sonnenburg JL. Microbiota-liberated host sugars facilitate post-antibiotic expansion of enteric pathogens. Nature. 2013;502(7469):96–9.

111. Huang YL, Chassard C, Hausmann M, von Itzstein M, Hennet T. Sialic acid catabolism drives intestinal inflammation and microbial dysbiosis in mice. Nat Commun. 2015;6:8141.

112. Robinson LS, Lewis WG, Lewis AL. The sialate O-acetylesterase EstA from gut Bacteroidetes species enables sialidase-mediated cross-species foraging of 9-O-acetylated sialoglycans. J Biol Chem. 2017;292(28):11861–72.

113. Owen CD, Tailford LE, Monaco S, Suligoj T, Vaux L, Lallement R, Khedri Z, Yu H, Lecointe K, Walshaw J, Tribolo S, Horrex M, Bell A, Chen X, Taylor GL, Varki A, Angulo J, Juge N. Unravelling the specificity and mechanism of sialic acid recognition by the gut symbiont Ruminococcus gnavus. Nature Communications. 2017;8:2196.

114. Bell A, Brunt J, Crost E, Vaux L, Nepravishta R, Owen CD, Latousakis D, Xiao A, Li W, Chen X, Walsh MA, Claesen J, Angulo J, Thomas GH, Juge N. Elucidation of a unique sialic acid metabolism pathway in mucus-foraging Ruminococcus gnavus unravels mechanisms of bacterial adaptation to the gut. Nat Microbiol. 2019;4(12):2393–404.

115. Zaramela LS, Martino C, Alisson-silva F, Rees SD, Diaz SL, Chuzel L, Ganatra MB, Taron CH, Secrest P, Zuniga C, Huang J, Siegel D, Chang G, Varki A, Zengler K. Gut bacteria respoding to dietary changes encode sialidases the exhibit preference for red meat-associated carbohydrates. Nature Microbiology. 2019;4(12):2082–9.

116. Davis JJ, Wattam AR, Aziz RK, Brettin T, Butler R, Butler RM, Chlenski P, Conrad N, Dickerman A, Dietrich EM, Gabbard JL, Gerdes S, Guard A, Kenyon RW, MacHi D, Mao C, Murphy-Olson D, Nguyen M, Nordberg EK, Olsen GJ, Olson RD, Overbeek JC, Overbeek R, Parrello B, Pusch GD, Shukla M, Thomas C, Vanoeffelen M, Vonstein V, Warren AS, Xia F, Xie D, Yoo H, Stevens R. The PATRIC Bioinformatics Resource Center: Expanding data and analysis capabilities. Nucleic Acids Research. 2020;48(D1):D606–12.

117. Stamatakis A. Using RAxML to Infer Phylogenies. Current Protocols in Bioinformatics. 2015;51(1):6.14.1-6.14.14.

118. Letunic I, Bork P. Interactive tree of life (iTOL) v3: an online tool for the display and annotation of phylogenetic and other trees. Nucleic Acids Res. 2016;44(W1):W242–5.

119. Dominguez-Bello MG, Costello EK, Contreras M, Magris M, Hidalgo G, Fierer N, Knight R. Delivery mode shapes the acquisition and structure of the initial microbiota across multiple body habitats in newborns. Proc Natl Acad Sci U S A. 2010 Jun 29;107(26):11971–5.

120. Underwood MA, German JB, Lebrilla CB, Mills DA. Bifidobacterium longum subspecies infantis: Champion colonizer of the infant gut. Vol. 77, Pediatric Research. Nature Publishing Group; 2015. p. 229–35.

121. Zivkovic AM, German JB, Lebrilla CB, Mills DA. Human milk glycobiome and its impact on the infant gastrointestinal microbiota. Proc Natl Acad Sci USA. 2011;108(Suppl 1):4653–8.

122. Ninonuevo MR, Park Y, Yin H, Zhang J, Ward RE, Clowers BH, German JB, Freeman SL, Killeen K, Grimm R, Lebrilla CB. A strategy for annotating the human milk glycome. Journal of Agricultural and Food Chemistry. 2006;54(20):7471–80.

123. Engfer MB, Stahl B, Finke B, Sawatzki G, Daniel H. Human milk oligosaccharides are resistant to enzymatic hydrolysis in the upper gastrointestinal tract. American Journal of Clinical Nutrition. 2000;71(6):1589–96.

124. Newburg DS, Ruiz-Palacios GM, Morrow AL. Human Milk Glycans Protect Infants Against Enteric Pathogens. Annual Review of Nutrition. 2005;25(1):37–58.

125. Martín-Sosa S, Martín MJ, Hueso P. The Sialylated Fraction of Milk Oligosaccharides Is Partially Responsible for Binding to Enterotoxigenic and Uropathogenic Escherichia coli Human Strains. The Journal of Nutrition. 2002;132(10):3067–72.

126. Idota T, Kawakami H, Murakami Y, Sugawara M. Inhibition of Cholera Toxin by Human Milk Fractions and Sialyllactose. Bioscience, Biotechnology, and Biochemistry. 1995;59(3):417–9.

127. Marcobal A, Barboza M, Froehlich JW, Block DE, German JB, Lebrilla CB, Mills DA. Consumption of Human Milk Oligosaccharides by Gut-related Microbes. J Agric Food Chem. 2010 May 12;58(9):5334–40.

128. Yu ZT, Chen C, Newburg DS. Utilization of major fucosylated and sialylated human milk oligosaccharides by isolated human gut microbes. Glycobiology. 2013 Nov;23(11):1281–92.

129. Lis-Kuberka J, Orczyk-Pawiłowicz M. Sialylated oligosaccharides and glycoconjugates of human milk. The impact on infant and newborn protection, development and well-being. Vol. 11, Nutrients. MDPI AG; 2019.

130. Sela DA, Chapman J, Adeuya A, Kim JH, Chen F, Whitehead TR, Lapidus A, Rokhsar DS, Lebrilla CB, German JB, Price NP, Richardson PM, Mills DA. The genome sequence of Bifidobacterium longum subsp. infantis reveals adaptations for milk utilization within the infant microbiome. Proc Natl Acad Sci USA. 2008;105(48):18964–9.

131. Sela DA, Li Y, Lerno L, Wu S, Marcobal AM, Bruce German J, Chen X, Lebrilla CB, Mills DA. An infant-associated bacterial commensal utilizes breast milk sialyloligosaccharides. Journal of Biological Chemistry. 2011 Apr 8;286(14):11909–18.

132. Garrido D, Kim JH, German JB, Raybould HE, Mills DA. Oligosaccharide binding proteins from bifidobacterium longum subsp. infantis reveal a preference for host glycans. PLoS ONE. 2011;6(3).

133. Kim JH, An HJ, Garrido D, German JB, Lebrilla CB, Mills DA. Proteomic Analysis of Bifidobacterium longum subsp. infantis Reveals the Metabolic Insight on Consumption of Prebiotics and Host Glycans. PLoS ONE. 2013;8(2).

134. Marcobal A, Sonnenburg JL. Human milk oligosaccharide consumption by intestinal microbiota. Clinical Microbiology and Infection. 2012;18(SUPPL. 4):12–5.

135. Schwab C, Gänzle M. Lactic acid bacteria fermentation of human milk oligosaccharide components, human milk oligosaccharides and galactooligosaccharides. FEMS Microbiology Letters. 2011;315(2):141–8.

136. Ruiz-Moyano S, Totten SM, Garrido DA, Smilowitz JT, Bruce German J, Lebrilla CB, Mills DA. Variation in consumption of human milk oligosaccharides by infant gut-associated strains of bifidobacterium breve. Applied and Environmental Microbiology. 2013;79(19):6040–9.

137. Wang B, Brand-Miller J, McVeagh P, Petocz P. Concentration and distribution of sialic acid in human milk and infant formulas. American Journal of Clinical Nutrition. 2001;74(4):510–5.

138. Nwosu CC, Aldredge DL, Lee H, Lerno LA, Zivkovic AM, German JB, Lebrilla CB. Comparison of the Human and Bovine Milk N-Glycome via High-Performance Microfluidic Chip Liquid Chromatography and Tandem Mass Spectrometry. J Proteome Res. 2012;11(5):2912–24.

139. Quin C, Vicaretti SD, Mohtarudin NA, Garner AM, Vollman DM, Gibson DL, Zandberg WF, Hart GW. Influence of sulfonated and diet-derived human milk oligosaccharides on the infant microbiome and immune markers. Journal of Biological Chemistry. 2020 Mar 20;295(12):4035–48.

140. Taylor RE, Gregg CJ, Padler-Karavani V, Ghaderi D, Yu H, Huang S, Sorensen RU, Chen X, Inostroza J, Nizet V, Varki A. Novel mechanism for the generation of human xeno-autoantibodies against the nonhuman sialic acid N-glycolylneuraminic acid. J Exp Med. 2010;207(8):1637–46.

141. Charbonneau MR, O'Donnell D, Blanton L V., Totten SM, Davis JCC, Barratt MJ, Cheng J, Guruge J, Talcott M, Bain JR, Muehlbauer MJ, Ilkayeva O, Wu C, Struckmeyer T, Barile D, Mangani C, Jorgensen J, Fan YM, Maleta K, Dewey KG, Ashorn P, Newgard CB, Lebrilla C, Mills DA, Gordon JI. Sialylated Milk Oligosaccharides Promote Microbiota-Dependent Growth in Models of Infant Undernutrition. Cell. 2016 Feb 25;164(5):859–71.

142. Feng L, Raman AS, Hibberd MC, Cheng J, Griffin NW, Peng Y, Leyn SA, Rodionov DA, Osterman AL, Gordon JI. Identifying determinants of bacterial fitness in a model of human gut microbial succession. Proc Natl Acad Sci U S A. 2020;117(5):2622–33.

143. Cowardin CA, Ahern PP, Kung VL, Hibberd MC, Cheng J, Guruge JL, Sundaresan V, Head RD, Barile D, Mills DA, Barratt MJ, Huq S, Ahmed T, Gordon JI. Mechanisms by which sialylated milk oligosaccharides impact bone biology in a gnotobiotic mouse model of infant undernutrition. Proc Natl Acad Sci U S A. 2019;116(24):11988–96.

144. Getz GS, Reardon CA. Animal Models of Atherosclerosis. Aterioscler Thromb Vasc Biol. 2012;32(5):1104–15.

145. Tanigaki K, Sacharidou A, Peng J, Chambliss KL, Yuhanna IS, Ghosh D, Ahmed M, Szalai A, Vongatanasin W, Mattrey RF, Chen Q, Azadi P, Lingvay I, Botto M, Holland WL, Kohler JJ, Sirsi SR, Hoyt K, Shaul PW, Mineo C. Hyposialylated IgG activates endothelial IgG receptor FcyRIIB to promote obesity-induced insulin resistance. J Clin Invest. 2018;128(1):309–22.

146. Jonsson AL, Bäckhed F. Role of gut microbiota in atherosclerosis. Nature Reviews Cardiology. 2017;14(2):79–87.

147. Jie Z, Xia H, Zhong SL, Feng Q, Li S, Liang S, Zhong H, Liu Z, Gao Y, Zhao H, Zhang D, Su Z, Fang Z, Lan Z, Li J, Xiao L, Li J, Li R, Li X, Li F, Ren H, Huang Y, Peng Y, Li G, Wen B, Dong B, Chen JY, Geng QS, Zhang ZW, Yang H, Wang J, Wang J, Zhang X, Madsen L, Brix S, Ning G, Xu X, Liu X, Hou Y, Jia H, He K, Kristiansen K. The gut microbiome in atherosclerotic cardiovascular disease. Nature Communications. 2017;8(1):1–11.

148. Gurung M, Li Z, You H, Rodrigues R, Jump DB, Morgun A, Shulzhenko N. Role of gut microbiota in type 2 diabetes pathophysiology. EBioMedicine. 2020;51:102590.

149. Hedlund M, Tangvoranuntakul P, Takematsu H, Long JM, Housley GD, Kozutsumi Y, Suzuki A, Wynshaw-Boris A, Ryan AF, Gallo RL, Varki N, Varki A. N-Glycolylneuraminic Acid Deficiency in Mice: Implications for Human Biology and Evolution. Mol Cell Biol. 2007;27(12):4340–6.

150. Perota A, Galli C. N-Glycolylneuraminic Acid (Neu5Gc) Null Large Animals by Targeting the CMP-Neu5Gc Hydroxylase (CMAH). Front Immunol. 2019;

151. Toju H, Peay KG, Yamamichi M, Narisawa K, Hiruma K, Naito K, Fukuda S, Ushio M, Nakaoka S, Onoda Y, Yoshida K, Schlaeppi K, Bai Y, Sugiura R, Ichihashi Y, Minamisawa K, Kiers ET. Core microbiomes for sustainable agroecosystems. Nature Plants [Internet]. 2018;4(5):247–57. Available from: http://dx.doi.org/10.1038/s41477-018-0139-4

152. Hu J, Wei Z, Friman VPP, Gu S hua H, Wang X fang F, Eisenhauer N, Yang T jie J, Ma J, Shen Q rong R, Xu Y chun C, Jousset A. Probiotic Diversity Enhances Rhizosphere Microbiome Function and Plant Disease Suppression. Mbio [Internet]. 2016;7(6):1–8. Available from: https://www.ncbi.nlm.nih.gov/pmc/articles/PMC5156302/pdf/mBio.01790-16.pdf

153. Vorholt JA, Vogel C, Carlström CI, Müller DB. Establishing Causality: Opportunities of Synthetic Communities for Plant Microbiome Research. Cell Host and Microbe. 2017;22(2):142–55.

154. Edwards J, Johnson C, Santos-Medellin C, Lurie E, Kumar Podishetty N, Bhatnagar S, Eisen JA, Sundaresan V. Structure, variation, and assembly of the root-associated microbiomes of rice. Proc Natl Acad Sci USA. 2015;112(8):E911–20.

155. Bai Y, Müller DB, Srinivas G, Garrido-Oter R, Potthoff E, Rott M, Dombrowski N, Münch PC, Spaepen S, Remus-Emsermann M, Hüttel B, McHardy AC, Vorholt JA, Schulze-Lefert P. Functional overlap of the Arabidopsis leaf and root microbiota. Nature. 2015;528(7582):364–9.

156. Niu B, Paulson JN, Zheng X, Kolter R. Simplified and representative bacterial community of maize roots. Proc Natl Acad Sci U S A. 2017;114(12):E2450–9.

157. Bodenhausen N, Bortfeld-Miller M, Ackermann M, Vorholt JA. A Synthetic Community Approach Reveals Plant Genotypes Affecting the Phyllosphere Microbiota. PLoS Genetics. 2014;10(4).

158. Lebeis SL, Paredes SH, Lundberg DS, Breakfield N, Gehring J, McDonald M, Malfatti S, del Rio TG, Jones CD, Tringe SG, Dangl JL. Salicylic acid modulates colonization of the root microbiome by specific bacterial taxa. Science (1979). 2015;349(6250):860–4.

159. Zengler K, Hofmockel K, Baliga NS, Behie SW, Bernstein HC, Brown JB, Dinneny JR, Floge SA, Forry SP, Hess M, Jackson SA, Jansson C, Lindemann SR, Pett-Ridge J, Maranas C, Venturelli OS, Wallenstein MD, Shank EA, Northen TR. EcoFABs: advancing microbiome science through standardized fabricated ecosystems. Nature Methods [Internet]. 2019;16(7):567–71. Available from: http://dx.doi.org/10.1038/s41592-019-0465-0

160. Castrillo G, Teixeira PJPL, Paredes SH, Law TF, de Lorenzo L, Feltcher ME, Finkel OM, Breakfield NW, Mieczkowski P, Jones CD, Paz-Ares J, Dangl JL. Root microbiota drive direct integration of phosphate stress and immunity. Nature [Internet]. 2017;543(7646):513–8. Available from: http://dx.doi.org/10.1038/nature21417

161. Herrera Paredes S, Gao T, Law TF, Finkel OM, Mucyn T, Teixeira PJPL, Salas González I, Feltcher ME, Powers MJ, Shank EA, Jones CD, Jojic V, Dangl JL, Castrillo G. Design of synthetic bacterial communities for predictable plant phenotypes. Vol. 16, PLoS Biology. 2018. 1–41 p.

162. Auchtung JM, Robinson CD, Britton RA. Cultivation of stable, reproducible microbial communities from different fecal donors using minibioreactor arrays (MBRAs). Microbiome [Internet]. 2015;3(1):1–15. Available from: http://dx.doi.org/10.1186/s40168-015-0106-5

163. J Cira N, Pearce MT, Quake SR. Neutral and selective dynamics in a synthetic microbial community. Proc Natl Acad Sci U S A. 2018;115(42):E9842–8.

164. Ehsani E, Hernandez-Sanabria E, Kerckhof FM, Props R, Vilchez-Vargas R, Vital M, Pieper DH, Boon N. Initial evenness determines diversity and cell density dynamics in synthetic microbial ecosystems. Scientific Reports [Internet]. 2018;8(1):1–9. Available from: http://dx.doi.org/10.1038/s41598-017-18668-1

165. Zuñiga C, Li CT, Yu G, Al-Bassam MM, Li T, Jiang L, Zaramela LS, Guarnieri M, Betenbaugh MJ, Zengler K. Environmental stimuli drive a transition from cooperation to competition in synthetic phototrophic communities. Nature Microbiology [Internet]. 2019;4(12):2184–91. Available from: http://dx.doi.org/10.1038/s41564-019-0567-6

166. Vega NM, Gore J. Simple organizing principles in microbial communities. Vol. 45, Current Opinion in Microbiology. Elsevier Ltd; 2018. p. 195–202.

167. Marx V. Model organisms on roads less traveled. Nature Methods [Internet]. 2021;18(3):235–9. Available from: http://dx.doi.org/10.1038/s41592-021-01086-7

168. Koornneef M, Meinke D. The development of Arabidopsis as a model plant. Plant Journal. 2010;61(6):909–21.

169. Blaser MJ, Cardon ZG, Cho MK, Dangl JL, Donohue TJ, Green JL, Knight R, Maxon ME, Northen TR, Pollard KS, Brodie EL. Toward a predictive understanding of earth's microbiomes to address 21st century challenges. mBio. 2016;7(3):1–16.

170. Busby PE, Soman C, Wagner MR, Friesen ML, Kremer J, Bennett A, Morsy M, Eisen JA, Leach JE, Dangl JL. Research priorities for harnessing plant microbiomes in sustainable agriculture. PLoS Biology. 2017;15(3):1–14.

171. Bosch TC, Mcfall-Ngai MJ. Metaorganisms as the new frontier. Zoology (Jena) [Internet]. 2011;114(4):185–90. Available from: https://www.ncbi.nlm.nih.gov/pmc/articles/PMC3992624/pdf/nihms569856.pdf

172. McDonald JAK, Schroeter K, Fuentes S, Heikamp-deJong I, Khursigara CM, de Vos WM, Allen-Vercoe E. Evaluation of microbial community reproducibility, stability and composition in a human distal gut chemostat model. Journal of Microbiological Methods [Internet]. 2013;95(2):167–74. Available from: http://dx.doi.org/10.1016/j.mimet.2013.08.008

173. Agostinho A, Hartman A, Lipp C, Parker A, Stewart P, James G. An in vitro model for the growth and analysis of chronic wound MRSA biofilms. Journal of Applied Microbiology. 2011;111(5).

174. Kim HJ, Li H, Collins JJ, Ingber DE. Contributions of microbiome and mechanical deformation to intestinal bacterial overgrowth and inflammation in a human gut-on-a-chip. Proc Natl Acad Sci U S A. 2016;113(1):E7–15.

175. Cremer J, Segota I, Yang CY, Arnoldini M, Sauls JT, Zhang Z, Gutierreza E, Groisman A, Hwa T. Effect of flow and peristaltic mixing on bacterial growth in a gut-like channel. Proc Natl Acad Sci U S A. 2016;113(41):11414–9.

176. Aranda-Díaz A, Ng KM, Thomsen T, Real-Ramírez I, Dahan D, Dittmar S, Gonzalez CG, Chavez T, Vasquez KS, Nguyen TH, Yu FB, Higginbottom SK, Neff NF, Elias JE, Sonnenburg JL, Huang KC. Establishment and characterization of stable, diverse, fecal-derived in vitro microbial communities that model the intestinal microbiota. Cell Host & Microbe. 2022 Jan;

177. Orcutt R, Gianni F, Judge R. Development of an "altered Schaedler flora" for NCI gnotobiotic rodents. Microecology and Therapy. 1987;17(59).

178. Brand MW, Wannemuehler MJ, Phillips GJ, Proctor A, Overstreet AM, Jergens AE, Orcutt RP, Fox JG. The altered schaedler flora: Continued applications of a defined murine microbial community. ILAR Journal. 2015;56(2):169–78.

179. Zengler K. Central Role of the Cell in Microbial Ecology. Microbiology and Molecular Biology Reviews. 2009;73(4):712–29.

180. Gao J, Sasse J, Lewald KM, Zhalnina K, Cornmesser LT, Duncombe TA, Yoshikuni Y, Vogel JP, Firestone MK, Northen TR. Ecosystem fabrication (EcoFAB) protocols for the construction of laboratory ecosystems designed to study plant-microbe interactions. Journal of Visualized Experiments. 2018;(134):1–16.

181. Vrancken G, Gregory AC, Huys GRB, Faust K, Raes J. Synthetic ecology of the human gut microbiota. Nature Reviews Microbiology [Internet]. 2019;17(12):754–63. Available from: http://dx.doi.org/10.1038/s41579-019-0264-8

182. McClure R, Naylor D, Farris Y, Davison M, Fansler SJ, Hofmockel KS, Jansson JK. Development and Analysis of a Stable, Reduced Complexity Model Soil Microbiome. Frontiers in Microbiology. 2020;11(August):1–15.

183. Ke J, Wang B, Yoshikuni Y. Microbiome Engineering: Synthetic Biology of Plant-Associated Microbiomes in Sustainable Agriculture. Trends in Biotechnology [Internet]. 2020;xx(xx):1–18. Available from: https://doi.org/10.1016/j.tibtech.2020.07.008

184. McCarty NS, Ledesma-Amaro R. Synthetic Biology Tools to Engineer Microbial Communities for Biotechnology. Trends in Biotechnology [Internet]. 2019;37(2):181–97. Available from: https://doi.org/10.1016/j.tibtech.2018.11.002

185. Sheth RU, Cabral V, Chen SP, Wang HH. Manipulating Bacterial Communities by in situ Microbiome Engineering. Trends in Genetics [Internet]. 2016;32(4):189–200. Available from: http://dx.doi.org/10.1016/j.tig.2016.01.005

186. Schommer NN, Gallo RL. Structure and function of the human skin microbiome. Vol. 21, Trends in Microbiology. 2013. p. 660–8.

187. Grice EA, Segre JA. The skin microbiome. Vol. 9, Nature Reviews Microbiology. 2011. p. 244–53.

188. Byrd AL, Belkaid Y, Segre JA. The human skin microbiome. Nature Reviews Microbiology [Internet]. 2018;16(3):143–55. Available from: http://dx.doi.org/10.1038/nrmicro.2017.157

189. Bjerre RD, Bandier J, Skov L, Engstrand L, Johansen JD. The role of the skin microbiome in atopic dermatitis: a systematic review. Vol. 177, British Journal of Dermatology. Blackwell Publishing Ltd; 2017. p. 1272–8.

190. Xu H, Li H. Acne, the Skin Microbiome, and Antibiotic Treatment. Vol. 20, American Journal of Clinical Dermatology. Springer International Publishing; 2019. p. 335–44.

191. Staudinger T, Pipal A, Redl B. Molecular analysis of the prevalent microbiota of human male and female forehead skin compared to forearm skin and the influence of make-up. Journal of Applied Microbiology. 2011 Jun;110(6):1381–9.

192. Urban J, Fergus DJ, Savage AM, Ehlers M, Menninger HL, Dunn RR, Horvath JE. The effect of habitual and experimental antiperspirant and deodorant product use on the armpit microbiome. PeerJ. 2016;2016(2).

193. Bouslimani A, da Silva R, Kosciolek T, Janssen S, Callewaert C, Amir A, Dorrestein K, Melnik A v., Zaramela LS, Kim JN, Humphrey G, Schwartz T, Sanders K, Brennan C, Luzzatto-Knaan T, Ackermann G, McDonald D, Zengler K, Knight R, Dorrestein PC. The impact of skin care products on skin chemistry and microbiome dynamics. BMC Biology. 2019 Jun 12;17(1).

194. Oh J, Byrd AL, Park M, Kong HH, Segre JA. Temporal Stability of the Human Skin Microbiome. Cell. 2016 May 5;165(4):854–66.

195. Ruuskanen MO, Vats D, Potbhare R, RaviKumar A, Munukka E, Ashma R, Lahti L. Towards standardized and reproducible research in skin microbiomes. Environmental Microbiology. 2022;

196. Tan J, Zuniga C, Zengler K. Unraveling interactions in microbial communities - from co-cultures to microbiomes. Vol. 53, Journal of Microbiology. Microbiological Society of Korea; 2015. p. 295–305.

197. Kong HH, Oh J. State of Residency: Microbial Strain Diversity in the Skin. Journal of Investigative Dermatology. Elsevier B.V.; 2021.

198. Larson PJ, Chong D, Fleming E, Oh J. Challenges in Developing a Human Model System for Skin Microbiome Research. Journal of Investigative Dermatology. 2021 Jan 1;141(1):228-231.e4.

199. Boxberger M, Cenizo V, Cassir N, la Scola B. Challenges in exploring and manipulating the human skin microbiome. Vol. 9, Microbiome. BioMed Central Ltd; 2021.

200. Sasse J, Kant J, Cole BJ, Klein AP, Arsova B, Schlaepfer P, Gao J, Lewald K, Zhalnina K, Kosina S, Bowen BP, Treen D, Vogel J, Visel A, Watt M, Dangl JL, Northen TR. Multilab EcoFAB study shows highly reproducible physiology and depletion of soil metabolites by a model grass. New Phytologist. 2018;222(2).

201. Xiao M, Zhou XK, Chen X, Duan YQ, Alkhalifah DHM, Im WT, Hozzein WN, Chen W, Li WJ. Lysobacter tabacisoli sp. nov., isolated from rhizosphere soil of Nicotiana tabacum L. International Journal of Systematic and Evolutionary Microbiology. 2019 Jul 1;69(7):1875–80.

202. Kim SJ, Ahn JH, Weon HY, Joa JH, Hong SB, Seok SJ, Kim JS, Kwon SW. Lysobacter solanacearum sp. nov., isolated from rhizosphere of tomato.

International Journal of Systematic and Evolutionary Microbiology. 2017 May 1;67(5):1102–6.

203. Park JH, Kim R, Aslam Z, Jeon CO, Chung YR. Lysobacter capsici sp. nov., with antimicrobial activity, isolated from the rhizosphere of pepper, and emended description of the genus Lysobacter. International Journal of Systematic and Evolutionary Microbiology. 2008 Feb;58(2):387–92.

204. Richardson J, Stead DE, Elphinstone JG, Coutts RHA. Diversity of Burkholderia isolates from woodland rhizosphere environments.

205. Caballero-Mellado J, Martínez-Aguilar L, Paredes-Valdez G, Estrada-de los Santos P. Burkholderia unamae sp. nov., an N2-fixing rhizospheric and endophytic species. International Journal of Systematic and Evolutionary Microbiology. 2004 Jul;54(4):1165–72.

206. Ramette A, LiPuma JJ, Tiedje JM. Species abundance and diversity of Burkholderia cepacia complex in the environment. Applied and Environmental Microbiology. 2005 Mar;71(3):1193–201.

207. Castanheira N, Dourado AC, Kruz S, Alves PIL, Delgado-Rodríguez AI, Pais I, Semedo J, Scotti-Campos P, Sánchez C, Borges N, Carvalho G, Barreto Crespo MT, Fareleira P. Plant growth-promoting Burkholderia species isolated from annual ryegrass in Portuguese soils. Journal of Applied Microbiology. 2016 Mar 1;120(3):724–39.

208. Schlatter DC, Yin C, Hulbert S, Paulitz TC. Core Rhizosphere Microbiomes of Dryland Wheat Are Influenced by Location and Land Use History. 2020; Available from: https://doi.org/10.1128/AEM

209. Dai Y, Yang F, Zhang L, Xu Z, Fan X, Tian Y, Wang T. Wheat-associated microbiota and their correlation with stripe rust reaction. Journal of Applied Microbiology. 2020 Feb 1;128(2):544–55.

210. Xu J, Zhang Y, Zhang P, Trivedi P, Riera N, Wang Y, Liu X, Fan G, Tang J, Coletta-Filho HD, Cubero J, Deng X, Ancona V, Lu Z, Zhong B, Roper MC, Capote N, Catara V, Pietersen G, Vernière C, Al-Sadi AM, Li L, Yang F, Xu X, Wang J, Yang H, Jin T, Wang N. The structure and function of the global citrus rhizosphere microbiome. Nature Communications. 2018 Dec 1;9(1).

211. Gao J lian, Sun Y chen, Xue J, Sun P, Yan H, Khan MS, Wang L wei, Zhang X, Sun J guang. Variovorax beijingensis sp. nov., a novel plant-associated bacterial species with plant growth-promoting potential isolated from different geographic regions of Beijing, China. Systematic and Applied Microbiology. 2020 Nov 1;43(6).

212. Kim SJ, Cho H, Ahn JH, Weon HY, Joa JH, Hong SB, Seok SJ, Kim JS, Kwon SW. Chitinophaga rhizosphaerae sp. Nov., isolated from rhizosphere soil of a tomato

plant. International Journal of Systematic and Evolutionary Microbiology. 2017 Sep 1;67(9):3435–9.

213. Chung EJ, Park TS, Jeon CO, Chung YR. Chitinophaga oryziterrae sp. nov., isolated from the rhizosphere soil of rice (Oryza sativa L.). International Journal of Systematic and Evolutionary Microbiology. 2012;62(12):3030–5.

214. Li L, Sun L, Shi N, Liu L, Guo H, Xu A, Zhang X, Yao N. Chitinophaga cymbidii sp. nov., isolated from Cymbidium goeringii roots. International Journal of Systematic and Evolutionary Microbiology. 2013 May 1;63(PART 5):1800–4.

215. Lee HG, An DS, Im WT, Liu QM, Na JR, Cho DH, Jin CW, Lee ST, Yang DC. Chitinophaga ginsengisegetis sp. nov. and Chitinophaga ginsengisoli sp. nov., isolated from soil of a ginseng field in South Korea. International Journal of Systematic and Evolutionary Microbiology. 2007 Jul;57(7):1396–401.

216. Yan ZF, Lin P, Wang YS, Gao W, Li CT, Kook MC, Yi TH. Niastella hibisci sp. nov., isolated from rhizosphere soil of mugunghwa, the Korean national flower. International Journal of Systematic and Evolutionary Microbiology. 2016 Dec 1;66(12):5218–22.

217. Akter S, Park JH, Mizanur Rahman M, Huq MA. Niastella soli sp. Nov., isolated from rhizospheric soil of a persimmon tree. International Journal of Systematic and Evolutionary Microbiology. 2021;71(7).

218. Zhang K, Wang Y, Tang Y, Dai J, Zhang L, An H, Luo G, Rahman E, Fang C. Niastella populi sp. nov., isolated from soil of Euphrates poplar (Populus euphratica) forest, and emended description of the genus Niastella. International Journal of Systematic and Evolutionary Microbiology. 2010 Mar;60(3):542–5.

219. Weon HY, Kim BY, Yoo SH, Lee SY, Kwon SW, Go SJ, Stackebrandt E. Niastella koreensis gen. nov., sp. nov. and Niastella yeongjuensis sp. nov., novel members of the phylum Bacteroidetes, isolated from soil cultivated with Korean ginseng. International Journal of Systematic and Evolutionary Microbiology. 2006 Aug;56(8):1777–82.

220. Madhaiyan M, Poonguzhali S, Lee JS, Senthilkumar M, Lee KC, Sundaram S. Mucilaginibacter gossypii sp. nov. and Mucilaginibacter gossypiicola sp. nov., plant-growth-promoting bacteria isolated from cotton rhizosphere soils. International Journal of Systematic and Evolutionary Microbiology. 2010 Oct;60(10):2451–7.

221. Lee HR, Han SI, Rhee KH, Whang KS. Mucilaginibacter herbaticus sp. nov., isolated from the rhizosphere of the medicinal plant Angelica sinensis. International Journal of Systematic and Evolutionary Microbiology. 2013 Aug;63(PART8):2787–93.

222. Ahn JH, Kim BC, Joa JH, Kim SJ, Song J, Kwon SW, Weon HY. Mucilaginibacter ginsengisoli sp. Nov., Isolated from a ginseng-cultivated soil. International Journal of Systematic and Evolutionary Microbiology. 2015 Nov 1;65(11):3933–7.

223. Li W, Ten LN, Kim MK, Lee SY, Kang IK, Jung HY. Mucilaginibacter segetis sp. nov., Isolated from Soil. Current Microbiology. 2021 Jun 1;78(6):2447–54.

224. Menon RR, Kumari S, Kumar P, Verma A, Krishnamurthi S, Rameshkumar N. Sphingomonas pokkalii sp. nov., a novel plant associated rhizobacterium isolated from a saline tolerant pokkali rice and its draft genome analysis. Systematic and Applied Microbiology. 2019 May 1;42(3):334–42.

225. Chung EJ, Jo EJ, Yoon HS, Song GC, Jeon CO, Chung YR. Sphingomonas oryziterrae sp. nov. and sphingomonas jinjuensis sp. nov. isolated from rhizosphere soil of rice (oryza sativa l.). International Journal of Systematic and Evolutionary Microbiology. 2011 Oct;61(10):2389–94.

226. Zhao JJ, Zhang J, Sun L, Zhang RJ, Zhang CW, Yin HQ, Zhang XX. Rhizobium oryziradicis sp. Nov., isolated from rice roots. Vol. 67, International Journal of Systematic and Evolutionary Microbiology. Microbiology Society; 2017. p. 963–8.

227. Ouyabe M, Tanaka N, Shiwa Y, Fujita N, Kikuno H, Babil P, Shiwachi H. Rhizobium dioscoreae sp. Nov., a plant growth-promoting bacterium isolated from yam (dioscorea species). International Journal of Systematic and Evolutionary Microbiology. 2020;70(9):5054–62.

228. Morvan S, Meglouli H, Lounès-Hadj Sahraoui A, Hijri M. Into the wild blueberry (Vaccinium angustifolium) rhizosphere microbiota. Environmental Microbiology. 2020 Sep 1;22(9):3803–22.

229. de Alencar Menezes Júnior I, Feitosa de Matos G, Moura de Freitas K, da Conceição Jesus E, Rouws LFM. Occurrence of diverse Bradyrhizobium spp. in roots and rhizospheres of two commercial Brazilian sugarcane cultivars. Brazilian Journal of Microbiology. 2019 Jul 1;50(3):759–67.

230. Qaisrani MM, Zaheer A, Mirza MS, Naqqash T, Qaisrani TB, Hanif MK, Rasool G, Malik KA, Ullah S, Jamal MS, Mirza Z, Karim S, Rasool M. A comparative study of bacterial diversity based on culturable and culture-independent techniques in the rhizosphere of maize (Zea mays L.). Saudi Journal of Biological Sciences. 2019 Nov 1;26(7):1344–51.

231. Jurelevicius D, Korenblum E, Casella R, Vital RL, Seldin L. Polyphasic analysis of the bacterial community in the rhizosphere and roots of Cyperus rotundus L. grown in a petroleum-contaminated soil. Journal of Microbiology and Biotechnology. 2010;20(5):862–70.

232. Andreote FD, Carneiro RT, Salles JF, Marcon J, Labate CA, Azevedo JL, Araújo WL. Culture-independent assessment of rhizobiales-related alphaproteobacteria

and the diversity of Methylobacterium in the rhizosphere and rhizoplane of transgenic eucalyptus. Microbial Ecology. 2009;57(1):82–93.

233. Poonguzhali S, Madhaiyan M, Yim WJ, Kim KA, Sa TM. Colonization pattern of plant root and leaf surfaces visualized by use of green-fluorescent-marked strain of Methylobacterium suomiense and its persistence in rhizosphere. Applied Microbiology and Biotechnology. 2008 Apr;78(6):1033–43.

234. Schmalenberger A, Tebbe CC. Bacterial community composition in the rhizosphere of a transgenic, herbicide-resistant maize (Zea mays) and comparison to its non-transgenic cultivar Bosphore. FEMS Microbiology Ecology. 2006 Jan 5;40(1):29–37.

235. Cheng J, Zhang MY, Zhao JC, Xu H, Zhang Y, Zhang TY, Wu YY, Zhang YX. Arthrobacter ginkgonis sp. Nov., an actinomycete isolated from rhizosphere of Ginkgo biloba L. International Journal of Systematic and Evolutionary Microbiology. 2017 Feb 1;67(2):319–24.

236. Fernández-González AJ, Martínez-Hidalgo P, Cobo-Díaz JF, Villadas PJ, Martínez-Molina E, Toro N, Tringe SG, Fernández-López M. The rhizosphere microbiome of burned holm-oak: Potential role of the genus Arthrobacter in the recovery of burned soils. Scientific Reports. 2017 Dec 1;7(1).

237. Upadhyay SK, Singh DP, Saikia R. Genetic Diversity of Plant Growth Promoting Rhizobacteria Isolated from Rhizospheric Soil of Wheat under Saline Condition. Current Microbiology. 2009 Nov;59(5):489–96.

238. Zhang Y, Zhang J, Fang C, Pang H, Fan J. Mycobacterium litorale sp. nov., a rapidly growing mycobacterium from soil. International Journal of Systematic and Evolutionary Microbiology. 2012 May;62(5):1204–7.

239. Bouam A, Armstrong N, Levasseur A, Drancourt M. Mycobacterium terramassiliense, Mycobacterium rhizamassiliense and Mycobacterium numidiamassiliense sp. nov., three new Mycobacterium simiae complex species cultured from plant roots. Scientific Reports. 2018 Dec 1;8(1).

240. Wang W, Zhai Y, Cao L, Tan H, Zhang R. Illumina-based analysis of core actinobacteriome in roots, stems, and grains of rice. Microbiological Research. 2016 Sep 1;190:12–8.

241. Li C, Cao P, Jiang M, Hou Y, Du C, Xiang W, Zhao J, Wang X. Rhodococcus oryzae sp. nov., a novel actinobacterium isolated from rhizosphere soil of rice (Oryza sativa L.). International Journal of Systematic and Evolutionary Microbiology. 2020;70(5):3300–8.

242. Li Z, Song C, de Jong A, Kuipers OP. Draft Genome Sequences of Six Bacillus Strains and One Brevibacillus Strain Isolated from the Rhizosphere of Perennial Ryegrass (Lolium perenne). 2019; Available from: https://doi.org/10.1128/MRA

243. Sheng M, Jia H, Zhang G, Zeng L, Zhang T, Long Y, Lan J, Hu Z, Zeng Z, Wang B, Liu H. Siderophore Production by Rhizosphere Biological Control Bacteria Brevibacillus brevis GZDF3 of Pinellia ternata and Its Antifungal Effects on Candida albicans. Journal of Microbiology and Biotechnology. 2020 May 28;30(5):689–99.

244. Jin F, Ding Y, Ding W, Reddy MS, Dilantha Fernando WG, Du B. Genetic diversity and phylogeny of antagonistic bacteria against phytophthora nicotianae isolated from tobacco Rhizosphere. International Journal of Molecular Sciences. 2011 May;12(5):3055–71.

245. Nehra V, Saharan BS, Choudhary M. Evaluation of Brevibacillus brevis as a potential plant growth promoting rhizobacteria for cotton (Gossypium hirsutum) crop. Springerplus. 2016 Dec 1;5(1).

246. Lee SA, Kim TW, Heo J, Sang MK, Song J, Kwon SW, Weon HY. Paenibacillus lycopersici sp. nov. and Paenibacillus rhizovicinus sp. nov., isolated from the rhizosphere of tomato (Solanum lycopersicum). Journal of Microbiology. 2020 Oct 1;58(10):832–40.

247. Zhang J, Ma XT, Gao JS, Zhang CW, Zhao JJ, Zhang RJ, Ma LA, Zhang XX. Paenibacillus oryzisoli sp. nov., isolated from the rhizosphere of rice. Antonie van Leeuwenhoek, International Journal of General and Molecular Microbiology. 2017 Jan 1;110(1):69–75.

248. Ran J, Jiao L, Zhao R, Zhu M, Shi J, Xu B, Pan L. Characterization of a novel antifungal protein produced by Paenibacillus polymyxa isolated from the wheat rhizosphere. Journal of the Science of Food and Agriculture. 2021 Mar 30;101(5):1901–9.

249. Carini P, Delgado-Baquerizo M, Hinckley ELS, Holland-Moritz H, Brewer TE, Rue G, Vanderburgh C, McKnight D, Fierer N. Unraveling the effects of spatial variability and relic DNA on the temporal dynamics of soil microbial communities. mBio. 2020;11(1):1–16.

250. Marotz CA, Sanders JG, Zuniga C, Zaramela LS, Knight R, Zengler K. Improving saliva shotgun metagenomics by chemical host DNA depletion. Microbiome. 2018;6(1):1–9.

251. Marotz C, Morton JT, Navarro P, Coker J, Belda-Ferre P, Knight R, Zengler K. Quantifying Live Microbial Load in Human Saliva Samples over Time Reveals Stable Composition and Dynamic Load. mSystems. 2021;6(1):1–16.

252. Leducq JB, Seyer-Lamontagne E, Condrain-Morel D, Bourret G, Sneddon D, Foster JA, Marx CJ, Sullivan JM, Shapiro BJ, Kembel SW, Keim P. Fine-Scale Adaptations to Environmental Variation and Growth Strategies Drive Phyllosphere Methylobacterium Diversity. 2022.

253. Ceja-Navarro JA, Wang Y, Ning D, Arellano A, Ramanculova L, Yuan MM, Byer A, Craven KD, Saha MC, Brodie EL, Pett-Ridge J, Firestone MK. Protist diversity and community complexity in the rhizosphere of switchgrass are dynamic as plants develop. Microbiome. 2021 Dec 1;9(1).

254. Sher Y, Baker NR, Herman D, Fossum C, Hale L, Zhang X, Nuccio E, Saha M, Zhou J, Pett-Ridge J, Firestone M. Microbial extracellular polysaccharide production and aggregate stability controlled by switchgrass (Panicum virgatum) root biomass and soil water potential. Soil Biology and Biochemistry. 2020 Apr 1;143.

255. Thompson LR, Sanders JG, McDonald D, Amir A, Ladau J, Locey KJ, Prill RJ, Tripathi A, Gibbons SM, Ackermann G, Navas-Molina JA, Janssen S, Kopylova E, Vázquez-Baeza Y, González A, Morton JT, Mirarab S, Xu ZZ, Jiang L, Haroon MF, Kanbar J, Zhu Q, Song SJ, Kosciolek T, Bokulich NA, Lefler J, Brislawn CJ, Humphrey G, Owens SM, Hampton-Marcell J, Berg-Lyons D, McKenzie V, Fierer N, Fuhrman JA, Clauset A, Stevens RL, Shade A, Pollard KS, Goodwin KD, Jansson JK, Gilbert JA, Knight R, Agosto Rivera JL, Al-Moosawi L, Alverdy J, Amato KR, Andras J, Angenent LT, Antonopoulos DA, Apprill A, Armitage D, Ballantine K, Bárta J, Baum JK, Berry A, Bhatnagar A, Bhatnagar M, Biddle JF, Bittner L, Boldgiv B, Bottos E, Boyer DM, Braun J, Brazelton W, Brearley FQ, Campbell AH, Caporaso JG, Cardona C, Carroll JL, Cary SC, Casper BB, Charles TC, Chu H, Claar DC, Clark RG, Clayton JB, Clemente JC, Cochran A, Coleman ML, Collins G, Colwell RR, Contreras M, Crary BB, Creer S, Cristol DA, Crump BC, Cui D, Daly SE, Davalos L, Dawson RD, Defazio J, Delsuc F, Dionisi HM, Dominguez-Bello MG, Dowell R, Dubinsky EA, Dunn PO, Ercolini D, Espinoza RE, Ezenwa V, Fenner N, Findlay HS, Fleming ID, Fogliano V, Forsman A, Freeman C, Friedman ES, Galindo G, Garcia L, Garcia-Amado MA, Garshelis D, Gasser RB, Gerdts G, Gibson MK, Gifford I, Gill RT, Giray T, Gittel A, Golyshin P, Gong D, Grossart HP, Guyton K, Haig SJ, Hale V, Hall RS, Hallam SJ, Handley KM, Hasan NA, Haydon SR, Hickman JE, Hidalgo G, Hofmockel KS, Hooker J, Hulth S, Hultman J, Hyde E, Ibáñez-Álamo JD, Jastrow JD, Jex AR, Johnson LS, Johnston ER, Joseph S, Jurburg SD, Jurelevicius D, Karlsson A, Karlsson R, Kauppinen S, Kellogg CTE, Kennedy SJ, Kerkhof LJ, King GM, Kling GW, Koehler A v., Krezalek M, Kueneman J, Lamendella R, Landon EM, Lanede Graaf K, LaRoche J, Larsen P, Laverock B, Lax S, Lentino M, Levin II, Liancourt P, Liang W, Linz AM, Lipson DA, Liu Y, Lladser ME, Lozada M, Spirito CM, MacCormack WP, MacRae-Crerar A, Magris M, Martín-Platero AM, Martín-Vivaldi M, Martínez LM, Martínez-Bueno M, Marzinelli EM, Mason OU, Mayer GD, McDevitt-Irwin JM, McDonald JE, McGuire KL, McMahon KD, McMinds R, Medina M, Mendelson JR, Metcalf JL, Meyer F, Michelangeli F, Miller K, Mills DA, Minich J, Mocali S, Moitinho-Silva L, Moore A, Morgan-Kiss RM, Munroe P, Myrold D, Neufeld JD, Ni Y, Nicol GW, Nielsen S, Nissimov JI, Niu K, Nolan MJ, Noyce K, O'Brien SL, Okamoto N, Orlando L, Castellano YO, Osuolale O, Oswald W, Parnell J, Peralta-Sánchez JM, Petraitis P, Pfister C, Pilon-Smits E, Piombino P, Pointing SB, Pollock FJ, Potter C, Prithiviraj B, Quince C, Rani A, Ranjan R, Rao S, Rees AP, Richardson M, Riebesell U, Robinson C, Rockne KJ, Rodriguezl SM, Rohwer F, Roundstone W, Safran RJ,

Sangwan N, Sanz V, Schrenk M, Schrenzel MD, Scott NM, Seger RL, Seguinorlando A, Seldin L, Seyler LM, Shakhsheer B, Sheets GM, Shen C, Shi Y, Shin H, Shogan BD, Shutler D, Siegel J, Simmons S, Sjöling S, Smith DP, Soler JJ, Sperling M, Steinberg PD, Stephens B, Stevens MA, Taghavi S, Tai V, Tait K, Tan CL, Taş N, Taylor DL, Thomas T, Timling I, Turner BL, Urich T, Ursell LK, van der Lelie D, van Treuren W, van Zwieten L, Vargas-Robles D, Thurber RV, Vitaglione P, Walker DA, Walters WA, Wang S, Wang T, Weaver T, Webster NS, Wehrle B, Weisenhorn P, Weiss S, Werner JJ, West K, Whitehead A, Whitehead SR, Whittingham LA, Willerslev E, Williams AE, Wood SA, Woodhams DC, Yang Y, Zaneveld J, Zarraonaindia I, Zhang Q, Zhao H. A communal catalogue reveals Earth's multiscale microbial diversity. Nature. 2017;551(7681):457–63.

256. Marotz C, Sharma A, Humphrey G, Gotte N, Daum C, Gilbert J, Eloe-Fadrosh E, Knight R. Triplicate PCR reactions for 16S rRNA gene amplicon sequencing are unnecessary. Biotechniques [Internet]. 2019;67(1):6–9. Available from: https://www.future-science.com/doi/pdf/10.2144/btn-2018-0192

257. Minich JJ, Humphrey G, Benitez RAS, Sanders J, Swafford A, Allen EE, Knight R. High-throughput miniaturized 16S rRNA amplicon library preparation reduces costs while preserving microbiome integrity. mSystems. 2018;3(6):e00166-18.

258. Bolyen E, Rideout JR, Dillon MR, Bokulich NA, Abnet CC, Al-Ghalith GA, Alexander H, Alm EJ, Arumugam M, Asnicar F, Bai Y, Bisanz JE, Bittinger K, Brejnrod A, Brislawn CJ, Brown CT, Callahan BJ, Caraballo-Rodríguez AM, Chase J, Cope EK, da Silva R, Diener C, Dorrestein PC, Douglas GM, Durall DM, Duvallet C, Edwardson CF, Ernst M, Estaki M, Fouquier J, Gauglitz JM, Gibbons SM, Gibson DL, Gonzalez A, Gorlick K, Guo J, Hillmann B, Holmes S, Holste H, Huttenhower C, Huttley GA, Janssen S, Jarmusch AK, Jiang L, Kaehler BD, Kang K bin, Keefe CR, Keim P, Kelley ST, Knights D, Koester I, Kosciolek T, Kreps J, Langille MGI, Lee J, Ley R, Liu YX, Loftfield E, Lozupone C, Maher M, Marotz C, Martin BD, McDonald D, McIver LJ, Melnik A v., Metcalf JL, Morgan SC, Morton JT, Naimey AT, Navas-Molina JA, Nothias LF, Orchanian SB, Pearson T, Peoples SL, Petras D, Preuss ML, Pruesse E, Rasmussen LB, Rivers A, Robeson MS, Rosenthal P, Segata N, Shaffer M, Shiffer A, Sinha R, Song SJ, Spear JR, Swafford AD, Thompson LR, Torres PJ, Trinh P, Tripathi A, Turnbaugh PJ, Ul-Hasan S, van der Hooft JJJ, Vargas F, Vázquez-Baeza Y, Vogtmann E, von Hippel M, Walters W, Wan Y, Wang M, Warren J, Weber KC, Williamson CHD, Willis AD, Xu ZZ, Zaneveld JR, Zhang Y, Zhu Q, Knight R, Caporaso JG. Reproducible, interactive, scalable and extensible microbiome data science using QIIME 2. Nature Biotechnology. 2019;37(8):852–7.

259. Amir A, Daniel M, Navas-Molina J, Kopylova E, Morton J, Xu ZZ, Eric K, Thompson L, Hyde E, Gonzalez A, Knight R. Deblur Rapidly Resolves Single-Nucleotide Community Sequence Patterns. mSystems [Internet]. 2017;2(2):1–7. Available from: http://genomebiology.biomedcentral.com/articles/10.1186/gb-2012-13-9-r79

260. Martino C, Morton JT, Marotz CA, Thompson LR, Tripathi A, Knight R, Zengler K. A Novel Sparse Compositional Technique Reveals Microbial Perturbations. mSystems. 2019;4(1):1–13.

261. R Core Team. R: A language and environment for statistical computing [Internet]. Vienna, Austria: R Foundation for Statistical Computing; 2016. Available from: https://www.r-project.org/

262. Wickham H, Francois R. dplyr: A Grammar of Data Manipulation [Internet]. 2016. Available from: https://cran.r-project.org/package=dplyr

263. McMurdie PJ, Holmes S. phyloseq: An R package for reproducible interactive analysis and graphics of microbiome census data. PLoS ONE. 2013;8(4):e61217.

264. Wickham H. ggplot2: Elegant Graphics for Data Analysis [Internet]. New-York: Springer-Verlag; 2009. Available from: http://ggplot2.org

265. Wickham H. scales: Scale Functions for Visualization [Internet]. 2016. Available from: https://cran.r-project.org/package=scales

266. Bolger AM, Lohse M, Usadel B. Trimmomatic: A flexible trimmer for Illumina sequence data. Bioinformatics. 2014 Aug 1;30(15):2114–20.

267. Langmead B, Salzberg SL. Fast gapped-read alignment with Bowtie 2. Nature Methods. 2012 Apr;9(4):357–9.

268. Oh J, Byrd AL, Deming C, Conlan S, Kong HH, Segre JA, Barnabas B, Blakesley R, Bouffard G, Brooks S, Coleman H, Dekhtyar M, Gregory M, Guan X, Gupta J, Han J, Ho SL, Legaspi R, Maduro Q, Masiello C, Maskeri B, McDowell J, Montemayor C, Mullikin J, Park M, Riebow N, Schandler K, Schmidt B, Sison C, Stantripop M, Thomas J, Thomas P, Vemulapalli M, Young A. Biogeography and individuality shape function in the human skin metagenome. Nature. 2014 Oct 2;514(7520):59–64.

269. Erin Chen Y, Fischbach MA, Belkaid Y. Skin microbiota-host interactions. Vol. 553, Nature. Nature Publishing Group; 2018. p. 427–36.

270. Khmaladze I, Leonardi M, Fabre S, Messaraa C, Mavon A. The skin interactome: A holistic “genome-microbiome-exposome” approach to understand and modulate skin health and aging. Vol. 13, Clinical, Cosmetic and Investigational Dermatology. Dove Medical Press Ltd; 2020. p. 1021–40.

271. Vollmer DL, West VA, Lephart ED. Enhancing skin health: By oral administration of natural compounds and minerals with implications to the dermal microbiome. Vol. 19, International Journal of Molecular Sciences. MDPI AG; 2018.

272. Heetfeld AB, Schill T, Schröder SS, Forkel S, Mahler V, Pfützner W, Schön MP, Geier J, Buhl T. Challenging a paradigm: skin sensitivity to sodium lauryl sulfate is

independent of atopic diathesis. British Journal of Dermatology. 2020 Jul 1;183(1):139–45.

273. Takagi Y, Shimizu M, Morokuma Y, Miyaki M, Kiba A, Matsuo K, Isoda K, Mizutani H. A new formula for a mild body cleanser: Sodium laureth sulphate supplemented with sodium laureth carboxylate and lauryl glucoside. International Journal of Cosmetic Science. 2014;36(4):305–11.

274. Thakur P, Saini NK, Thakur VK, Gupta VK, Saini R v., Saini AK. Rhamnolipid the Glycolipid Biosurfactant: Emerging trends and promising strategies in the field of biotechnology and biomedicine. Vol. 20, Microbial Cell Factories. BioMed Central Ltd; 2021.

275. Fischer F, Achterberg V, Mä rz A, Puschmann S, Rahn CD, Lutz V, Blatt T, Wenck H, Gallinat S. Folic acid and creatine improve the firmness of human skin in vivo.

276. Peirano RI, Achterberg V, Dusing HJ, Akhiani M, Koop U, Jaspers S, Kruger A, Schwengler H, Hamann T, Wenck H, Stab F, Gallinat S, Blatt T. Dermal penetration of creatine from a face-care formulation containing creatine, guarana and glycerol is linked to effective antiwrinkle and antisagging efficacy in male subjects. Journal of Cosmetic Dermatology. 2011;10:273–81.

277. Lenz H, Schmidt M, Welge V, Schlattner U, Wallimann T, Elsä HP, Wittern KP, Wenck H, Stä F, Blattw T. The Creatine Kinase System in Human Skin: Protective Effects of Creatine Against Oxidative and UV Damage In Vitro and In Vivo. 2004.

278. Love MI, Huber W, Anders S. Moderated estimation of fold change and dispersion for RNA-seq data with DESeq2. Genome Biology. 2014 Dec 5;15(12).

279. Fournière M, Latire T, Souak D, Feuilloley MGJ, Bedoux G. Staphylococcus epidermidis and cutibacterium acnes: Two major sentinels of skin microbiota and the influence of cosmetics. Vol. 8, Microorganisms. MDPI AG; 2020. p. 1–31.

280. Dréno B, Dagnelie MA, Khammari A, Corvec S. The Skin Microbiome: A New Actor in Inflammatory Acne. Vol. 21, American Journal of Clinical Dermatology. Adis; 2020. p. 18–24.

281. Turesky RJ. Mechanistic evidence for red meat and processed meat intake and cancer risk: A follow-up on the international agency for research on cancer evaluation of 2015. Chimia (Aarau). 2018;72(10):718–24.

282. Canto JG et al. Number of coronary heart disease risk factors and mortality in patients with first myocardial infarction. JAMA. 2011;306:2120–7.

283. Organization WH. Cardiovascular diseases (CVDs) [Internet]. 2015. Available from: http://www.who.int/mediacentre/factsheets/fs317/en/

284. Tabas I, Garcia-Cardena G, Owens G. Recent insights into the cellular biology of atherosclerosis. J Cell Biol. 2015;209(1):13–22.

285. Varki N, Anderson D, Herndon JG, Pham T, Gregg CJ, Cheriyan M, Murphy J, Strobert E, Fritz J, Else JG, Varki A. Heart disease is common in humans and chimpanzees, but is caused by different pathological processes. Evol Appl. 2009;2(1):101–12.

286. Varki N, Strobert E, Dick EJ, Benirschke K, Varki A. Biomedical differences between human and nonhuman hominids: potential roles for uniquely human aspects of sialic acid biology. Annu Rev Pathol. 2011;6:365–93.

287. Laurence H, Kumar S, Owston M, Lanford R, Hubbard G, Dick EJ. Natural mortality and cause of death analysis of the captive chimpanzee (Pan troglodytes): A 35-year review. J Med Primatol. 2017;46(3):106–15.

288. Libby P, Buring JE, Badimon L, Hansson GK, Deanfield J, Sommer Bittencourt M, Tokgozoglu L, Lewis EF. Atherosclerosis. Nature Reviews Disease Primers. 2019;5.

289. Alisson-Silva F, Kawanishi K, Varki A. Human risk of diseases associated with red meat intake: Analysis of current theories and proposed role for metabolic incorporation of a non-human sialic acid. Vol. 51, Molecular Aspects of Medicine. Elsevier Ltd; 2016. p. 16–30.

290. Peri S, Kulkarni A, Feyertag F, Berninsone PM, Alvarez-Ponce D. Phylogenetic Distribution of CMP-Neu5Ac Hydroxylase (CMAH), the Enzyme Synthetizing the Proinflammatory Human Xenoantigen Neu5Gc. Genome Biol Evol. 2018;10(1):207–19.

291. Banda K, Gregg CJ, Chow R, Varki NM, Varki A. Metabolism of vertebrate amino sugars with N-glycolyl groups: Mechanisms underlying gastrointestinal incorporation of the non-human sialic acid xeno-autoantigen N-glycolylneuraminic acid. Journal of Biological Chemistry. 2012 Aug 17;287(34):28852–64.

292. Schwarzkopf M, Knobeloch K, Rohde E, Hinderlich S, Wiechens N, Lucka L, Horak I, Reutter W, Horstkorte R. Sialylation is essential for early development in mice. Proc Natl Acad Sci USA. 2002;99(8):5267–70.

293. Varki A, Cummings RD, Esko JD, Stanley P, Hart GW, Aebi M, Darvill AG, Kinoshita T, Packer NH, Prestegard JH, Schnaar RL, Seeberger PH, editors. Essentials of Glycobiology. 3rd ed. Cold Spring Harbor, NY: Cold Spring Harbor Laboratory Press; 2015.

294. Wang B. Sialic acid is an essential nutrient for brain development and cognition. Annu Rev Nutr. 2009;29:177–222.

295. Tangvoranuntakul P, Gagneux P, Daiz S, Bardor M, Varki N, Varki A, Muchmore E. Human uptake and incorporation of an immunogenic nonhuman dietary sialic acid. Proc Natl Acad Sci USA. 2003;100(21):12045–50.

296. Banda K, Gregg CJ, Chow R, Varki NM, Varki A. Metabolism of Vertebrate Amino Sugars with N-Glycolyl Groups: mechanisms underlying gastrointestinal incorporation of the non-human sialic acid xeno-autoantigen N-glycolylneuraminic acid. J Biol Chem. 2012;287(34):28852–64.

297. Samraj AN, Pearce OMT, Laubli H, Crittenden AN, Bergfeld AK, Banda K, Gregg CJ, Bingman AE, Secrest P, Diaz SL, Varki NM, Varki A. A red meat-derived glycan promotes inflammation and cancer progression. Proc Natl Acad Sci USA. 2015;112(2):542–7.

298. Gao B, Long C, Lee W, Zhang Z, Gao X, Landsittel D, Ezzelarab M, Ayares D, Huang Y, Cooper DK, Wang Y, Hara H. Anti-Neu5Gc and anti-non-Neu5Gc antibodies in healthy humans. PLoS One. 2017;12(7):e0180768.

299. Zhu A, Hurst R. Anti-N-glycolylneuraminic acid antibodies identified in healthy human serum. Xenotransplantation. 2002;

300. Padler-Karavani V, Yu H, Cao H, Chokhawala H, Karp F, Varki N, Chen X, Varki A. Diversity in specificity, abundance, and composition of anti-Neu5Gc antibodies in normal humans: Potential implications for disease. Glycobiology. 2008;18(10):818–30.

301. Dhar C, Sasmal A, Varki A. From “Serum Sickness” to “Xenosialitis”: Past, Present, and Future Significance of the Non-human Sialic Acid Neu5Gc. Front Immunol. 2019;10:807.

302. Paul A, Padler-Karavani V. Evolution of sialic acids: Implications in xenotransplant biology. Xenotransplantation. 2018;25(8):e12424.

303. Ghaderi D, Taylor RE, Padler-Karavani V, Diaz S, Varki A. Implications of the presence of N-glycolylneuraminic acid in recombinant therapeutic glycoproteins. Nature Biotechnology. 2010 Aug;28(8):863–7.

304. Samraj AN, Bertrand KA, Luben R, Khedri Z, Yu H, Nguyen D, Gregg CJ, Diaz SL, Sawyer S, Chen X, Eliassen H, Padler-Karavani V, Wu K, Khaw KT, Willett W, Varki A. Polyclonal human antibodies against glycans bearing red meat-derived non-human sialic acid N-glycolylneuraminic acid are stable, reproducible, complex and vary between individuals: Total antibody levels are associated with colorectal cancer risk. PLoS ONE. 2018 Jun 1;13(6).

305. Malykh YN, Schauer R, Shaw L. N-Glycolylneuraminic acid in human tumours. Biochimie. 2001 Jul;83(7):623–34.

306. Hedlund M, Padler-Karavani V, Varki NM, Varki A. Evidence for a human-specific mechanism for diet and antibody-mediated inflammation in carcinoma progression. Proc Natl Acad Sci USA2. 2008;105(48):18936–41.

307. Shewell LK, Day CJ, Kutasovic JR, Abrahams JL, Wang J, Poole J, Niland C, Ferguson K, Saunus JM, Lakhani SR, von Itzstein M, Paton JC, Paton AW, Jennings MP. N-glycolylneuraminic acid serum biomarker levels are elevated in breast cancer patients at all stages of disease. BMC Cancer. 2022 Dec;22(1).

308. Kawanishi K, Dhar C, Do R, Varki N, Gordts PLSM, Varki A. Human Species-Specific Loss of CMP-N-acetylneuraminic Acid Hydroxylase Accelerates Atherosclerosis via Intrinsic and Extrinsic Mechanisms. Proc Natl Acad Sci USA. 2019;116(32).

309. Kawanishi K, Coker JK, Grunddal K v., Dhar C, Hsiao J, Zengler K, Varki N, Varki A, Gordts PLSM. Dietary neu5ac intervention protects against atherosclerosis associated with human-like neu5gc loss- brief report. Arteriosclerosis, Thrombosis, and Vascular Biology. 2021;2730–9.

310. Zaramela LS, Martino C, Alisson-silva F, Rees SD, Diaz SL, Chuzel L, Ganatra MB, Taron CH, Secrest P, Zuniga C, Huang J, Siegel D, Chang G, Varki A, Zengler K. Gut bacteria respoding to dietary changes encode sialidases the exhibit preference for red meat-associated carbohydrates. Nature Microbiology. 2019;4(12):2082–9.

311. Tran C, Turolla L, Ballhausen D, Buros SC, Teav T, Gallart-Ayala H, Ivanisevic J, Faouzi M, Lefeber DJ, Ivanovski I, Giangiobbe S, Caraffi SG, Garavelli L, Superti-Furga A. The fate of orally administered sialic acid: First insights from patients with N-acetylneuraminic acid synthase deficiency and control subjects. Molecular Genetics and Metabolism Reports. 2021 Sep 1;28.

312. Lee-Sundlov MM, Ashline DJ, Hanneman AJ, Grozovsky R, Reinhold VN, Hoffmeister KM, Lau JTY. Circulating blood and platelets supply glycosyltransferases that enable extrinsic extracellular glycosylation. Glycobiology. 2017;27(1):188–98.

313. Manhardt CT, Punch PR, Dougher CWL, Lau JTY. Extrinsic sialylation is dynamically regulated by systemic triggers in vivo. Journal of Biological Chemistry. 2017 Aug 18;292(33):13514–20.

314. Alberts B, Johnson A, Lewis J, Raff M, Roberts K, Walter P. Blood Vessels and Enodthelial Cells. In: Molecular Biology of the Cell. 4th ed. New York: Garland Science; 2002.

315. Samraj AN, Pearce OMT, Läubli H, Crittenden AN, Bergfeld AK, Band K, Gregg CJ, Bingman AE, Secrest P, Diaz SL, Varki NM, Varki A, Kornfeld SA. A red meat-derived glycan promotes inflammation and cancer progression. Proc Natl Acad Sci U S A. 2015 Jan 13;112(2):542–7.

316. Manzi AE, Diaz S, Varki A. High-Pressure Liquid Chromatography of Sialic Acids on a Pellicular Resin Anion-Exchange Column with Pulsed Amperometric Detection: A Comparison with Six Other Systems'. Vol. 3, ANALYTICAL BIOCHEMISTRY. 1990.

317. Dance A. Studying life at the extremes. Nature. 2020 Nov 5;587:165–6.